ABSTRACT

TANG, QIANHONG. Modeling Tropical Cyclone Induced Inland Flooding at Tar Pamlico River Basin of North Carolina. (Under the direction of Dr. Lian Xie).

Landfalling tropical cyclones often produce heavy precipitation and result in river and flash floods. Such floods can not only cause loss of human lives and properties, but also lead to ecological disasters in the affected watershed areas, estuaries and coastal waters. In order to better understand and simulate large coastal watershed hydrology and hydro-meteorological processes associated with tropical cyclones (TC) - induced inland flooding, the Weather Research and Forecasting (WRF) model and the Annualized Agricultural Nonpoint Source Pollution Model (AnnAGNPS) have been employed in this study. The study focuses on four major hydro-meteorological identities and their interactions: 1) previous rainfall events, 2) synoptic atmospheric environment, 3) landfalling hurricane, and 4) surface and ground water hydrology. The research is divided into two parts. Part one focuses on the investigation of the impacts of previous rainfall events on watershed surface runoff while part two studies the impacts of the synoptic atmospheric environment on landfalling hurricanes and the resulting effect on surface runoff. Hurricane Floyd was chosen in this study as a special case because it produced massive floodingas a result of the combined effects of previous rainfall events from Hurricane Dennis and the synoptic atmospheric environment.

The modeling results indicate that the AnnAGNPS model performs well in predicting the total amount of watershed runoff. However Muskingum channel routing is needed for AnnAGNPS to improve the hydrographs of flow discharge during hurricane events.

Sensitivity analysis of soil saturated hydrological conductivity (K_s) indicates that both base flow and event total runoff are sensitive to K_s. Base flow increases as K_s increases when $K_s \leq$ 15 m/day, but slightly decreases when K_s > 15 m/day which is out of assumption of linear relationship from Darcy's law. Peak runoff exponentially decreases as K_s increases. The results show that without the preceding Hurricane Dennis, the outlet discharge as a result of Hurricane Floyd would have been as much as 37% lower than that caused by the combined Dennis-Floyd effect.

Precipitation during the landfall of Hurricane Floyd (1999) was simulated by using the WRF model with two-way nested domains. The horizontal grid spacing of the inner-most domain is 2 km. The WRF model could reproduce the northeast- southwest oriented narrow and intense band of precipitation that developed just inland of the coast over North Carolina. The distribution pattern of accumulated precipitation is consistent with the observed precipitation pattern. The magnitudes of the simulated precipitation are generally within 30% of the observed values at the weather stations in the study area.

The effects of large-scale atmospheric environment on Hurricane Floyd - induced precipitation and flooding have also been investigated. Through a vortex removal technique, Hurricane Floyd vortex was mostly removed to obtain the large-scale atmospheric environmental field at the model initial time. It is shown that the environment-induced precipitation can be as high as 21.5% of total precipitation in domain 3 which covers most of the North Carolina and 7.3% in the focused hydrological study area. Idealized hydrological simulation results demonstrate that without large scale environmental impacts the discharge

would have been as much as 10.4% lower at the Tarboro gauge station if assuming TC and synoptic environment interaction is linear.

Using simulated precipitation from the WRF, AnnAGNPS model along with Muskingum routing was able to reproduce the hydrograph and total volume of surface runoff at the watershed outlet. This implies that with improved precipitation forecasts from numerical weather prediction models such as WRF, it is possible to make skillful river runoff forecasts using distributed hydrological models.

Modeling Tropical Cyclone Induced Inland Flooding at Tar Pamlico River Basin of North Carolina

by
Qianhong Tang

A dissertation submitted to the Graduate Faculty of
North Carolina State University
in partial fulfillment of the
requirements for the degree of
Doctor of Philosophy

Marine, Earth, and Atmospheric Sciences

Raleigh, North Carolina

July 2010

APPROVED BY:

_____	_____
Lian Xie Chair of Advisory Committee	Gary M. Lackmann
_____	_____
Sethu Raman	Fredrick H. M. Semazzi

DEDICATION

To Xu Qiang, a very close friend and sister who passed away during my PhD study. In memory for her love, support, and kindness to me and many other Chinese students at NCSU, I dedicate this dissertation to her.

BIOGRAPHY

Qianhong Tang grew up in Qinghai Province of northwestern China, a very remote highland with the elevation of 2200 meters above the sea level. Although both the economy and climate in Qinghai were very poor, she grew up in a very warm family with positive guidance of her parents and the company of her two brothers. She got her early college education at Nanjing Institute of Meteorology, China. After finishing her bachelor's degree, she worked at Qinghai Meteorological Institute for 10 years. She then followed her husband to Thailand and worked as a GIS specialist at a consulting firm in Bangkok for 7 years. She felt that she needed to get further education to fresh her knowledge so she went to Kansas State University to pursue her master's degree education in the Department of Biological and Agricultural Engineering in 2000. She finished her study there in 2002 with a Master of Engineer degree. In 2006, she started her PhD study in MEAS department, North Carolina State University and has been studying and doing research there since then.

She married her high school classmate and college mate, Hechu Chen and they have a lovely 20-years-old daughter – Minlu Chen. She is very thankful for the loves from her parents, relatives, friends, daughter and husband.

ACKNOWLEDGMENTS

I owe a debt beyond my ability to express to many people who made it possible for me to complete this study. The first and the most important person I would like to express my gratitude is: Dr. Lian Xie, my advisor, who provided me with the opportunity to pursue my lifetime dream. Without his guidance, encouragement and continuous support, I could not possibly finish my study. I am deeply impressed by his academic intelligence and sensitivity. His patience, tolerance and sincerity towards his students will be the example I will follow for the rest of my life. I also want to express my appreciation to Dr. Lackmann, who guided me at each step of the study programs and inspired me in many difficult situations of my study. His constructive suggestions have been assimilated particularly in the major two parts of my dissertation. Without his encouragement, I could not accomplish this. I am also grateful to Dr. Raman, I learned a lot from him through his advices and his class. My appreciation is also to Dr. Fred H. M. Semazzi for his willingness to serve as my committee member and for his valuable time in advising me in different perspectives within his expertise. I thank Dr. Gerald S. Janowitz for his continuous generous helps and great advices through the graduate study program. Dr. Wei Ning Xiang served on my committee for a period of time. His kind personality and guidance left me with deep impression.

I learnt a lot from classes taught by different professors at MEAS in NCSU and wish to reward the department in the future. I would also like to thank the following people and university staff for their help: Ms. Connie Hockaday for administrating my stay in the department and their continuous supports and great helps; Susan, Laura, Christine, Office of

International Student Services for taking care of our immigration issue; department staff for their silent support to make our research smooth.

Other people I want to express my acknowledgement to are Drs. Ronald Bingner and Yongping Yang from USDA for their great helps in AnnAGNPS model and related issues.

I thank my best friend Mr. Xiang Rong for spending his valuable time reading my manuscripts carefully and correct all of the errors many times. His friendship would be invaluable treasure of my life. Dr. Yongqiang Liu's advising, suggestions and great helps are valuable to this dissertation.

To my colleagues within Dr. Xie's Coastal Fluid Dynamics Laboratory, Drs. Machuan Peng, Tingzhuang Yan, Huiqing Liu, Xuejing Zhang, Bin Liu, Yanyun Liu, I want to express my gratitude for their prompt assistance with all scopes of my study and life. They have made my life at Raleigh more colorful. I would like to express my special appreciation to Dr. Bin Liu for his friendly advice academically and other broader perspective. His tremendous helps, patience and kindness helped finishing this research.

This study is supported by U.S. National Oceanic and Atmospheric Administration Grant #NA07NWS4680002, all awarded to North Carolina State University and MEAS department. Acknowledgment is also made to the NCAR/NCEP for making available of the WRF model and NARR data, USDA for AGNPS model, USGS for all hydrological data and North Carolina State Climate Office for both surface and ground water data.

There are many friends who helped and supported me both financially and spiritually in the past several years. I would like to express my deep appreciation to all of them. They are John and Jean Young, Jian and Grace Zhang, Jinyi Li and Yongxin Sun, David and Pat

Lee, Vicky Wang, Wanxian Lin, Jonathan and Ruth Hou, Joe and Cindy Li, Jan and Winnie Lin, Joe and Amy Liu, Jack Bowers and Betty J. Fisher, Zifeng and Zhuying Li, Xiang Rong and Lin Wang, Weiping Zhao, Huaxiao Zhang, Qiang Xu and Benhui Liu, Yu Luo and Huixia Wang, Andrew and Alice Liao.

I especially thank my college roommates: Ms. Qianhong Li and Ms. Bin Liu. Their friendship and great helps inspired me through these years. How simple thanks can express my appreciation to them.

Finally, I want to thank my family. I thank my mother-in-law for her tremendous sacrifice and unconditional love to me and my family. I thank her for taking care of my husband when I have been thousands of miles away from him for all these years. Thanks to my parents, brothers and sisters for their consistent encouragement, understanding and their unconditional love. My father has been trying very hard to fight with cancer so that he can see the day I reach my goal. Without his encouragement, I could not have been strong enough to pursue my PhD study. Of course, my pretty daughter, she spent many years with me in US with laughs, tears, happiness and joy. We have studied together and grown up throughout the life. We have made this dream come true. I am so thankful to have her in my life. Most of all, I must thank my husband - Hechu Chen for his understanding, unlimited support and love. Without him, I would never have made it through this endeavor. He helped and encouraged me to reach my potential.

TABLE OF CONTENTS

LIST OF TABLES

LIST OF FIGURES

CHAPTER 1 Introduction

1.1 Motivation

Forecasting inland flooding associated with heavy rainfall induced by landfalling tropical cyclones (TCs) is a difficult task, which can be complicated by existing internal and external features that may enhance the precipitation preceding or during landfall of the TC. The damage of inland floods can often exceed the coastal damage of these life-threatening storms (Rappaport 2000). Such floods can not only cause loss of human lives and properties, but also lead to ecological disasters in watershed areas, estuaries and coastal waters. Previous studies (Hilderbrand 2002; Croke 2005) indicated that approximately 40% of the damages from landfalling tropical cyclones in North Carolina were caused by inland flooding. The fact that same amount of precipitation can result in very different levels of flooding and flood damage due to different spatial distributions of precipitation and different characteristics of watersheds such as land use and soil types, slopes and aspects, creates a major challenge for inland flood forecasting. Groundwater hydrology which influences the base flow of watersheds, adds an additional degree of difficulty in inland flood forecasting.

In the United States, inland flooding is the predominant cause of deaths associated with TCs. Hurricane Floyd in September 1999 caused the loss of 57 lives in the US. It was the deadliest hurricane in the United States since Hurricane Agnes in 1972 and before Hurricane Katrina of 2005. The storm also was one of the costliest in the nation's history, amounting to $4.5 billion dollars (Pasch et al. 1999). Most of the deaths and damage were

from inland, freshwater flooding in eastern North Carolina. There were 35 lives lost in this event in North Carolina.

Operationally, the National Weather Service River Forecast System (NWSRFS) has been used at all thirteen National Weather Service River Forecast Centers (NWSRFCs) (NOAA 2005). The NWSRFS is a continuous simulation, conceptual, lumped-parameter model for stream flow simulation. Originally released in 1972, the model is capable of simulating historical stream flows for various types of design studies. The forecast system contains a variety of hydrologic models and procedures that can be connected in whatever sequence which is needed for a particular application.

The two approaches typically used by the NWS for flood forecasting are either the use of a rainfall runoff model, or by empirical estimation of flood potential based on area rainfall amounts (Gupta 2006). The River Forecast Centers (RFC's) apply the former approach, using two continuous, lumped rainfall-runoff models -- the physically-based Sacramento Soil Moisture Accounting Model (SAC-SMA; Burnash et al 1973), and the empirically-based Continuous-API Model (CONT-API; Sittner *et al.* 1969) based on the Antecedent Precipitation Index (API; Kohler and Linsley 1951). The Mid-Atlantic RFC (MARFC) uses the CONT-API method. Depending upon the developmental stage and needs of the RFC, these models run at either 1-hour or 6-hour time steps. The rainfall-runoff models need to be calibrated for several key parameters before they can provide reliable forecasts in an operational setting (NWSRFS website).

Sacramento Model, also called Sacramento Soil Moisture Accounting (SAC-SMA) model, of the NWSRFS has been originally developed by NWS Sacramento, California River

Forecast Center (Burnash et al. 1973). The NWS model can be partitioned into two major components, the Sacramento soil moisture accounting model and the flow routing model. The Sacramento soil moisture accounting model is a continuous, conceptual, lumped input and lumped parameter model that transforms the rainfall input in the land phase of the hydrologic cycle into channel inflows (Whol 2000). Sacramento model also has been developed into a semi-distributed model. Ajami et al. (2004) compared lumped, semi-lumped and semi-distributed versions of the SAC-SMA (Sacramento Soil Moisture Accounting) model for the Illinois River basin at Watts (OK). Their results did not show any improvement by semi-distributed SAC-SMA model. The flow routing model is responsible for routing the channel inflows to the basin or sub-basin outlet by using unit hydrograph and Muskingum routing methods (Methods et al. 2003).

The Southeast River Forecast Center (SERFC) operates five southeastern states and all basins covered by these states (). The Southeast River Forecast Center (SERFC) is experimenting with the Hydrologic Engineering Centers River Analysis System (HEC-RAS) model in its river basins (Joshua Palmer, *personal communication*). This includes areas like Northeast Florida along the St. Johns River and the extreme eastern Coastal Plain of North Carolina. However, HEC-RAS only does not account for rainfall/runoff, so the Sacramento model is used as a supplement to HEC-RAS at certain points along the river or rivers to incorporate rainfall/runoff as additional water to the flow being routed from upstream.

An alternative to the use of HEC-RAS is the application of a distributed watershed model to simulate watershed surface runoff at different outlets and then use a channel routing

model to route the water downstream. In this study, a river forecast model is developed based on the Annualized Agricultural Nonpoint Source Pollution Model (AnnAGNPS) distributed watershed model and the Muskingum channel routing scheme (Methods et al. 2003). The AnnAGNPS is developed by the AnnAGNPS model development group in U. S. Department of Agriculture for studying agriculture runoff and nonpoint source water pollution (Bingner et al. 2007). It is originally designed for relatively small watersheds. However, dividing a large watershed into several sub-watersheds can give us better solution in the simulation. The selection of the AnnAGNPS for this study is based on the comparison studies (Migliaccio and Srivastava 2007; Borah and Bera 2003, 2004; Parajuli et al. 2009) of currently available watershed models, including those of Areal Nonpoint Source Watershed Environment Response Simulation (ANSWERS‐2000), Hydrologic Simulation Program - Fortran (HSPF), Soil and Water Assessment Tool (SWAT), Watershed Assessment Model (WAM), and Water Erosion Prediction Project (WEPP). The study indicates that for short-range forecasting of TC related flooding, AnnAGNPS along with SWAT are more appropriate than the other models included in the study. Thus, this study selects the AnnAGNPS and applies it to the Tar-Pamlico River Basin in North Carolina.

Appling a hydrological model in a large coastal watershed during Tropical Cyclones (TCs)/hurricane landfall is a major challenge because the watershed itself not only is receiving heavy and intense precipitation but also interacting with ocean tides, strong waves and storm surges. Besides, antecedent rainfall events and extremely high degree of stream-aquifer interaction in the coastal watershed makes the situation more complex. Figure 1.1 demonstrates the interaction of these components. Large scale of atmospheric environment

prior or during hurricane landfall may enhance/reduce the precipitation. Previous precipitation will increase soil moisture in the watershed and creates storm surge over the ocean. All of these will then impact on the watershed hydrological processes and further contribute to coastal watershed flooding. This study is to find solutions of these interactions and tends to provide a potential and additional ensemble tool for the better river flood forecasting during TCs landfalls in the future.

1.2 Objectives

Based on the background study, the following research questions are proposed: How much impact did previous rainfall events have on Hurricane Floyd flooding? How much surface runoff would be reduced without previous rainfall events during Floyd? What role did the large scale synoptic environment play? What would be the amount of precipitation induced by the synoptic environment? The objectives of this study are then to explore important hydrological parameters that impact watershed flooding during hurricane events; assess the effects of different distributions of precipitation on watershed hydrology; quantify the contributions of antecedent rainfall events to flooding of hurricane Floyd; and quantify the amount of precipitation induced by synoptic atmospheric environment.

The rest of this dissertation is organized as follows. The first chapter is introduction. The second chapter is Modeling the impacts of Previous Rainfall Events on Inland Flooding in Tar Pamlico River Basin of North Carolina. Chapter 3 is Modeling impacts of Large-Scale Atmospheric Environmental on Inland Flooding during Floyd landfall in 1999. The last chapter is Concluding Remarks and Future Works.

REFERENCES

Ajami, N. K., H. Gupta, T. Wagener and S. Sorooshian, 2004: Calibration of a semi-distributed hydrologic model for streamflow estimation along a river system. J. hydro 298(2004): 112-135.

Burnash, R.J.C., Ferral, R.L., McGuire, R.A., 1973. A generalized streamflow simulation system-conceptual modeling for digital computers, US Department of Commerce, National Weather Service and State of California, Department of Water Resources.

Croke, M. S., 2005: Examining Planetary, Synoptic and Mesoscale Features That Enhance Precipitation Associated with Landfalling Tropical Cyclones in North Carolina. North Carolina State University Master Thesis.

Dyhouse, G., J. Hatchett and J. Benn, 2003. Floodplain Modeling Using HEC-RAS. First Edition. Haestad press. Waterbury, CT. USA.

Ellen E. Wohl, 2000. Inland Flood Hazards - Human, Riparian, and Aquatic Communities. Colorado State University. Cambridge University Press.

Finnerty, B. D., M. B. Smith, D. J. Seo, V. Koren and G. Moglen, 2008. Sensitivity of the Sacramento Soil Moisture Accounting Model to Space-Time Scale Precipitation Inputs from NEXRAD. http://www.hydro.washington.edu/~tazebe/tasks2.html

Gebert, W. A., M. J. Radloff, E. J. Condidine and J. L. Kennedy, 2007. Use streamflow data to estimate baseflow recharge in Wisconsin. J. American Water Recourses Association 43(1): 220-236.

Gupta, H., 2006. Development of a site-specific flash flood forecasting model for the Western region. Final report for COMET proposal entitled. University of Arizona.

Hilderbrand, D. C., 2002: Risk Assessment of North Carolina Tropical Cyclones (1925 – 2000). North Carolina State University Master Tthesis.

Hydrology Handbook, 1996. Task Committee on Hydrology Handbook. American Society of Civil Engineers. New York.

Linsley, R. K., M. A. Kohler and J. L. Paulhus. 1975. Hydrology for Engineers, 2nd edition. New York: McGraw-Hill, Inc.

Martin, K., 2002. NWSRFS calibration parameter selection and geologic reasoning: Pacific Northwest cases. J. American Water Recourses Association 38(5): 1349-1362.

NASA, 2000. Assessing Floyd's floods. Earth Observatory, National Aeronautics and Space Administration. http://earthobservatory.nasa.gov/Features/FloydSediment/sediment_2.php

NOAA, 2000. NOAA Service Assessment Report of Hurricane Floyd Floods of September 1999. June.

NWSRFS Manuel, 2005. http://www.nws.noaa.gov/oh/hrl/nwsrfs/users_manual/htm/formats.php

Parajuli, P. B., N. O. Nelson, L. D. Frees and K. R. Mankin, 2009: Comparison of AnnAGNPS and SWAT model simulation results in USDA-CEAP agricultural watersheds in south-central Kansas. *Hydrol. Process,*. **23**, 748-763.

Pasch, R. J., T. B. Kimberlain and S. R. Stewart, 1999: Preliminary Report Hurricane Floyd 7 - 17 September, 1999. National Hurricane Center, NOAA. http://www.nhc.noaa.gov/1999floyd_text.html

Rappaport, E. N., 2000: Loss of life in the United States associated with recent Atlantic tropical cyclones. *Bull. Amer. Meteor. Soc.*, **81**, 2065-2073.

Reed, S., V. Korean, M. Smith, Z. Zhang, F. Moreda, D. J. Seo and DMIP participants, 2004: Overall distributed model intercomparison project results. J. Hydro. 298 (2004): 27-60.

Tewolde, M. H., 2005. Flood Routing in Ungauged Catchments using Muskingum Methods.Universal publishers, Florida, USA.

Viessman, W and G. L. Lewis, 1996. Introduction to Hydrology. Fourth Edition. HarperCollins College Publishers.

Yuan, Y., 2000. Tile-drained Watershed SCS-curve Number Model. Ph.D. dissertation, University of Illinois at Urbana-Champaign, United States -- Illinois. Retrieved December 8, 2008, from Dissertations & Theses: A&I database. (Publication No. AAT 9955685).

TABLE 1.1 Summary of NWSRFS major operational models

Types of operations	Operation included	Model description	Input	Output	Advantages	Disadvantages
Rainfall/Runoff models	Sacramento Soil Moisture Accounting (SAC SMA)	Consider soil moisture, two layer soils, base flow and evaporation. It is physical model.	Historic time series of T, P, runoff	Predicted time series of T, P and runoff	Soil moisture accounted. Simple model. Time frame is flexible.	Too coarse to consider physical mechanism of hydrological process. No surface condition input.
	NWS RFC Antecedent Precipitation Index Models (API) (Ohio, Middle Atlantic, Central, Colorado Basin)	According antecedent precipitation, two layer soil, base flow and evaporation. Model is linear and empirical.	Historic time series of T, P, runoff	Predicted time series of T, P and runoff	Ensemble models with others can create forecast of river flow, time frame is flexible.	Surface condition only considered as imperviousness. No distributed model. No GIS linkage.
	HEC-GEO	Detailed consideration of channel flow	Upper stream flow and stage	Downstream flow and stage	Channel crossection, flow routing	No watershed surface consideration
Temporal distribution of runoff	Unit hydrograph	Semi-distributed model using unit hydrograph.	Area, Precipitation intensity, channel information	Discharge	Considered drainage area and channel conditions	Did not consider slope of surface.

Synthesized from 1) National Weather Service River Forecast System website
2) Gupta, 2006
3) NWSRFS manuals
4) Hydrology handbook, 1996
5) Martin, 2002

TABLE 1.2 Record floods at NWS forecast points for Hurricane Floyd (1999) (NOAA, 2000)

Date	Location	Flood Stage (Ft)	Old	New
9/17/99	Tar River at Louisburg, NC	20	25.34	26.05
9/17/99	Tar River near Rocky Mount, NC	15	23.67	32.35
9/18/99	Fishing Creek near Enfield, NC	16	17.72	21.65
9/20/99	Tar River at Tarboro, NC	19	31.77	41.51
9/21/99	Tar River at Greenville, NC	13	22.07	29.72

Table 1.3 Verification of NWS Forecast for Hurricane Floyd at Tar-Pamlico River Basin, NC (NOAA, 2000)

Station	Flood Stage (feet)	River Flood Warning/ Statement Time++	Forecast Crest (feet)	Observed Crest (ft)/time of Crest	Departure (forecast crest – observed crest) (feet)	Lead Time (issuance to observed Crest)
Rocky Mount (WFO Raleigh)	15	15/1430	23	32.4 9/16/99 - 1900 EDT+	-9.4	28 hr, 30 min
		16/0940	34-35		+1.6 to +2.6	9 hr, 20 min
Tarboro (WFO Raleigh)	19	15/1409	26	41.5 9/19/99 - 1500 EDT	-15.5	96 hr, 51 min
		16/0940	33-34		-8.5 to -7.5	77 hr, 20 min
		16/2204	34		-7.5	64 hr, 56 min
		17/2000	38		-3.5	43 hr
Greenville (WFO Morehead City)	13	15/1310	18.0	29.73 9/21/99 - 1000EDT	-11.73	140 hr, 50 min
		16/1000	24-25		-4.73	120 hr
		17/1425	26.5		-3.23	91 hr, 35 min
		18/1135	28.5		-1.23	70 hr, 25 min
		18/1925	29		-0.73	62 hr, 35 min
		19/1245	29.5-30		-0.23 to +0.27	45 hr, 15 min
		20/1300	30		+0.27	27 hr

+ EDT – Eastern Daylight Time

++ Only warnings/statements with updated crest values and/or times are included.

Table from NOAA Service Assessment Report of Hurricane Floyd Floods of September 1999.

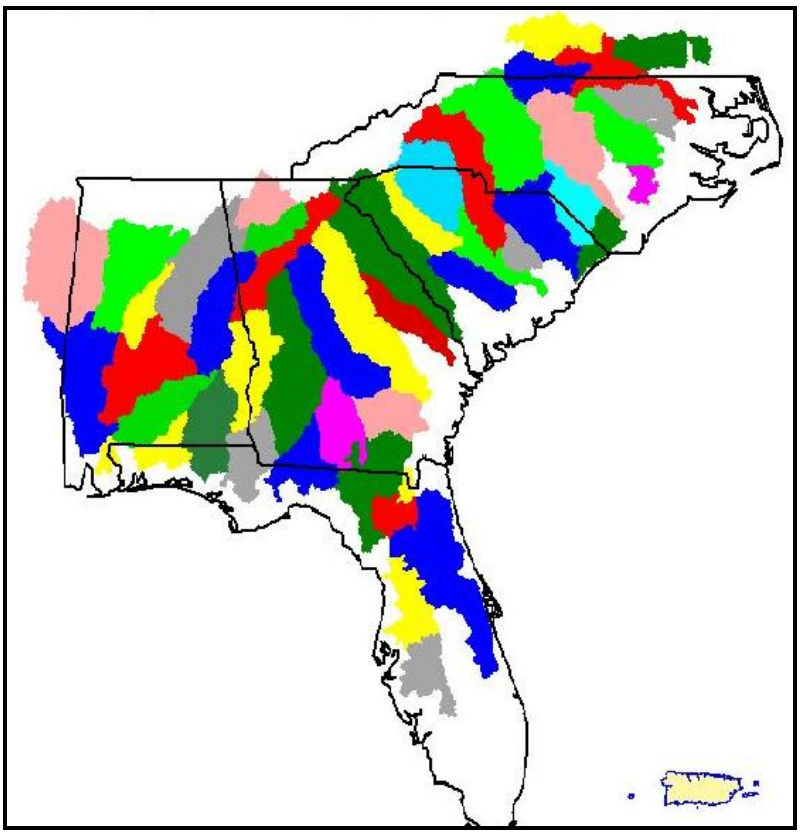

FIG 1.1 River basins by Southeastern River Forecast Center (SERFC website). The grey color area in the northeast of North Carolina is Tar-Pamlico River Basin.

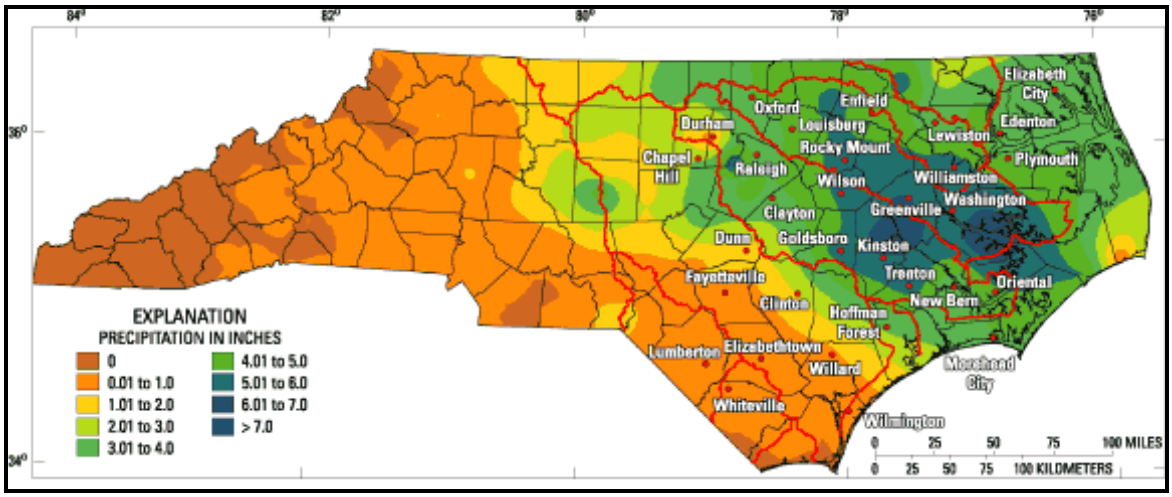

FIG 1.2 Rainfall during Hurricane Dennis, September 4–5, 1999. Rainfall map from State Climate Office of North Carolina.

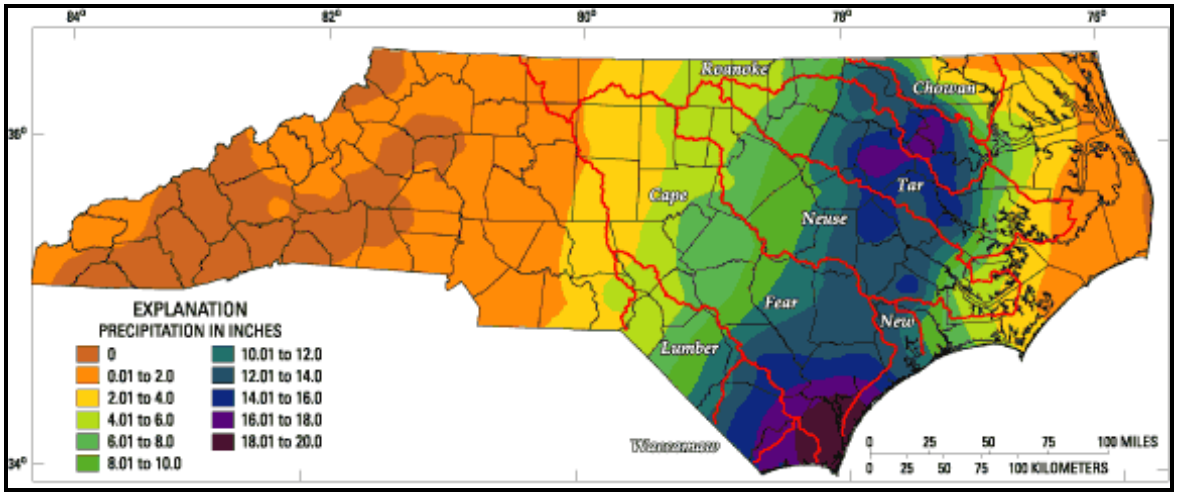

FIG 1.3 Rainfall during Hurricane Floyd, September 14–16, 1999. Rainfall map from State Climate Office of North Carolina.

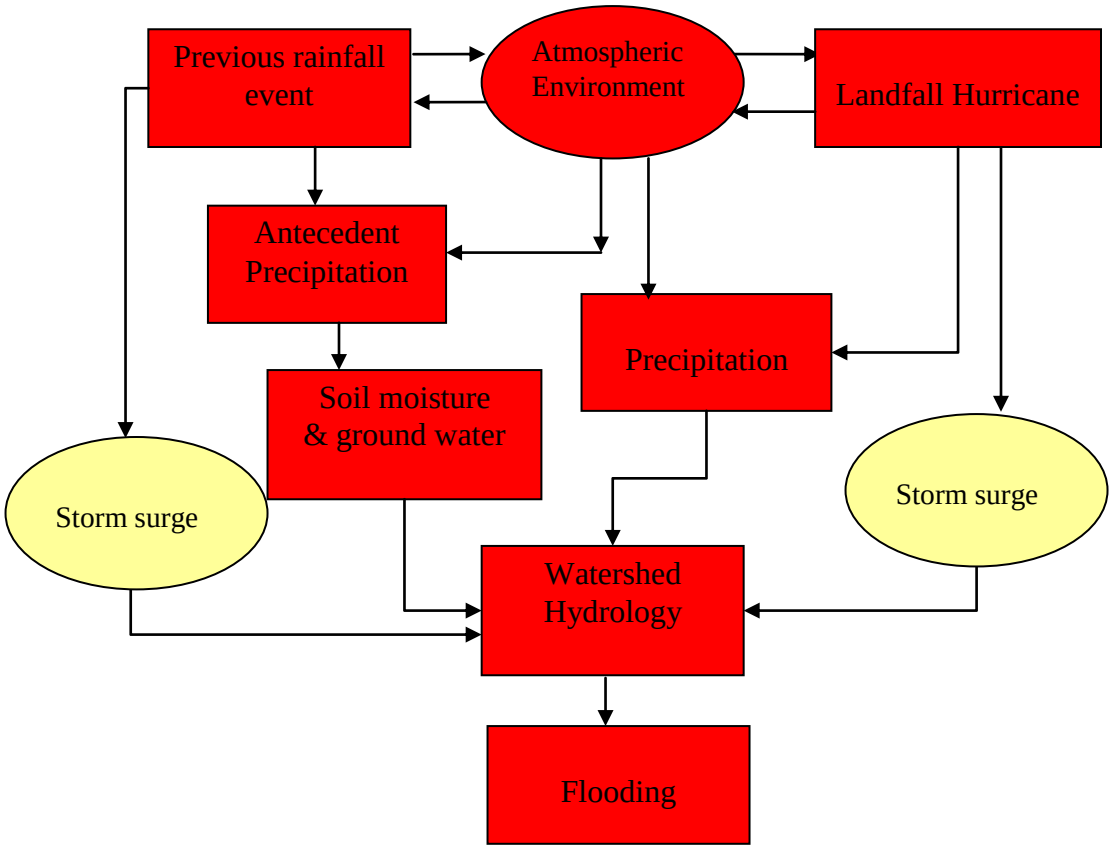

FIG 1.4 The schematic interaction map of antecedent precipitation, atmospheric environment and landfall tropical cyclone induced precipitations, watershed hydrological response and storm surges. The yellow color boxes are not studied in the research.

CHAPTER 2 Modeling the Impacts of Previous Rainfall Events on Inland Flooding in Tar Pamlico River Basin of North Carolina

2.1 Introduction

Landfalling tropical cyclones often produce heavy precipitation, resulting in river and flash floods. It is imperative that accurate forecasting of flooding in coastal watershed caused by landfalling cyclones is provided to decision makers and the public to reduce the storm damages. However, there are several factors that make this task challenging. First, the same amount of precipitation can result in very different levels of flooding and flood damage due to distinct spatial distributions of precipitation (e.g., Opitz et al. 1995; Castro et al. 2009). Second, the characteristics of watersheds such as land use and soil types, slopes and aspects further complicates inland flood forecasting (e.g. Miller et al. 2007; Wang and Melesse 2006). Finally, groundwater hydrology, which influences the base flow of watersheds, adds an additional dimension to the difficulty in inland flood forecasting (Stewart et al. 2007; Zhu and Day 2009).

Many watershed hydrological models have been developed to understand the hydrological-meteorological processes and make prediction of key hydrological variables in the past. These models can be divided into three groups based on their primary applications. The first group is developed from engineering fields, such as HEC- RAS (Hydrologic Engineering Centers River Analysis System, Methods et al. 2003), SHE (Systeme Hydrologique Europeen, Abbotte et al. 1986a, b) and TOPMODEL (a TOPography based

hydrological MODEL, Beven and Kirkby 1979). These models focus on channel hydraulics and hydrology in order to construct dams and channels to prevent flooding. However this class of model generally lacks adequate consideration of overland flow and spatial viability of rainfall.

The second group is from meteorological fields. Current operational models are dominated by lumped or semi lumped models (Gupta et al. 2006), such as the Sacramento Soil Moisture Accounting Model (SAC-SMA; Burnash et al. 1973) and the empirically-based Continuous-API Model (CONT-API; Sittner *et al.* 1969) which is based on the Antecedent Precipitation Index (API; Kohler and Linsley 1951). The original meteorological river forecast models were developed based on the relationship between precipitation and stream flow and thus are called rainfall-runoff models. A shortcoming of these models is that they do not treat surface watershed characteristics and ground water hydrology in sufficient spatial details. It is interesting to note that despite a lack of detailed treatment of surface watershed characters, these lumped models may perform better than physically based distributed models for large watersheds (e.g. Reed et al. 2004; Karen et al. 2004; Kling and Gupta 2009) because it is often difficult to accurately describe large watersheds in distributed models.

The third group is the hydrological component of non-point source pollution models developed by the U. S. Department of Agriculture (USDA) and Environmental Protection Agency (EPA) to predict the pollution from overland. The most widely used models are the Annualized Agricultural Nonpoint Source Pollution Model (AnnAGNPS, previously AGNPS), the Soil and Water Assessment Tool (SWAT) developed by USDA, the Hydrologic Simulation Program - Fortran (HSPF), and the Better Assessment Science

Integrating point & Non-point Sources (BASINS) developed by EPA. These models are based on well developed structures to simulate watershed topology, surface land use, soil type, ground water and river channel flow, and are usually applied to small agricultural watersheds for the purpose of predicting non point source pollution. Distributed rainfall information can be incorporated into these models. Although small watersheds have been the target of application at the beginning of the model development, these models have been applied to large watersheds in recent years (e.g. Bhuyan et al. 2002a, b, 2003a, b). Sub-divided watersheds can be used to provide more detailed information as subwatershed. The total volume of water at the outlet of the entire watershed can then be obtained by summing up the outputs from multiple sub-watersheds.

The AnnAGNPS (Bingner et al. 2007) is selected in the study because it accounted for detailed surface topology, soil, land use, ground water hydrology and river channel flow. At the same time, up to 99 distributed rainfall stations can be accepted in the model. The GIS is used to manage the data processes. In this study, we will use the AnnAGNPS model with Muskingum routing method on a large coastal watershed to simulate inland flooding and the meteorological and hydrological processes associated with the flooding.

The rest of this chapter 2 is organized as follows. The second section is model description. In this section, the AnnAGNPS model, schematic diagram, water balance equation, SCS-CN method and subsurface flow are described. The third section is the description of study area, data and methods. The fourth section presents the results and discussion, followed by a summary and conclusion section.

2.2 Model Description

2.2.1 The AnnAGNPS Model

AnnAGNPS (Bingner et al. 2007) is a watershed hydrology and water quality model developed by the USDA. It is a batch process, continuous-simulation, surface-runoff, pollutant loading (PL) computer model written in standard ANSI Fortran 90. It simulates loadings of daily river discharge, peak runoff and non-point source pollutants (e.g., sediments, nutrients – nitrogen and phosphorus, herbicide and other variables). It has been widely applied in the United States and many other countries, such as Australia (Baginska et al. 2003), China (Hong et al. 2005), Germany (Grunwald and Norton 1999) and Canada (Das et al. 2006). Bhuyan et al. (2002a, 2002b, 2003a, 2003b) applied AnnAGNPS in a watershed in south central Kansas with a total area of 2404 km^2. They concluded that integrated modeling process was found to be effective for smaller watersheds that had adequate rainfall data. Perrone and Madramootoo (1997) determined the predictive capability of the AnnAGNPS model with respect to surface runoff, peak flow, and sediment yield produced by rainfall-runoff events on a 26 km^2 watershed in Quebec, Canada. They concluded that AnnAGNPS was reliable for surface runoff and sediment yield predictions, but generally over-predicted peak flow. Mostaghimi et al. (1997) found better agreement between simulated and observed runoff volumes than between simulated and observed peak flow rates, sediment or nutrient yields by AnnAGNPS.

AnnAGNPS operates on daily time step and uses the Soil Conservation Service Curve Number method (SCS-CN) to determine overland runoff (USDA-NRCS, 1986). The model

accounts for lateral subsurface and tile drainage (tile drainage is the drainage on agricultural cultivated land which is not considered here). Runoff in channels is calculated using Manning's equation (Polyakov et al. 2007).

2.2.2 Schematic diagram

The schematic diagram of AnnAGNPS model is shown in FIG 2.1. Digital elevation model data is processed in the GIS-based Flownet Generator to create cells and reaches (detailed in 3.c.) which then match with land use and soil type layers. Meteorological data was imported by assigned each weather station in their represented each Thiessen's polygons in the watershed. Then Thiessen's polygon was overlaid with cells so that each cell contains the assigned weather station. Other information such as groundwater level, soil hydrological characters and antecedent moisture condition (AMC) and correspondent curve number (CN) for each cell were manually imported into AnnAGNPS. The daily weather data was imported from 1989 – 2008 in this study in order to simulate hurricanes induced flooding within this period. For each targeted rainfall event, a three-year spin-up run was carried out to produce the initial soil moisture content. After completing the Input Editor, AnnAGNPS is then ready for calibration runs.

2.2.3 Water balance equation

The water budget equation used in AnnAGNPS model is presented by Bingner et al. (2007) in equation (1) that soil moisture change from time t to t+1 equals the sum of

precipitation, surface runoff, subsurface lateral flow, evapotranspirition and percolation. In AnnAGNPS, time interval is one day. For each individual cell, the water budget is represented by equation (1):

$$SM_{t+1} = SM_t + WI_t - Q_t - q_t - ET_t - PERC_t \quad (1)$$

where *SM* is soil moisture content (mm) for each soil layer, *WI* water input (mm), consisting of precipitation or snowmelt plus irrigation water, *Q* runoff (mm), *q* subsurface lateral flow and drainage, *ET* evapotranspiration (mm) (including evaporation and transpiration), and *PERC* percolation of water (mm) (including infiltration) out of each soil layer. Subscript t and t+1 indicate that the value are taken at the present and next time step. Water balance is computed for two soil layers. The first layer is the top 2 meters from the surface and is usually treated as the tillage layer. The second layer is from 2 meters to the impervious layer or user defined depth in a soil profile. In the computation, the soil moisture (SM) is considered to be valid for the beginning of a day. In the absence of actual initial soil moisture SM_t data (observations), simulated using soil moisture data from the previous three years is conducted to generate the initial soil moisture at the beginning of the time step. The runoff (Q_t) is determined using the Soil Conservation Service Curve Number method (SCS-CN) (USDA-SCS 1972). Evapotranspiration (ET_t) is calculated using the Penman equation (Bingner et al. 2007). Subsurface lateral flow and drainage (q_t) is computed by Darcy's equation (detailed in Section 2e). For the second soil layer, the water input (WI) is the percolation from the first layer (percolation is the downward drainage of soil water into lower

layers by gravity). The simulation of runoff (Q) is described in the next section with a initial value at zero.

2.2.4 SCS-CN method for surface runoff

The Natural Resources Conservation Service (NRCS) Soil Conservation Service Curve Number method (SCS-CN) (USDA-SCS 1972; Mishra and Singh 2003) has currently been heavily used in watershed models for estimation of direct runoff. This CN method is employed in watershed models such as SWAT (Soil and Water Assessment Tool) (Arnold et al. 1998) and AnnAGNPS (Bingner et al. 2007) as well as point/plot/field scale models such as GLEAMS (Groundwater Loading Effects of Agricultural Management Systems) (Leonard et al. 1987) and EPIC (Erosion Productivity Impact Calculator or Environmental Policy Integrated Climate) (Williams et al. 1984; Williams and Meinardus 2004). This popularity of the CN method is due to its easy application and a lack of suitable alternatives (Hjelmfelt 1991) although it has been questioned by Garen and Moore (2005) and discussed by Walter and Shaw (2005) for its weak physical basis since it funded on the empirical runoff relation of Mockus (1949) and soil vegetation land use complex of Andrews (1954). The advantages of this method includs its simplicity, predictability, stability, reliance on one parameter (CN), and responsiveness to major runoff-producing watershed properties (Ponce and Hawkins 1996). The SCS-CN method is based on the water balance equation and two fundamental hypotheses (Mishra and Singh 2003). The first hypothesis equates the ratio of the amount of direct surface runoff Q to the total rainfall P (or maximum potential surface to the runoff) with the ratio of the amount of infiltration F_c amount of the potential maximum retention S. The second to the

potential hypothesis relates the initial abstraction I_a maximum retention. Therefore, estimation of Curve Number (CN) becomes one of the most important focuses of researchers (Bhuyan et al. 2003a, b; Hjelmfelt 1991; Yuan 2000, 2006, 2008). The original SCS-CN equation (USDA-SCS 1972) is given as:

$$Q = \frac{(P - 0.2S)^2}{(P + 0.8S)} \tag{2}$$

$$S = 254\left[\frac{100}{CN} - 1\right] \tag{3}$$

where Q is direct runoff in mm, P is total rainfall in mm, S is potential retention in mm and CN is runoff curve number (dimensionless). Equations (2) and (3) are empirical equations that may be best used to transform a rainfall frequency distribution to a runoff frequency distribution. The CN varies from event to event, according to antecedent moisture condition (AMC), soil condition, land use type, etc. The AMC II value represents the central tendency while AMC I represents dry condition and AMC III represents wet condition. The variability of the curve number leads to difficulty in attempting to determine its value. Wet antecedent conditions are associated with high curve numbers. Dry antecedent conditions are associated with a wide spectrum of curve numbers. Apparently, other watershed and storm characteristics become important for factors affecting the value of CN under dry conditions (Hjelmfelt 1991).

2.2.5 Subsurface flow

Subsurface lateral flow and drainage components are developed within AnnAGNPS by Yuan et al. (2006) to more effectively evaluate the impact of management practices for

watersheds that produce a significant amount of subsurface flow. Subsurface lateral flow is determined using Darcy's equation and assuming steady state condition.

$$q_{lat} = -K_s \frac{dh}{dx}$$

where q_{lat} = subsurface lateral flow (mm per time step); K_s = saturated lateral hydraulic conductivity for each soil layer (mm per time step); *dh/dx* = hydraulic gradient (non-dimensional). It represents the slope of water table or aquifer; *h* = hydraulic head (mm). The accuracy of this method relies on the accuracy of the K_s estimates. Sources of uncertainty in K_s estimation include the uncertainties related to the measurement of hydraulic conductivity, the applicability of data at the field scale as opposed to the laboratory scale, and the spatial variability in K_s. In addition, because K_s is strongly dependent on ambient soil moisture content, uncertainty exists because of the nonlinear relation between K_s and ambient soil moisture content (Coes et al. 2007). The hydraulic gradient *dh/dx* is approximated by the local surface topographic slope (Yuan et al. 2006).

2.3 Description of study area, data and methods

2.3.1 Study Area

The Tar-Pamlico River Basin (FIG 2.2) is selected for this study because it covers a large area reaching the east coast and has experienced frequent severe inland floodings due to tropical cyclones such as Bertha (1996), Fran (1996), Floyd (1999) and Isabel (2003). Hurricane Floyd created a 500-year flooding in the Tar Pamlico River Basin and caused 57

human deaths. Tar Pamlico River Basin is one of the watersheds located entirely within the state of North Carolina. With a total area of 14,089 square kilometers, it is the fourth largest river basin in the state (NCDWQ 2004). The basin encompasses all or part of 16 counties and 51 municipalities. A sub-area was selected for the upper reaches of the Tar-Pamlico River Basin located above the USGS gage station at Tarboro. The watershed area with its outlet at Tarboro covers an area of 5605 km^2. This subwatershed is used to calibrate the model. This study area was further divided into seven subwatersheds as depicted in FIG 2.3. The elevation of the study area varies from 7 to 240 meters above sea level. The land use types in the study area are dominated by forest and cropland. No large water body is present in the study area.

2.3.2 Data acquisition and automation

GIS provides advantages associated with the full utilization of spatially distributed data by automatically extracting digital terrain data to analyze hydrological processes (Chang et al. 2000). ArcView version 3.0 has been used to develop the interface for AnnAGNPS for its digital data ingestion, managing and processing. Digital data required to run the watershed model are available from several public sources. However, selecting the proper scale of the dataset is a difficult task. A dataset of small scale may not provide sufficient coverage to simulate a real world watershed, while a dataset of a large scale with good resolution to represent the real world, requires huge works, especially for large watersheds. Blöschl and Sivapalan (1995) proposed an optimal scale for different types of watershed. According to

their study, an optimal scale for the Tar-Pamlico River Basin is 1:250, 000 for Digital Elevation Model (DEM) with a resolution of 90m x 90m. The projection system of NAD 83 State Plane North Carolina FIPS_3200 was chosen so that all collected datasets could be projected or transformed into a single coordinate system.

2.3.3 Digital Elevation Model (DEM)

DEM data is processed by a set of Flownet generator modules of the AnnAGNPS to generate cell and stream network information, and to provide a link to the location where upland streams enter the channel and then routed downstream (Bingner et al. 2007). FIG 2.4 illustrates 1035 cells and 419 reaches (river channels) created in the study area according to the slope and aspect of the DEM data. Each cell can be treated as a sub-watershed with unique soil and land cover as well as other characteristics.

2.3.4 Soil data

There are two sources of soil data available: the Soil Survey Geographic (SSURGO) Database and the State Soil Geographic (STATSGO) Database. The SSURGO dataset is a set of digital soil survey data and generally has the most detailed level of soil geographic data developed by the National Cooperative Soil Survey. However, SSURGO data for Warren and Pitt counties were under development at the time of this study. It is also not practical to estimate soil data at the county level since the polygons of soil type varies from a few square feet to acres. Therefore, soil information in this study was extracted from the STATSGO

Database. The STATSGO dataset is a digital general soil association map of North Carolina developed by the National Cooperative Soil Survey. It consists of a broad based inventory of soils and nonsoil areas that occur in a repeatable pattern on the landscape and that can be cartographically shown at the scale mapped.

Since STATSGO represents more general data (some data are estimated) instead of real soil survey data, the data may not be appropriate for use in watershed models. To test the validity of using STATSGO for watershed models, Wang and Melesse (2006) compared the effects of using SSURGO and STATSGO in a small watershed in the SWAT model. Their results indicated that both did a good and comparable job of predicting the high stream flows, although SSURGO provided an overall better prediction of the discharges than STATSGO did. However, STATSGO predicted the low stream flows more accurately and had a slightly better performance during the validation period. Hence, it is comfortable to use STATSGO in our study. Sensitivity analyses for soil parameters such as soil saturated hydrological conductivity (see section 2.4.2) were also performed to adjust and correct the errors.

STATSGO provides general soil types. But a great deal of detailed soil profile information have to be calculated in the Map Unit Use File (MUUF) software (Baumer et al. 1994). STATSGO data were overlaid with cells created from Flownet generator module. TABLE 2.1 shows soil types in the study area. Soil identity of NC074 with major soil type of sand clay has the highest percentage (29%) in the watershed. Within NC074, CECIL soil is the major soil series with 17%. ROANOKE with major soil type of loam sand is the major soil series for both NC010 and NC027, representing 19% and 53%, respectively. Examples of the results from MUUF searches include up to 5 layer soil texture types, depth (up to 2.5

meters), organic matter, bulk density, saturated soil conductivities, rock fragments, clay ratio, silt ratio and sand ratio, very fine sand, fine sand, wilting point, etc.

2.3.5 Land cover

Land cover was extracted from the National Land Cover Database 2001 (http://seamless.usgs.gov) as TIF files. The TIF files were then converted to ArcGrid format. After being merged and projected to State Plane NAD83, the land cover data were reclassified and dissolved in GIS. Forest land (Tree) accounts for 67.8% of the total study area, followed by crop (22.5%), grass land (4.2%), built up area (2.8%) and wet area (2.6%).

2.3.6 Groundwater level and hydrogeological aquifers

Groundwater level in coastal areas is very important for watershed simulation since groundwater recharge to surface water when high groundwater level exists in some stations. Aquifer data in GIS format were downloaded from USGS website (http://water.usgs.gov/GIS/). FIG 2.5 depicts the aquifers and groundwater stations (data from North Carolina State Climate Office) in the study area. There are only three types of aquifers in the study area: igneous and metamorphic rock aquifers in the upper Tar-Pamlico River Basin, semiconsolidated sand aquifers in the lower Tar-Pamlico River Basin and a small portion of carbonate-rock aquifers.

Unlike climate stations, groundwater level data measured in well stations are not all in continuous time series format (only measured in a period of time). It is hard to represent

the entire study area. Data were manually input into each cell of the AnnAGNPS model based on the available well stations in the surroundings, elevation of each cell and distance from river.

2.3.7 Climate and weather data

The real time climate data are provided by the North Carolina State Climate Office at stations shown in FIG 2.6. However, not all stations have observation data from 1/1/1989 – 12/31/2008. Many of the stations only have the three required parameters, namely daily maximum temperature, daily minimum temperature and precipitation. Some stations only measure precipitation. Therefore, daily wind speed, dew point and solar radiation required in the AnnGNPS model are derived by the GEM model (The Generation of Weather Elements for Multiple applications program) and the Raleigh-Durham station is set as the referenced station. Details of the GEM model can be found in Johnson et al. (2000). GEM is a climate data generator that generates synthetic climatic data using 100 assigned weather stations in the United States. Since precipitation is the most important parameter in this research, real time precipitation dataset is used for all stations.

2.3.8 Muskingum channel routing

It should be pointed out that modeling hydrological process in a large coastal watershed such as the Tar-Pamlico River Basin during Tropical Cyclones (TCs) landfall is a challenging task due to the difficulties in quantifying the heavy precipitation and its spatial

and temporal distribution. Antecedent rainfall events and an extremely high degree of stream-aquifer interaction in the coastal watershed also complicate the modeling work. FIG 2.7 illustrates the interactions between major hydro-meteorological processes that affect the watershed hydrology of a coastal watershed. Large-scale atmospheric environment during hurricane landfall may increase the precipitation. Prior precipitation will increase soil moisture in the watershed, and strong winds from landfall hurricanes can create large storm surge over the coastal ocean which slows down the drainage. These processes create complex interactions that impact the watershed hydrological processes which contribute to coastal watershed flooding. The AnnAGNPS needed to be modified to include channel routing before it could be applied to a large watershed such as the Tar-Pamlico River Basin.

The Muskingum method has been widely applied in natural river/channel routing. Muskingum equation can be expressed as (Viessman and Lewis 1996):

$$O_2 = C_0 I_2 + C_1 I_1 + C_2 O_1$$

where I is the inflow rate to the reach and O is the outflow rate from the reach while subscripts 1 and 2 denote the beginning and ending times of Δt . C_0, C_1 and C_2 can be calculated by:

$$C_0 = \frac{-KX + 0.5\Delta t}{K - KX + 0.5\Delta t}$$

$$C_1 = \frac{KX + 0.5\Delta t}{K - KX + 0.5\Delta t}$$

$$C_2 = \frac{K - KX - 0.5\Delta t}{K - KX + 0.5\Delta t}$$

where K is the storage time constant for the reach and can be estimated by reach length (L) divided by average velocity of the flood wave (V_W). Average velocity (V_W) can be obtained from river discharge divided by area of river cross section. X is a weighting factor that varies between 0 and 0.5 (averaged about 0.2).

2.3.9 Study procedure

First, scale analysis was carried to find the most important parameters in the water balance equation. Second, sensitivity analysis was performed to quantify model uncertainties and determine the appropriate range of model, including the curve number, soil hydrological conductivity and other related parameters. Third, AnnAGNPS model was then calibrated by running historical hurricane cases and compared them to the measured stream flow data. Hurricanes ranging from heavy, middle and light rainfall events, such as hurricane Bertha (1996), Fran (1996), Floyd (1999), Isabel (2003) and Hanna (2008) are selected (see Fig 2.10). Finally, after calibration, the special case of the hurricane Floyd was studied.

2.4 Results and discussion

2.4.1 Scale analysis for water balance equation at Tar-Pamlico River Basin

Scale analysis, or scaling, is a convenient technique for estimating the magnitudes of various terms in the governing equations for a particular type phenomenon. In scaling, typical expected values of the following quantities are specified: 1) magnitudes of the field

variables; 2) amplitudes of fluctuations in the field variables; and 3) the characteristic length, depth, and time scales on which these fluctuations occur. These typical values are then used to compare the magnitudes of various terms in the governing equations (Holton 2004). Scale analysis of water balance equation (1) (detailed in 2.2.3) in a unit area of Tar-Pamlico River Basin has been performed and the results (TABLE 2.2) are described below and the time period is about 5 – 7 days during a hurricane landfall event.

SM_{t+1}-SM_t (soil moisture content changes in mm): during a hurricane event followed with heavy precipitation, soil moisture can be saturated within a very short period. The time needed to reach saturated soil moisture varies from a few minutes to a few hours, depending on types of soils and intensity of the precipitation. Once soil is saturated, this term will not change. The magnitude of this term is relatively small (from 0 to 1) and can be neglected when saturated.

WI_t (precipitation in unit area, irrigation and snow melt not considered here): in last 20 years, the maximum daily precipitation of 280 mm (11 inches) in the study area occurred on September 16, 1999 during Hurricane Floyd's landfall. So the scale of precipitation can be set to 0 - 10^2 mm for this event.

Q_t (runoff in mm in unit area): although a 500-year storm event of Hurricane Floyd created high daily precipitation of 280 mm on September 16, 1999, runoff at USGS station 02083500 only created 30 mm/day per unit area. However, this amount of runoff continuously flowed for several days and the total event runoff has almost 200 mm per unit area. So the scale of

runoff is 10^1 mm on daily scale and can be cumulated to 10^2 mm for a hurricane event such as Floyd.

q_t (subsurface lateral flow and drainage): q_t is hard to measure and no real time observation is available. Subsurface lateral flow can be estimated through delaying runoff at the outlet of the Basin. The magnitude of this term can be comparable to surface runoff. Due to flatness of the Tar-Pamlico River Basin, the scale of this item is estimated at 10^1 mm. However, during a hurricane event, this term can be as high as 10^2 mm as it contributes to direct surface runoff. This value is combined with surface runoff (Q_t).

ET_t (evapotranspiration rate in mm): annual evapotranspiration in the US is about 40-60% of annual precipitation. During the short period of a hurricane event, it can be very small due to heavy rainfall and high humidity in the atmosphere. According to the historical evapotranspiration record, highest evapotranspiration is around 36 mm/day (May 27, 2005 at Upper Coastal Plain Research Station, Edgecombe county) in recent 20 years. So the scale of this term can be set to 0 - 10^1 mm during a hurricane event.

$PERC_t$ (percolation in unit of time as infiltration rate in mm/day): the magnitude of $PERC_t$ depends on different soil conditions. It ranges from 1 mm/hr in clay to 30 mm/hr in sand. It also depends on soil moisture condition. The higher the soil moisture content, the slower the infiltration rate will be. During a hurricane event, soil moisture content is very high after rainfall. The scale of 0 - 10^1 mm/day has been used.

From the scale analysis, it is obvious that precipitation, surface runoff, subsurface lateral and drainage flow have the magnitude of 10^2. Therefore they are more important than soil moisture change and evapotranspiration during a hurricane event. Therefore, sensitivity analysis will focus on these three terms.

2.4.2 Sensitivity of soil conductivity

Subsurface flow and groundwater recharge are especially important in the coastal area compared to mid-west US such as in the previous study of Kansas (Tang 2002) due to the humid climate, high soil moisture contents during hurricanes and high groundwater level. Increases of humid climate, dense vegetation, permeable soil and steep, subsurface stormflow dominate the hydrograph volumetrically. Coes et al. (2007) estimated mean historical annual groundwater recharge rate at three sites in the North Carolina Coastal Plain. Their results indicated that recharge rates are high, > 50% of rainfall if groundwater tables are high at these sites ranging from 0 – 3.1 meters below surface. In the study area, peak flow results more from groundwater return flow than from direct surface runoff due to precipitation.

Initial saturated hydraulic conductivity K_s in the watershed for the AnnAGNPS model is calculated from MUUF by STATSGO. Therefore, model sensitivity to K_s is performed. FIG 2.8 presents the sensitivity analysis of the relation between base flow and K_s value. At low K_s values (<=15 m/day), base flow sharply increases with K_s. These K_s values occur in most common soil types. High K_s value (> 15 m/day) will not vary much of base flow. FIG 2.9 gives the highest daily runoff during a hurricane event (such as Hurricane Floyd). Peak

runoff decreases when the K_s value increases. Before K_s reaches 15 mm/day, peak runoff drops rapidly as K_s increases. After the K_s becomes greater than 15, peak runoff drops slightly. This is because when soil saturated conductivity increases at beginning, base flow then increases quickly. When the soil saturated conductivity reach to certain point, the base flow could not increase any more. The same situation is applied to peak runoff. Therefore, Ks of 15 mm/day is the turning point. Therefore, both surface runoff and base flow is very sensitive to Ks. Careful selection of proper Ks is crucial to watershed modeling.

2.4.3 Calibration

FIG 2.10 is the correlation between model simulated and USGS measured total runoffs for hurricanes Bertha (1996), Fran (1996), Floyd (1999), Isabel (2003) and Hanna (2008). Different color points represent different hurricane events. Floyd has to be choosen because it is once in 500 hundreds years flooding events. Without this event, the higher runoff value would not be existed. The linear relationship with R squared score of 0.867 indicates that there is a good agreement between simulated total runoff at outlets and those measured by USGS gages. The confidence level is 99%.

2.4.4 Hydrological response to heavy precipitation in the Tar-Pamlico River Basin

Hydrological response to heavy precipitation in the Tar-Pamlico River Basin depends on topographic conditions, soil texture, channel flow, subsurface flow, etc. To better evaluate the effected characteristics of the Tar-Pamlico River Basin on watershed hydrology, seven

sub-basins were defined where each outlet of a sub-basin contains a USGS water monitoring station so that comparisons of model output with measured runoff can be performed. FIG 2.11 depicts daily river discharges at USGS gage stations in September 1999 in the study area. Please see FIG 2.3 for distribution of these gage stations. The top axis presents daily precipitation at Wilson 3 SW station (see FIG 2.6 for location). This figure indicates that the highest stream flow discharge often delayed several days after the heavy rainfall. Such as the highest discharge is on 19th while highest precipitation is on 16th which is three days differences at USGS station 02083500 (Tarboro). FIG 2.12 quantifies the relationship between sub-watershed drainage area and the highest discharge delaying days after the peak precipitation. At the upper Tar-Pamlico Basin of gage station 02081500, the highest surface runoff occurred on the same day as the highest rainfall event. For gage stations farther downstream, which corresponds to a larger drainage area, the highest discharge happens 1-5 days after the highest rainfall. At the study outlet gage station 02083500 (Tarboro), the highest discharge occurs 3 days after the heaviest rainfall. This is perhaps because a) Tar-Pamlico River Basin is dominated by sandy, sandy loam and sandy clay soil (TABLE 2.1) with high infiltration rates; b) Tar-Pamlico River Basin is a very flat area where surface runoff moves slowly from the top of the Basin to the outlet. c) Subsurface flow and groundwater recharge would also play an important role in this basin. More detailed studies are needed to test these hypotheses.

2.4.5 Distribution of precipitation

Precipitation is one of the most important parameters in the model as shown by the scale analysis in Section 2.4.1. The Tar-Pamlico River Basin covers a relatively large area. The variation of spatial distribution of precipitation during hurricane events is large. As demonstrated in FIG 2.13 (Palmer 2008), precipitation tapered off from east to west during Hurricane Floyd. From east coast to higher elevation to the west in the Piedmont area, both cumulated precipitation during the period of September 13-17 and single daily precipitation on September 16, 1999 showed a decreasing trend.

Two different climate data sets were tested in the study. The distribution of the first eight climate stations is shown in FIG 2.6. The simulation of total runoff during Hurricane Floyd demonstrates that at the two upper Tar-Pamlico stations 02081500 and 0208 1747, stream flow rates are underestimated (FIG 2.15). There is a large difference between simulated and measured runoffs at Station 02082950. This is due to USGS data were estimated and it was found that the value was overestimated from the analysis of distribution of precipitation and area covered by the station. However, it will not affect the total area at the downstream outlet of station 02083500. Another set of climate data was provided by the North Carolina State Climate Office recently. Since there are many missing values at these stations, data are not regularly published. After data quality control processes and interpolation, the precipitation data can be very useful for our model simulation during tropical cyclone landfall. Locations of these stations are shown in FIG 2.14. FIG 2.16 is a comparison chart by AnnAGNPS using both the first and second climate data set with USGS

gauged data. The results indicate that the second climate data set improved simulated runoff at the upper Tar-Pamlico stations (02081500 and 02081747).

2.4.6 Simulation of hydrograph for TC events

It has been shown in the sensitivity analysis that total runoff for TC events can be well simulated by AnnAGNPS as long as accurate precipitation data are provided.

To create accurate hydrographs for the hurricane events, the Muskingum method (e.g. Gill 1978; Kshirsagar et al. 1995; Methods et al. 2003) was applied in the river/channel routing in seven subwatersheds. FIG 2.17 shows that the simulated hydrograph compared reasonably with the USGS measured data. It is clear that simulation results for the upper Tar at stations 02081500 and 02081747 are more accurate than those for the lower Tar at station 02083500 where runoff peak is 3 to 5 days after the peak rainfall.

2.4.7 Impacts of pre-existing TCs

Hurricane Floyd made landfall and passed the East Coast of the United States from Sept. 14 – 17, 1999. Torrential rains fell from the Carolinas to New England, resulting in massive flooding in major rivers and surrounding areas.

Hurricane Floyd produced large amount of precipitation. On top of that, soil moisture content and groundwater levels were both very high before the arrival of Hurricane Floyd due to the previous landfall of Hurricane Dennis on Sept 5, 1999. According to historical groundwater records, groundwater level at station N22Y1 (see FIG 2.5 for location) in the

lower Tar-Pamlico near the outlet of the watershed was merely 0.05 (m) below the surface on Sept. 10, 1999. That was just 5 days before Hurricane Floyd's landfall at 0630 UTC/GMT (Coordinated Universal Time, also referred to as Greenwich Mean Time corresponding to 2:30 am Eastern Daylight Time) on Sept. 16, 1999. In other words, before Hurricane Floyd's landfall, the groundwater recharge at the outlet of the Tar-Pamlico River Basin almost reached the surface. Thus, any additional precipitation after Hurricane Dennis would likely cause flooding.

In order to estimate the impacts of the preceding TC, simulations were conducted for the following scenario: 1) both Dennis and Floyd, 2) Floyd only, and 3) Dennis only (FIG 2.18). The results of the simulation indicate that without Hurricane Dennis the discharge would have been as much as 37% lower than the actual event at gage station 02083500 (Tarboro).

Once the total amount of surface runoff is calculated from the AnnAGNPS model, flood area can be simulated using the software MicroDEM (available at http://www.usna.edu/Users/oceano/pguth/website/microdem/microdem.htm). With these advanced techniques, it is easy to generate flood maps once the water level at the gage site is known, as demonstrated in FIG 2.19.

2.5 Summary and Conclusions

In summary, AnnAGNPS has been applied to simulate the hydrological processes in a large coastal watershed area in the event of TC induced inland flooding and the results are summarized below:

a. For the large watershed of Tar-Pamlico River Basin with a total area of 5605 km^2, AnnAGNPS can be used to simulate the total streamflow in the event of TC induced inland flooding. Channel routing must be incorporated into the mdoel in order to simulate the hydrograph. This is the first attempt of such to use AnnAGNPS to simulate hydrological processes in a large coastal watershed in the event of TC induced inland flooding. The study indicated that the upper small sub-watersheds at stations 02081500 and 02081747 are better than larger sub-watershed such as stations 02082770 and 02082950. But overall, it still provides good hydrographs.

b. Scale analysis indicates that the important parameters affecting watershed flooding are precipitation, surface runoff and subsurface flow.

c. The sensitivity analysis and calibration through TCs of Bertha (1996), Fran (1996), Floyd (1999), Isabel (2003) and Hanna (2008) indicate that the AnnAGNPS model can be reliably used to simulate event total runoff.

d. Sensitivity analysis of soil saturated hydrological conductivity K_s indicates that peak runoff at gages exponentially decreases as K_s increases and base flow increases as K_s increases at lower level of K_s value (0 – 15 m/day) while base flow slightly decreases when K_s value increases at higher level of K_s value (> 15 m/day). This is because

when soil saturated conductivity increases at beginning, base flow then increases quickly. When the soil saturated conductivity reach to certain point, the base flow could not increase any more. The same situation is applied to peak runoff. Therefore, Ks of 15 mm/day is the turning point.

e. Previous TC or precipitation could saturate the soil of the watershed so that additional landfalling TC would more easily causes flooding. In the case of Hurricane Dennis which immediately preceded Hurricane Floyd, total runoff caused by Hurricane Floyd at the outlet without Hurricane Dennis would have been as much as 37% lower than the actual observations.

The severe flooding in the coastal watershed is caused by the interaction of antecedent precipitation, large scale atmospheric environment and hurricane induced precipitation, watershed hydrological response and storm surge as indicated in Fig. 2.7. This study focuses such a role of precipitation and hydrological characteristics of the watershed on stream flow. The impact of large scale environmental to watershed hydrology will be studied in the next chapter.

REFERENCES

Abbott, M.B., J. C. Bathurst, J. A. Cunge, P. E. O'Connell and J. Rasmussen, 1986a: An introduction to European hydrological system - system hydrologique Europeen, 'SHE', 1 history and philosophy of a physically-based distributed modeling system. *J. of Hydrol*, **87**, 45-59.

Abbott, M.B., J. C. Bathurst, J. A. Cunge, P. E. O'Connell and J. Rasmussen, 1986a: An introduction to European hydrological system - system hydrologique Europeen, 'SHE', 2 Structure of a physically-based distributed modeling system. *J. of Hydrol*, **87**, 61-77.

Arnold, J. G., R. Srinivasan, R. S. Muttiah, and J. R. Williams, 1998: Large area hydrologic modeling and assessment – Part I: Model development. *J. Amer. Water Resour. Assoc*., **34**, 73-89.

Baginska, B., W. Milne‐Home, and P. S. Cornish, 2003: Modelling nutrient transport in Currency Creek, NSW, with AnnAGNPS and PEST. *J. Environ. Modelling and Software*, **18**, 801-808.

Baumer, O., P. Kenyon and J. Bettis, 1994: MUUF v2.14 User's Manual. USDA Natural Resource Conservation Service, Lincoln, Nebraska.

Beven, K. J. and Kirkby, M. J. 1979: A physically based variable contributing area model of catchment hydrology, *Hydrol. Sci. Bull.*, **24**, 43-69.

Bhuyan, S. J., P. K. Kalita, K. Janssen, P. L. Barnes, 2002a: Soil loss redictions with three erosion simulation models. *J. Environ. Modeling and Software*, **17**, 137-146.

——, L. Marzen, J. K. Koelliker, J. A. Harrington, 2002b: Assessment of runoff and sediment yield using remote sensing, GIS, and AGNPS. *J. Soil and Water Conserv.*, **57**, 351–364.

——, K. R. Mankin and J. K. Koelliker, 2003a: Watershed-scale AMC selection for hydrologic modeling. *Trans. ASAE*, **46,** 303-310.

——, J. K. Koelliker, L. J. Marzen and J. A. Harrington, 2003b: An integrated approach for water quality assessment of a Kansas watershed. *J. Environ. Modelling and Software* **18**, 473-484.

Bingner, R. L., F. D. Theurer and Y. Yuan, 2007: AnnAGNPS technical processes. Version 4.0. USDA-ARS documentation.

Blöschl, G. and M. Sivapalan, 1995: Scale issues in hydrological modelling: A review. *Hydrol Processes*. **9,** 251-290.

Burnash, R.J.C., R. L. Ferral, and R. A. McGuire, 1973: A generalized streamflow simulation system—Conceptual modeling for digital computers. Joint Federal–State River Forecast Center Tech. Rep., Department of Water Resources, State of California and National Weather Service, 204 pp.

Castro, C. L., A. B. Beltran-Przekurat and R. A. Pielke Sr. , 2009: Spatiotemporal variability of precipitation, modeled soil moisture, and vegetation greenness in North America within the recent observational record. *J. Hydrometeor*., **10,** 1355-1378.

Chang, T. J., M. H. Hsu, W. H. Teng and C. J. Huang, 2000: A GIS-assisted distributed watershed model for simulating flooding and inundation. *J. Amer. Water Resour. Assoc*., **36**, 975-988.

Coes, A. L., T. B. Spruill and M. J. Thomasson, 2007: Multiple-method estimation of recharge rate at diverse locations in the North Carolina Coastal Plain, USA. *Hydrogeol J.*, **15**, 773–788.

Das, S., R. P. Rudra, P. K. Goel, B. Gharabaghi, and N. Gupta, 2006: Evaluation of AnnAGNPS in cold and temperate regions. *Water Sci. Tech.*, **53**, 263-270.

Garen, D. C. and D. S. Moore, 2005: Curve number hydrology in water quality modeling: uses, abuses, and future directions. *J. Amer. Water Resour. Assoc*., **41**, 377-388.

Gill, M. A., 1978: Flood routing by the Muskingum method. *J. Hydrol.,* **36**, 353-363.

Grunwald, S. and L. D. Norton, 1999: An AGNPS-based runoff and sediment yield model for two small watersheds in Germany. *Trans. ASAE.,* **42**, 1723-1731.

Gupta, H.V., S. Sorooshian, T. Wagener, T. S. Hogue, D. Goodrich, G. Sampson, M. Schaffner and E. Bersack, 2006: Development of a Site-Specific Flash Flood Forecasting Model for the Western Region. Final Report to NWSHRL, NOAA, Silver Spring, MD.

Hilderbrand, D. C., 2002: Risk Assessment of North Carolina Tropical Cyclones (1925 – 2000). North Carolina State University. MS thesis.

Hjelmfelt, A. T., 1991: Investigation of curve number procedure. *J. Hydraulic Eng*., **117**, 725-737.

Holton, J. R. 2004: An introduction to Dynamic Meteorology. Elsevier Academic Press, 535 pp.

Hong, H. S., J. L. Huang, L. P. Zhang, and P. F. Du. 2005: Modelling pollutant loads and management alternatives in Jiulong River watershed with AnnAGNPS. *Huan Jing Ke Xue*, **26**, 63-69.

Johnson, G. L., C. Daly, G. H. Taylor and C. L. Hanson, 2000: Spatial variability and interpolation of stochastic weather simulation model parameters. *J. Appl. Meteor*. **39**, 778-796.

Karen, V., S. Reed, M. Smith, Z. Zhang, and D.-J. Seo, 2004: Hydrology Laboratory Research Modeling System (HL-RMS) of the National Weather Service. *J. Hydrol.*, **291,** 297–318.

Kling, H. and H. Gupta, 2009: On the development of regionalization relationships for lumped watershed models: The impact of ignoring sub-basin scale variability. *J. Hydrol.*, **373**, 337–351

Kohler, M. A. and R. K. Linsley, 1951. Predicting Runoff From Storm Rainfall. U.S. Weather Bureau, Research Paper 34.

Kshirsagar, M. M., B. Rajagopalan and U. Lall, 1995: Optimal parameter estimation for Muskingum routing with ungauged lateral inflow. *J. Hydrol.*, **169**, 25-35.

Leonard, R. A., W. G. Knisel and D. A. Still, 1987: GLEAMS - Groundwater loading effects of agricultural management systems. *Trans. ASAE,* **30**, 1403-1418.

Methods, H., G. Dyhouse, J. Hatchett and J. Benn, 2003: *Floodplain Modeling Using HEC-RAS.* 1st ed. Haestad Press, 581 pp.

Migliaccio, K. W. and P. Srivastava, 2007: Hydrologic components of watershed-scale models. *Trans. ASABE,* **50**, 1695-1703.

Miller, S. N., D. P. Guertin and D. C. Goodrich, 2007: Hydrologic modeling uncertainty resulting from land cover misclassification. *J. Amer. Water Resour. Assoc*., **43**, 1065-1075.

Mishra, S. K. and V. P. Singh, 2003: Soil Conservation Service Curve Number (SCS-CN) Methodology. Kluwer Academic Publishers, Netherlands.

Mockus, V. 1949: Estimation of total (peak rates of) surface runoff for individual storms. Exhibit A of Appendix B, Interim Survey Report Grand (Neosho) River Watershed, U.S. Department of Agriculture., Dec. 1.

Mostaghimi, S., S. W. Park, R. A. Cooke and S. Y. Wang, 1997: Assessment of management alternatives on a small agricultural watershed. *Wat. Res.*, **31,** 1867-1878.

NCDWQ, 2004: Basinwide planning program: 2004 Tar-Pamlico River Basinwide water quality plan. North Carolina Division of Water Quality website: http://h2o.enr.state.nc.us/basinwide/tarpam_draft_dec2003.html

Opitz, H. H., S. G. Summer, D. A. Wert, W. R. Snyder, R. J. Kane, R. H. Brady, P. M. Stokols, S. C. Kuhl and G. M. Carter, 1995: The challenge of forecasting heavy rain and flooding throughout the eastern region of the National Weather Service. Part II: forecast techniques and applications: *Wea. Forecasting*, **10**, 91-104.

Palmer, J. M. 2008: Geostatistical modeling of subclimatic tropical precipitation in the Carolinas. North Carolina State University. MS thesis.

Perrone, J. and C. A. Madramootoo, 1997: Use of AGNPS for watershed modeling in Quebec. *Trans. ASAE*, **40**, 1349-1354.

Polyakov, V., A. Fares, D. Kubo, J. Jacobi and C. Smith, 2007: Evaluation of a non-point source pollution model, AnnAGNPS, in a tropical watershed. *Environ. Modelling Software*, **22,** 1617-1627.

Ponce, V. M. and R. H. Hawkins, 1996: Runoff curve number: has it reached maturity? *J. Hydrol. Engineer.*, **1,** 11-19.

Reed, S., V. Koren, M. Smith, Z. Zhang, F. Moreda, D.-J. Seo, and DMIP Participants, 2004: Overall Distributed Model Intercomparison Project results. *J. Hydrol.,* **298,** 27–60.

Sittner, W., C. Schauss, and J. Monro, 1969: Continuous Hydrograph Synthesis with an API-Type Hydrologic Model. *Water Resources Research,* **5**, 1007-1022.

Steward, M., J. Cimino and M. Ross, 2007: Calibration of base flow separation methods with streamflow conductivity. *Ground Water,* **45**, 17-27.

Tang, Q., 2002: Water Quality Modeling in Black Vermillion Watershed with AGNPS 2001. MS thesis, Kansas State University.

USDA-NRCS, 1986: Urban hydrology for small watersheds, TR-55. [Available online at http://www.nrcs.usda.gov.]

USDA-SCS (U.S. Department of Agriculture-Soil Conservation Service), 1972: SCS National Engineering Handbook, Section 4, Hydrology. Chapter 10, Estimation of Direct Runoff From Storm Rainfall. *U.S. Department of Agriculture, Soil Conservation Service,* Washington, D.C., 10.1-10.24 pp.

Viessman W. and G. L. Lewis, 1996: Introduction to hydrology. 4th edition. HarperCollins College Publishers, 235pp.

Walter, M. T. and S. B. Shaw, 2005: Discussion: "Curve Number Hydrology in Water Quality Modeling: Uses, Abuses, and Future Directions," by David C. Garen and Daniel S. Moore. *J. Amer. Water Resour. Assoc.*, **41**, 1491-1492.

Wang, X. and A. M. Melesse, 2006: Effects of STATSGO and SSURGO as inputs on SWAT model's snowmelt simulation. *J. Amer. Water Resour. Assoc.*, **40**, 1217-1236.

Williams, J. and A. Meinardus, 2004: EPIC. [Available online at http://www.brc.tamus.edu/epic.]

Williams, J. R., C. A. Jones and P. T. Dyke, 1984: A Modeling Approach to Determining the Relationship Between Erosion and Soil Productivity. *Trans. the ASAE*, **27**, 129-144.

Yuan, Y., 2000: Tile-drained Watershed SCS-curve Number Model. Ph.D. dissertation, University of Illinois at Urbana-Champaign, United States -- Illinois. Retrieved December 8, 2008, from Dissertations & Theses: A&I database. (Publication No. AAT 9955685).

——, R. L. Bingner and F. D. Theurer, 2006: Subsurface flow component for AnnAGNPS. *Appl. Eng. Agric.*, **22**, 231-241.

——, M. A. Locke and R. L. Bingner, 2008: Annualized Agricultural Non-Point Source model application for Mississippi Delta Beasley Lake watershed conservation practices assessment. *J. Soil and Water Conserv.*, **63**, 542-551.

Zhu, Y. and R. L. Day, 2009: Regression modeling of streamflow, baseflow, and runoff using geographic information systems. *J. Environ. Manag.*, **90**, 946-953

TABLE 2.1 Soil Types in the study area.

SOIL_ID	Representative Soil Series	Component Percentage	Area (km^2)	% of Total Area	Major soil types
NC003	CHEWACLA	34	53	0.9	Silt loam, silt clay
NC010	ROANOKE	19	238	4.2	Loam sand
NC027	ROANOKE	53	97	1.7	Loam sand
NC034	RAINS	29	152	2.7	Silt
NC035	NORFOLK	34	945	16.9	Loam sand
NC038	AUTRYVILLE	21	713	12.7	Sand, sand clay
NC057	WHITE STORE	15	49	0.9	Silt loam, clay
NC061	HERNDON	16	439	7.8	Silt loam, silt clay
NC068	WEDOWEE	30	689	12.3	Sand loam, loam
NC074	CECIL	17	1,625	29.0	Sand clay
NC075	PACOLET	14	309	5.5	Fine sandy loam
NC083	ENON	22	245	4.4	Fine sandy loam
NC086	IREDELL	17	21	0.4	Loam
NC087	WILKES	22	30	0.5	Fine sandy loam
TOTAL			5605	100.0	

TABLE 2.2 Scale analysis of water balance equation in a unit area of Tar-Pamlico River Basin.

	SM_{t+1}-SM_t	WI_t	Q_t	q_t	ET_t	$PERC_t$
Hurricane Event scale (mm)	10^0	10^2	10^2	10^2	10^1	10^1

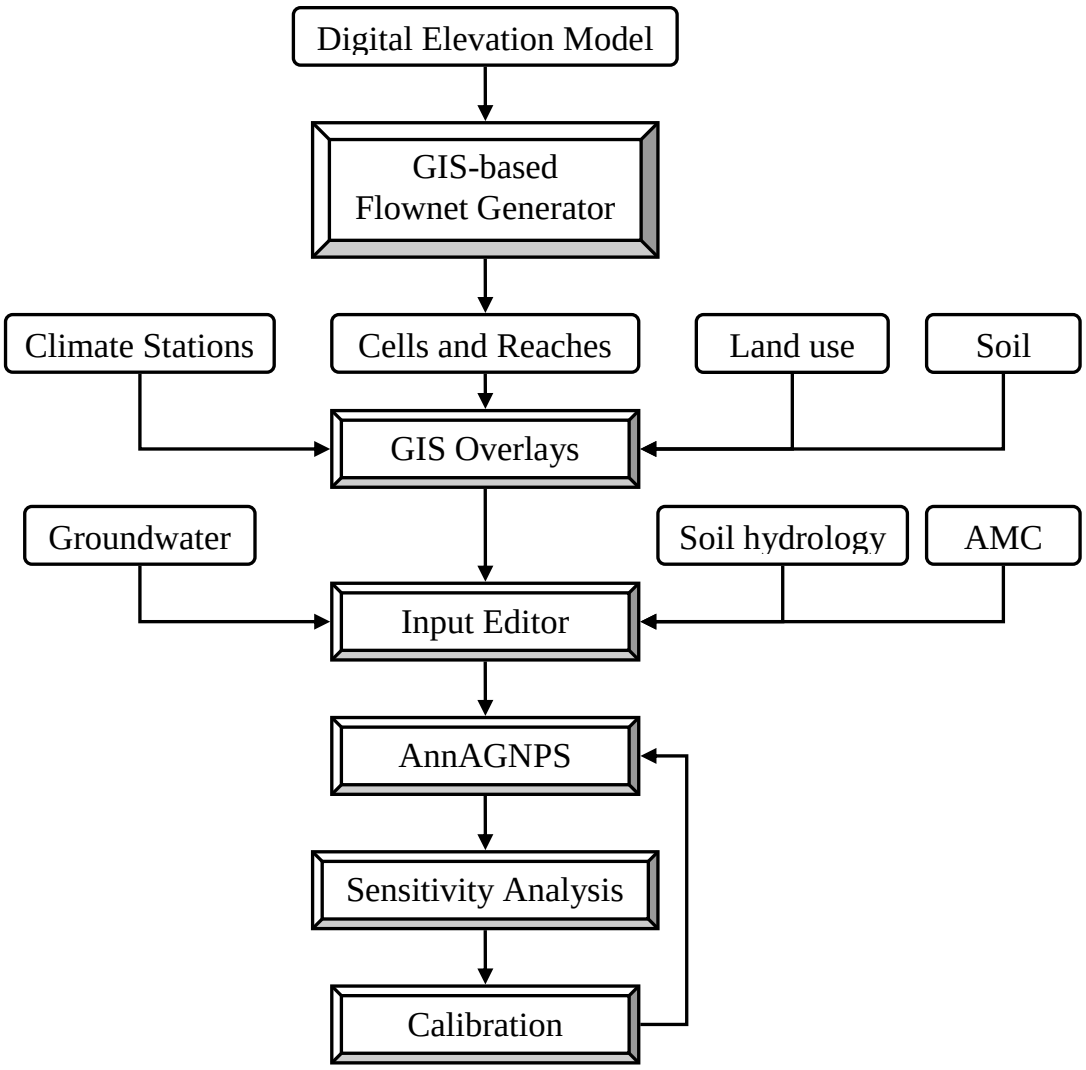

FIG 2.1 Schematic Diagram for AnnAGNPS.

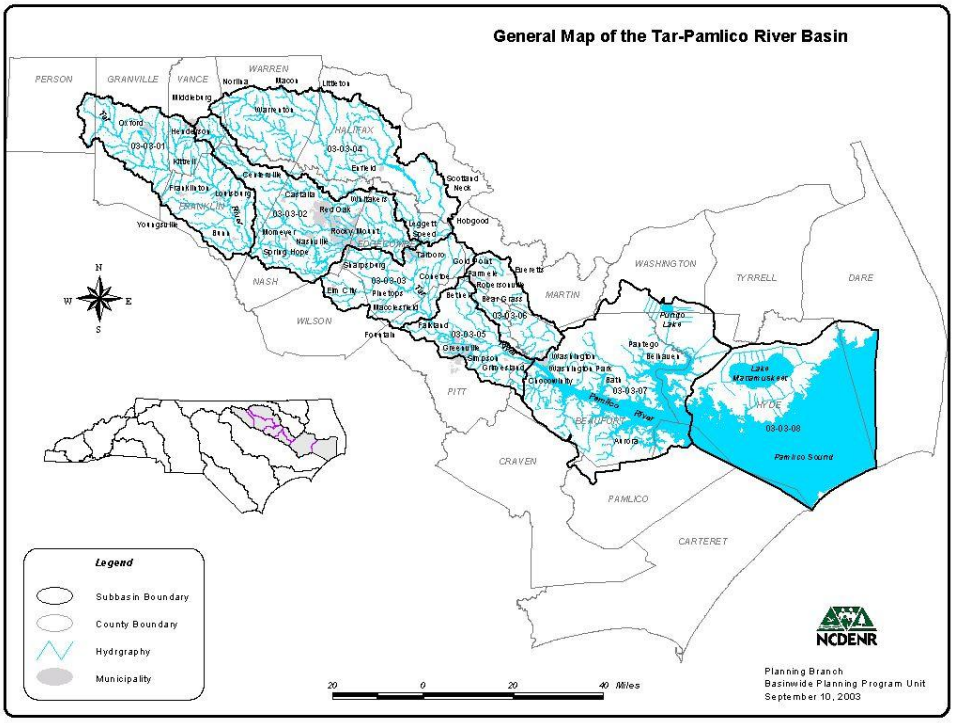

FIG 2.2 The study area – Tar-Pamlico River Basin (From NCDENR).

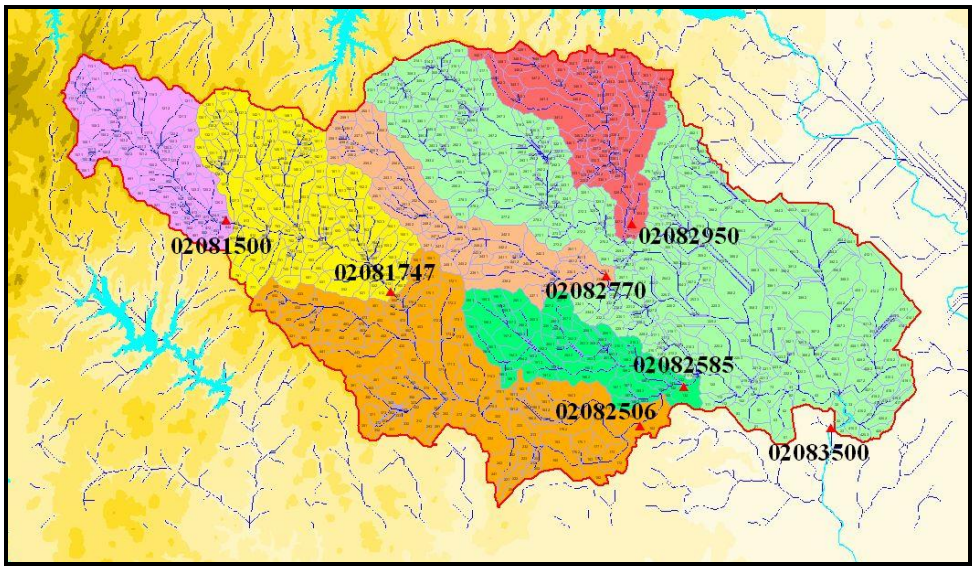

FIG 2.3 USGS streamflow gages (triangle points) and corresponding areas in AnnAGNPS in Tar-Pamlico River Basin (Each downstream gage area covers all upper gage areas).

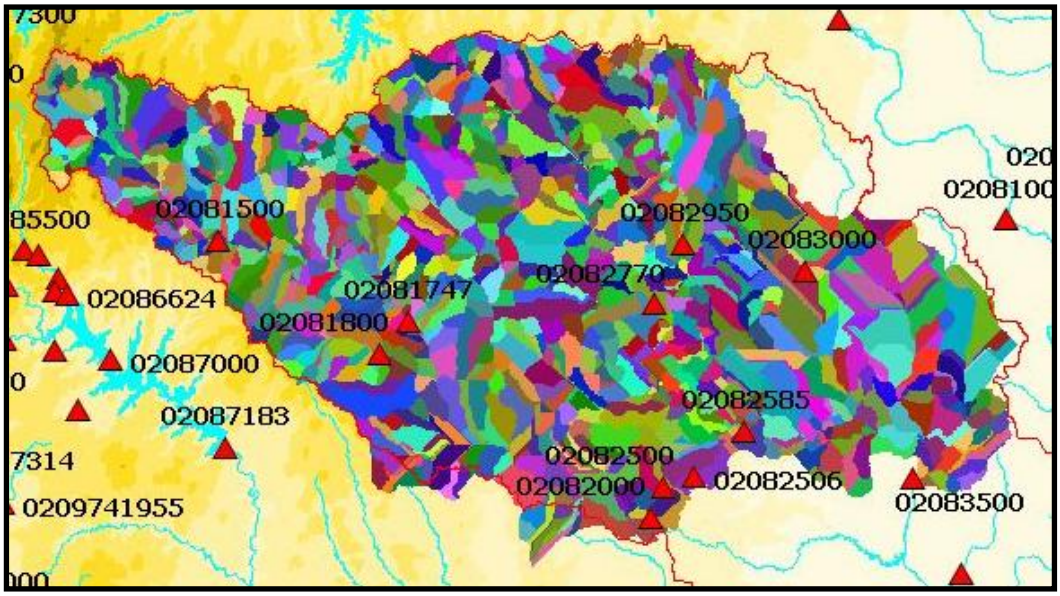

FIG 2.4 DEM created cells (1035 cells created).

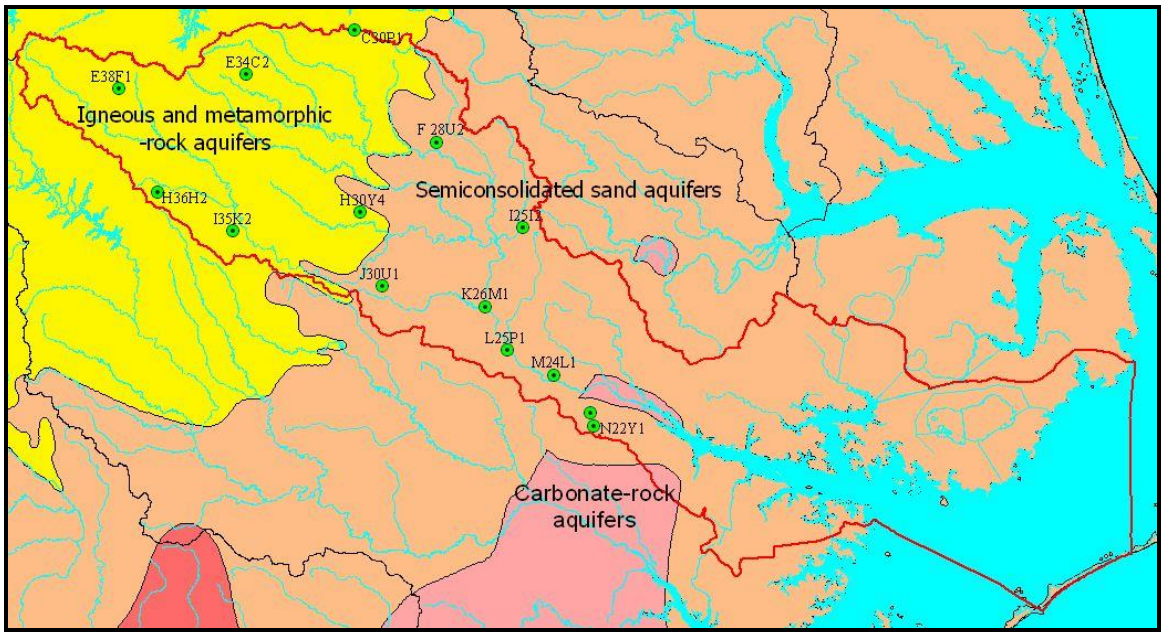

FIG 2.5 Groundwater stations and aquifers in the study area.

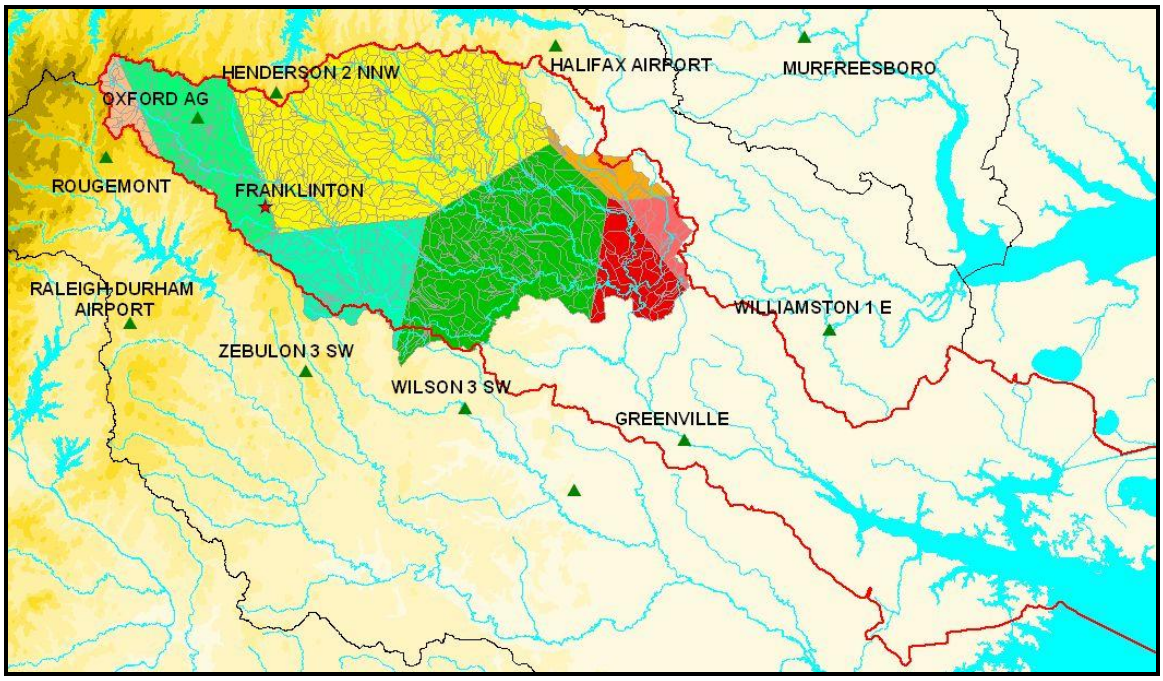

FIG 2.6 Climate stations and their Thiessen polygons in the study area.

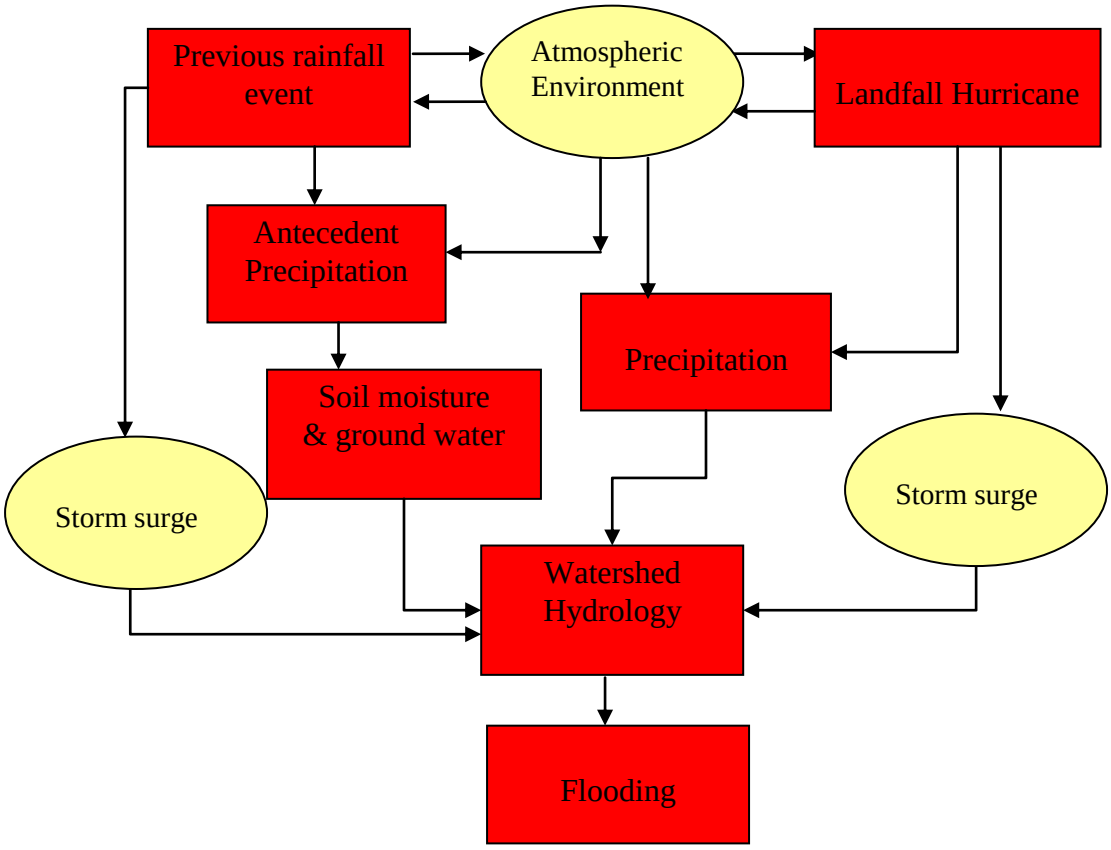

FIG 2.7 The interaction of antecedent precipitation, atmospheric environment and landfall tropical cyclone induced precipitations, watershed hydrological response and storm surges.

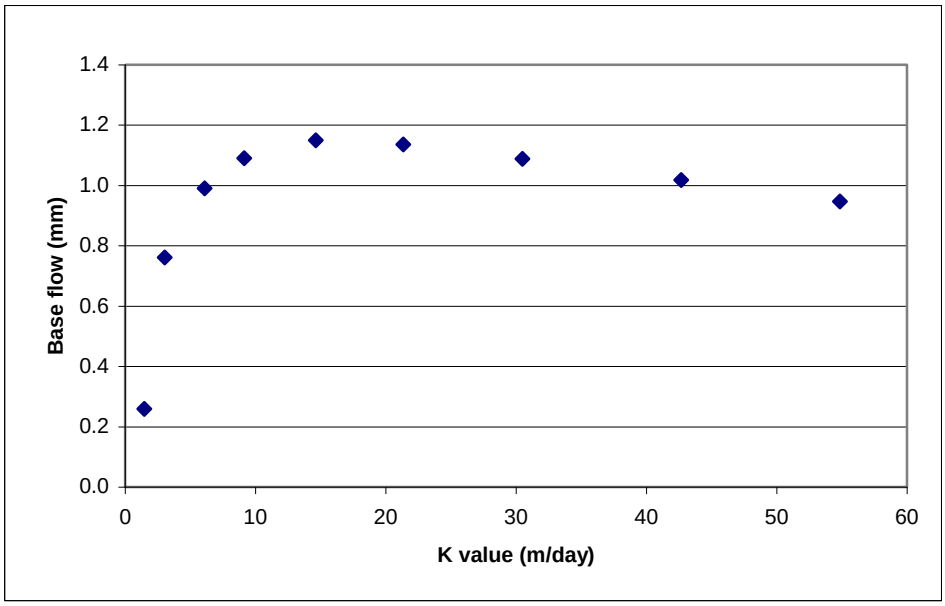

FIG 2.8 Sensitivity analysis of the relation between base flow (mm) and soil saturated hydrological conductivity K_s value (m/day).

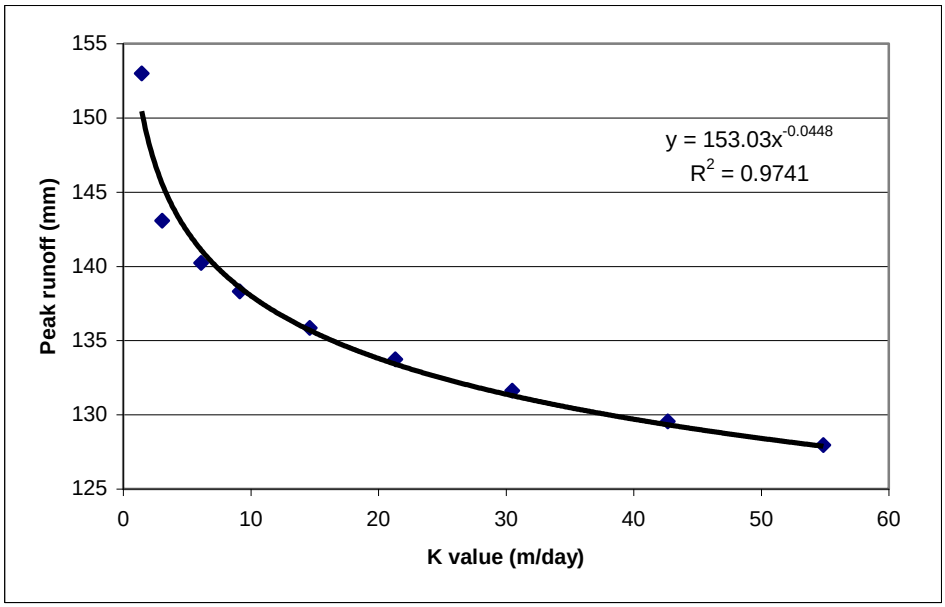

FIG 2.9 Sensitivity analysis of the relation between peak runoff (mm) and soil saturated hydrological conductivity K_s value (m/day).

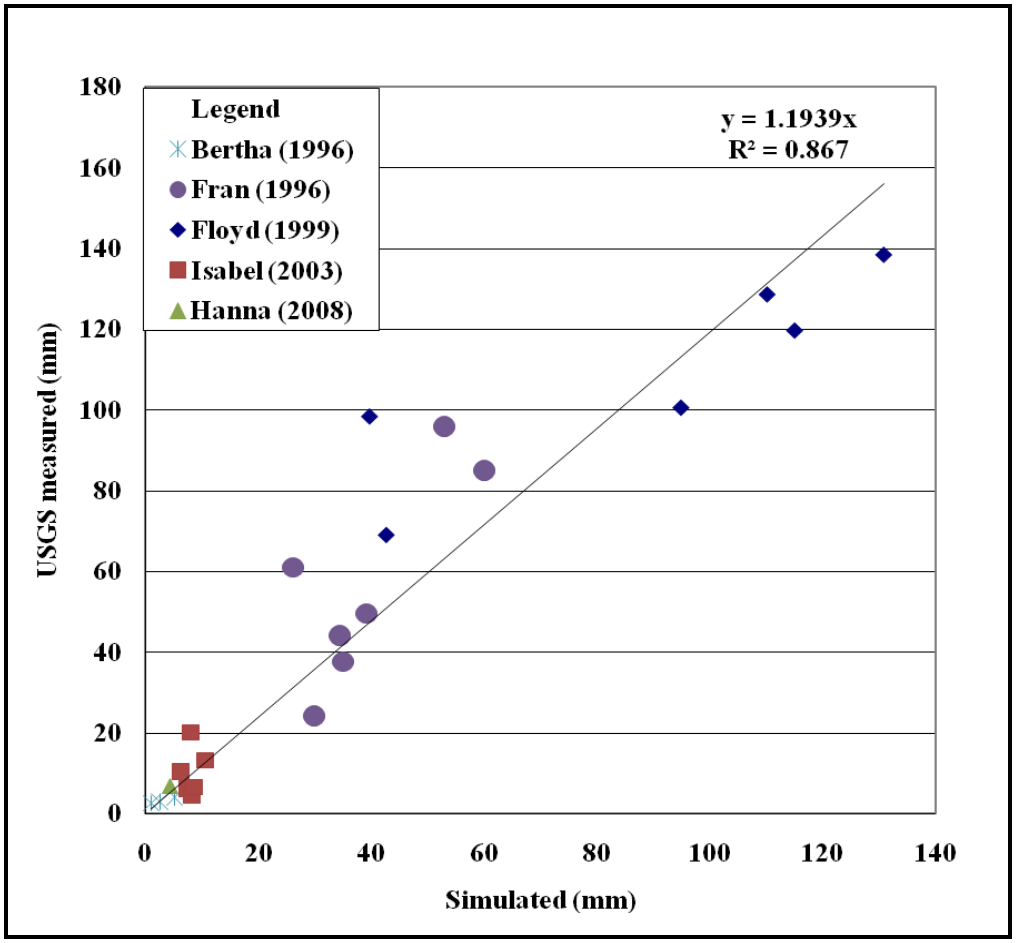

FIG 2.10 Relationship between AnnAGNPS simulated and USGS measured runoff.

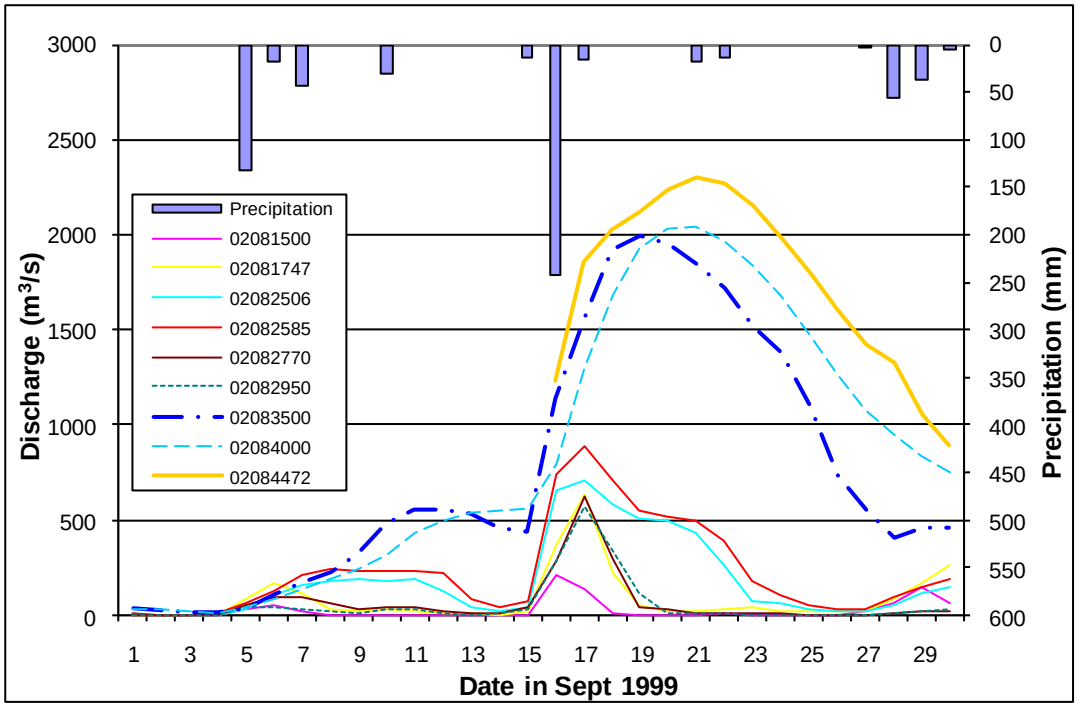

FIG 2.11 Daily river discharges (m^3 s^{-1}) at USGS gage stations and daily precipitation at Wilson 3 SW station in Sept 1999 in the study area (this figure has two additional downstream stations than Figure 3: 02084000 and 02084472).

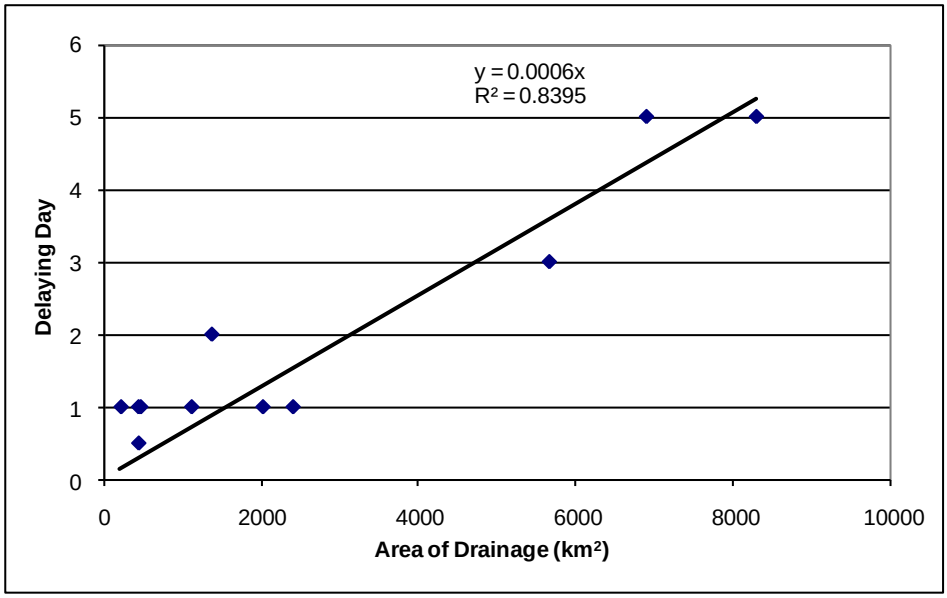

FIG 2.12 Relationship between drainage area (km^2) and peak discharge delaying days.

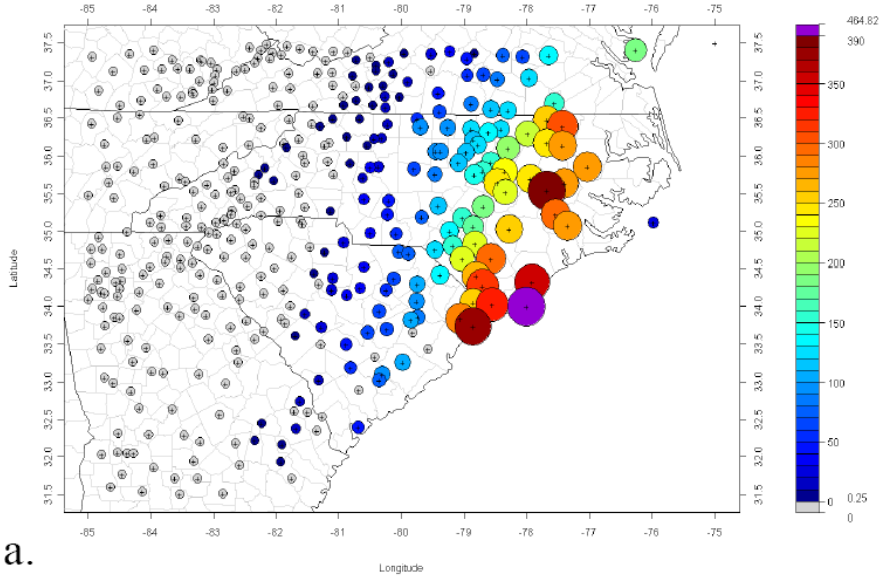

a.

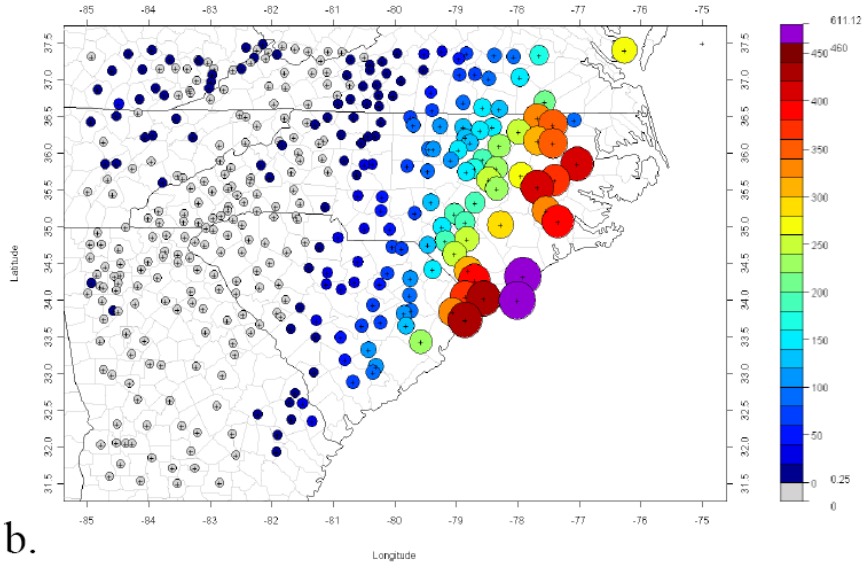

b.

FIG 2.13 Polka-dot plot for daily precipitation for a) 16 September 1999 b) 13 – 17 September 1999 (Palmer, 2008).

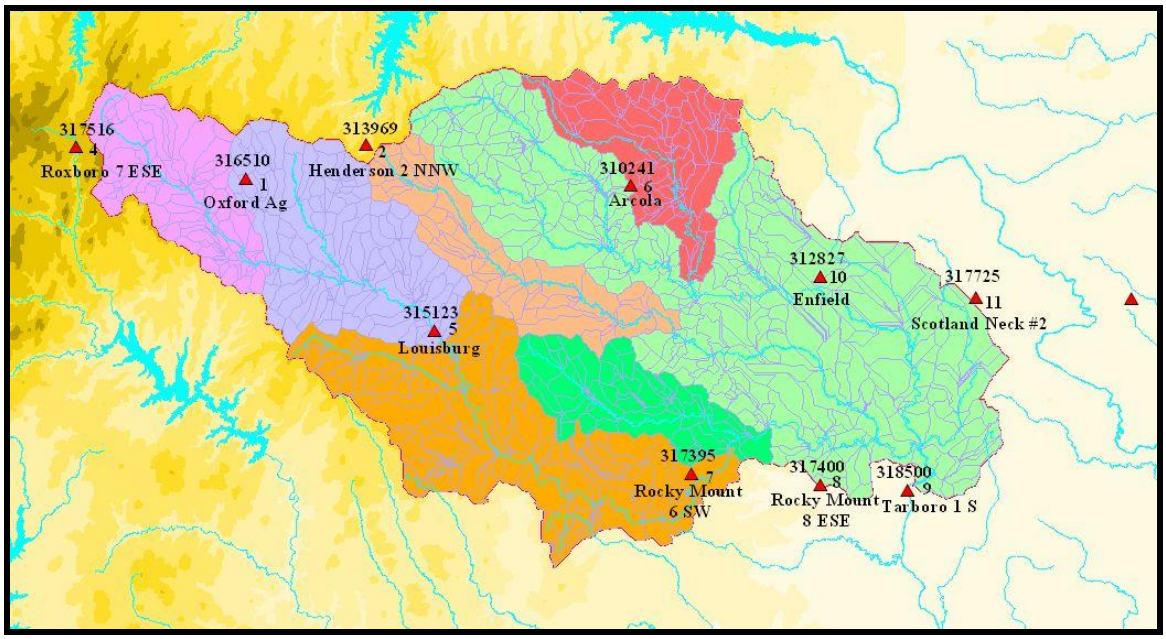

FIG 2.14 Climate station set 2.

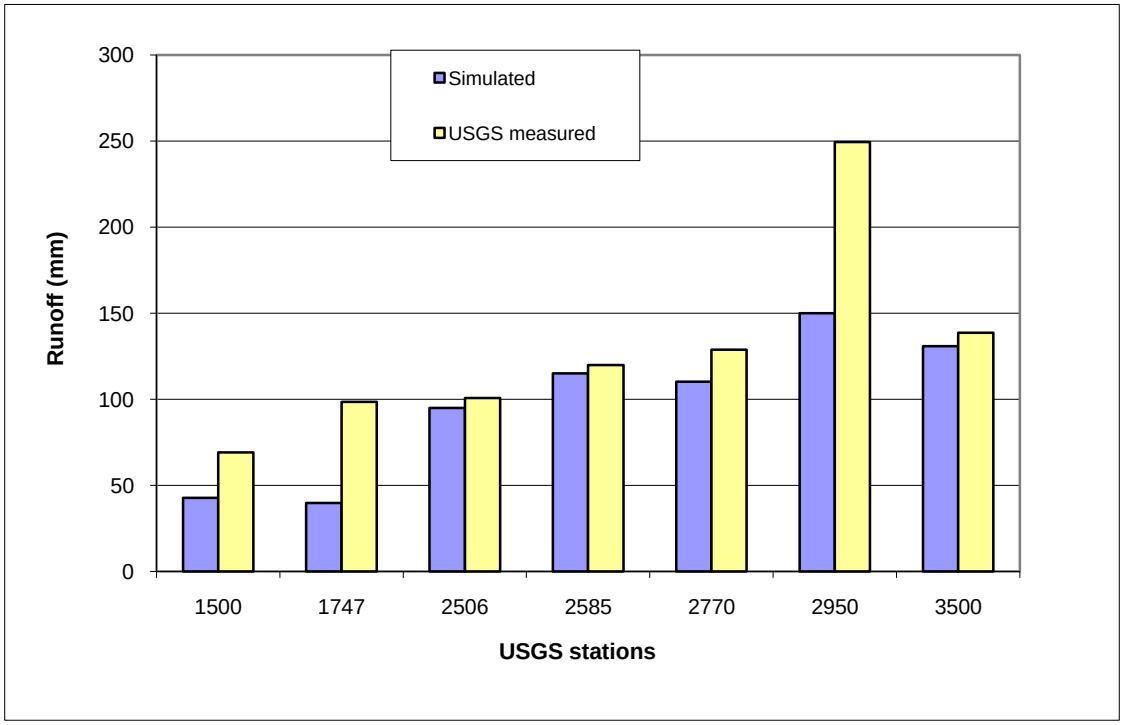

FIG 2.15 Comparison of AnnGNPS model output with USGS gage data during Hurricane Floyd (Sep 15 – 18, 1999) (mm per unit area).

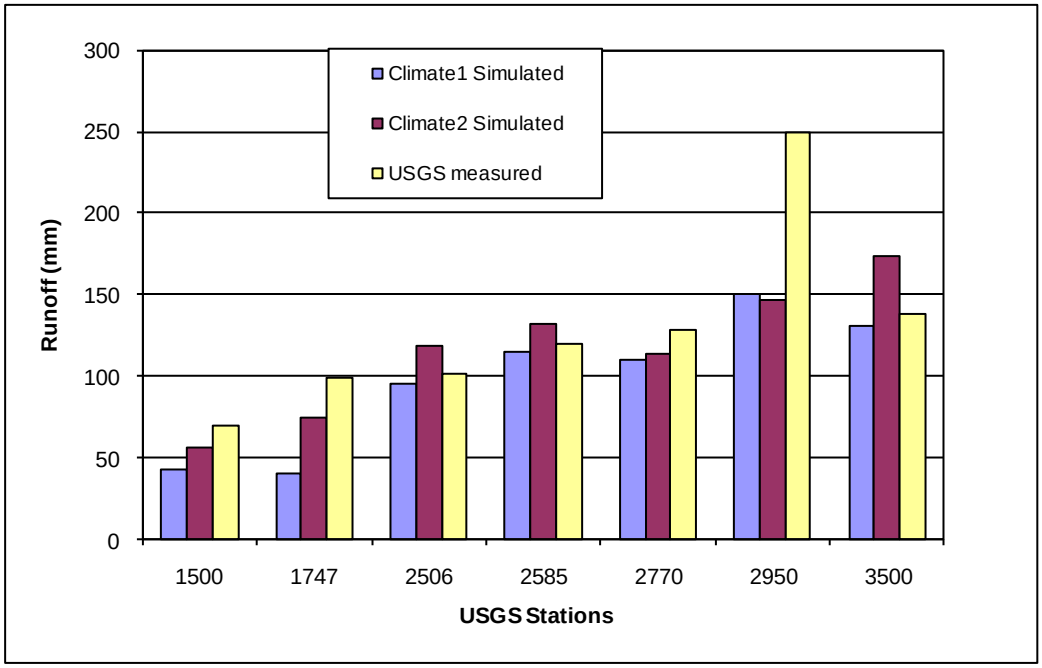

FIG 2.16 Comparison of AnnGNPS model output using data from climate stations set 1 and climate stations set 2 with USGS gage data during Hurricane Floyd (Sep 15 – 18, 1999) (mm/unit area).

FIG 2.17 Comparison of AnnGNPS simulated with USGS measured river discharges hydrographs in September 1999 at gages a) 02081500 and b) 02081747 c) 02082506 and d) 02082585 e) 02082770 and f) 02082950 g) 02083500 (Note: Dennis on Sept 5 and Floyd on Sept 16, 1999).

(a)

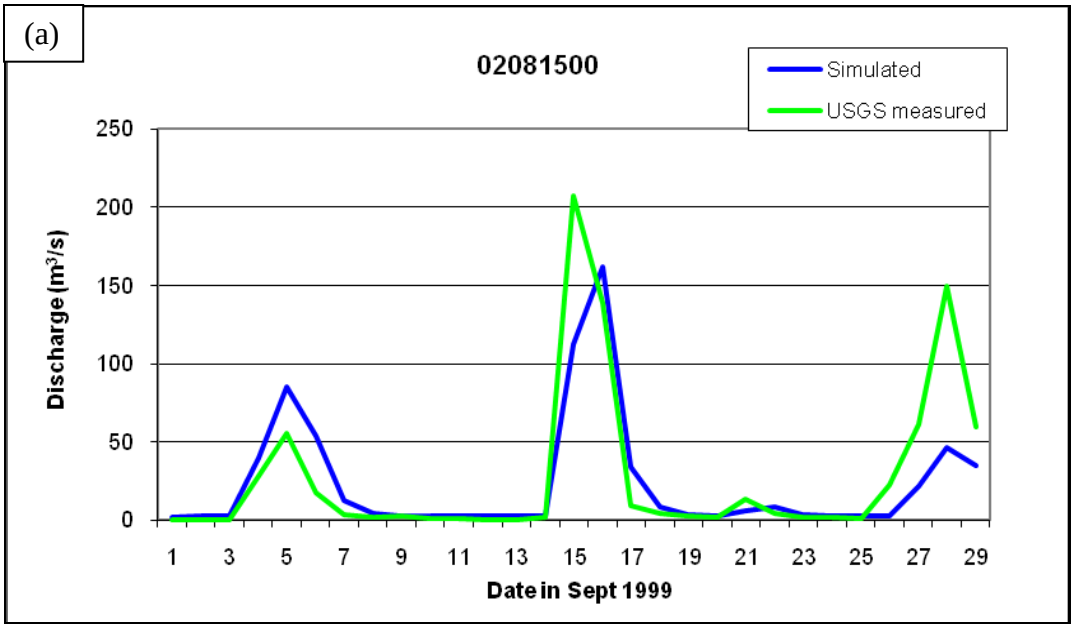
02081500
Simulated
USGS measured
Discharge (m³/s)
250
200
150
100
50
0
1 3 5 7 9 11 13 15 17 19 21 23 25 27 29
Date in Sept 1999

(b)

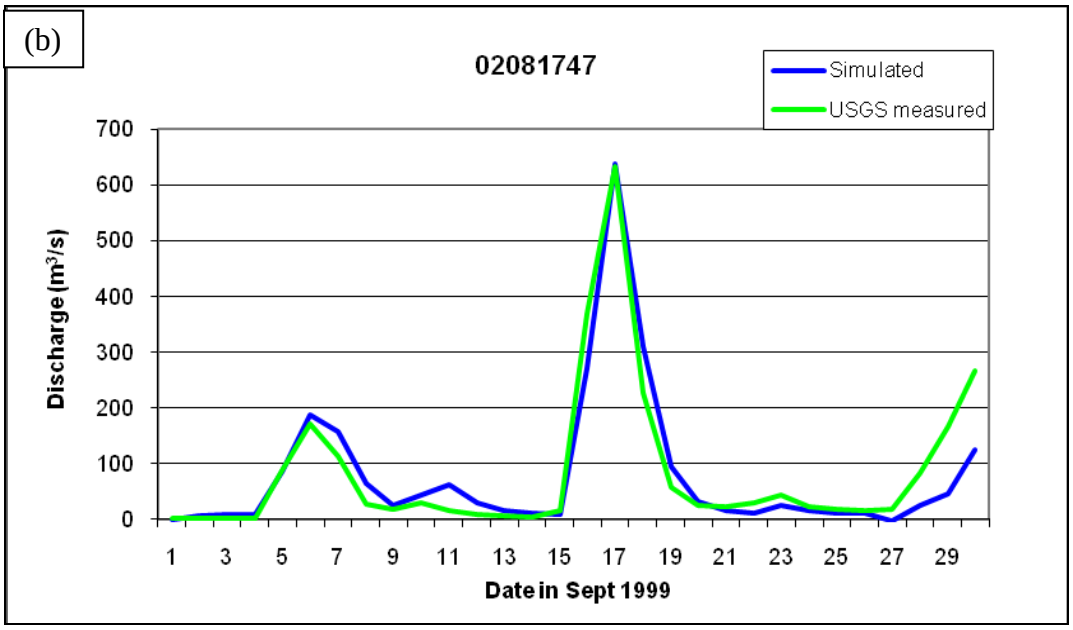
02081747
Simulated
USGS measured
Discharge (m³/s)
700
600
500
400
300
200
100
0
1 3 5 7 9 11 13 15 17 19 21 23 25 27 29
Date in Sept 1999

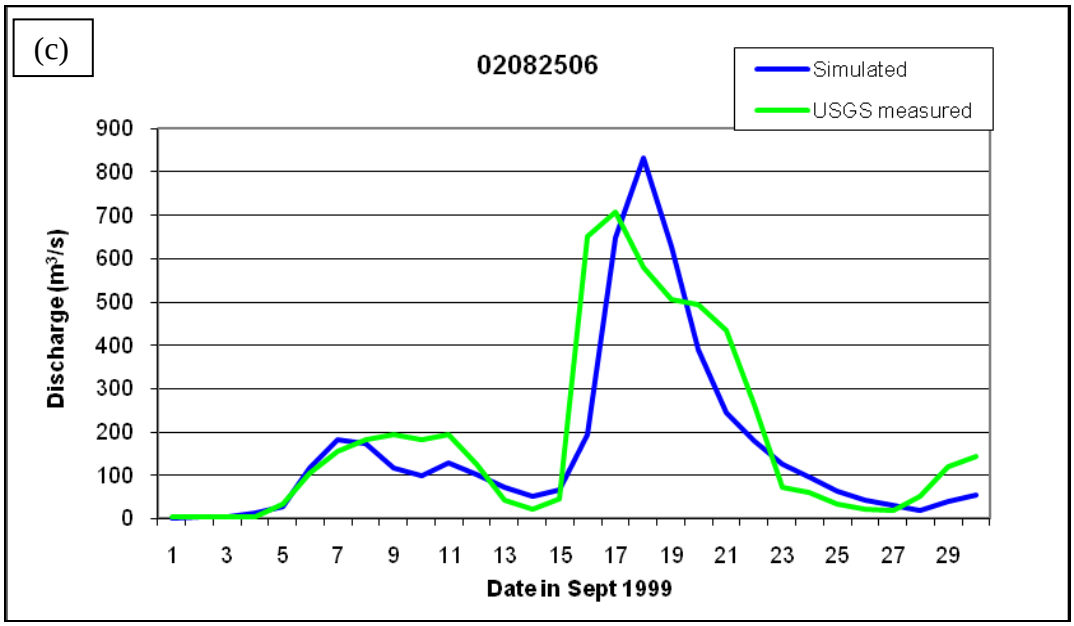
(c)
02082506
Simulated
USGS measured
Discharge (m³/s)
900
800
700
600
500
400
300
200
100
0
1 3 5 7 9 11 13 15 17 19 21 23 25 27 29
Date in Sept 1999

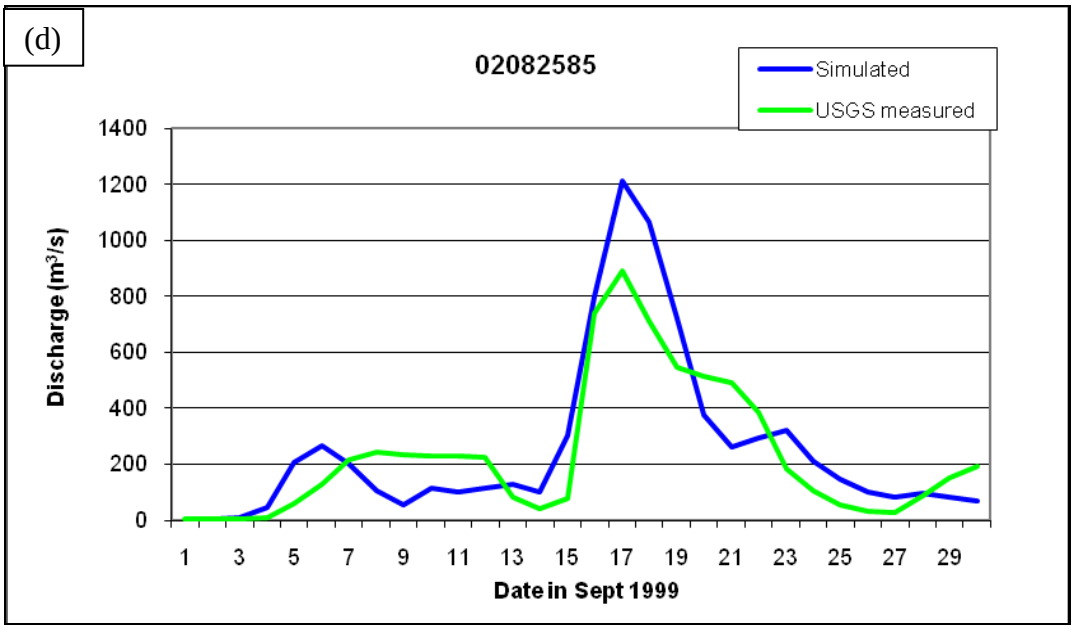
(d)
02082585
Simulated
USGS measured
Discharge (m³/s)
1400
1200
1000
800
600
400
200
0
1 3 5 7 9 11 13 15 17 19 21 23 25 27 29
Date in Sept 1999

(e)

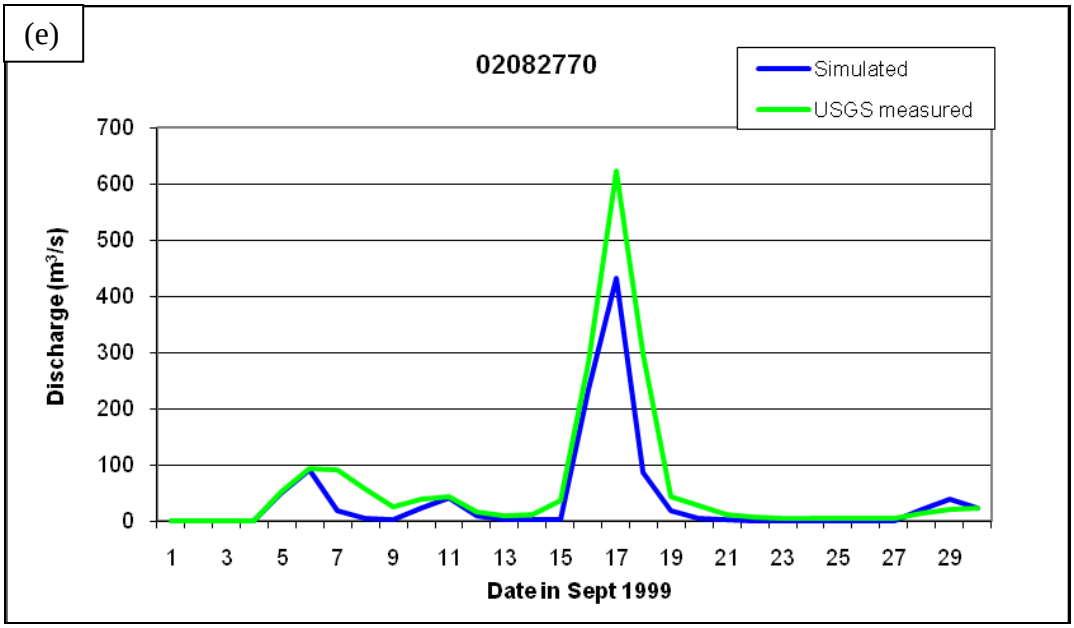
02082770
Simulated
USGS measured
Discharge (m³/s)
700
600
500
400
300
200
100
0
1 3 5 7 9 11 13 15 17 19 21 23 25 27 29
Date in Sept 1999

(f)

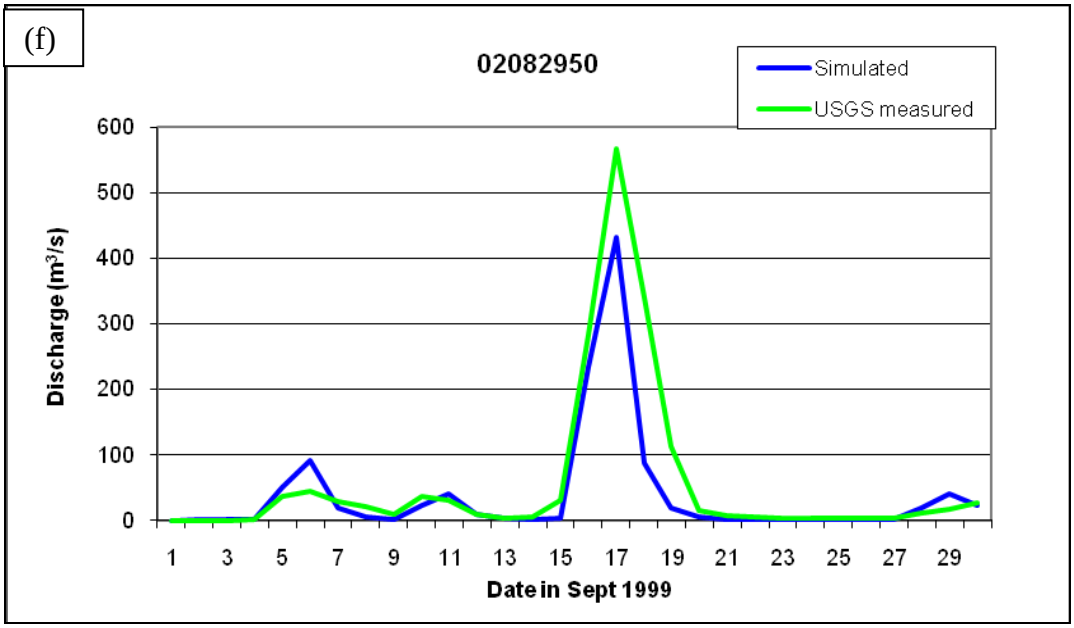
02082950
Simulated
USGS measured
Discharge (m³/s)
600
500
400
300
200
100
0
1 3 5 7 9 11 13 15 17 19 21 23 25 27 29
Date in Sept 1999

(g)

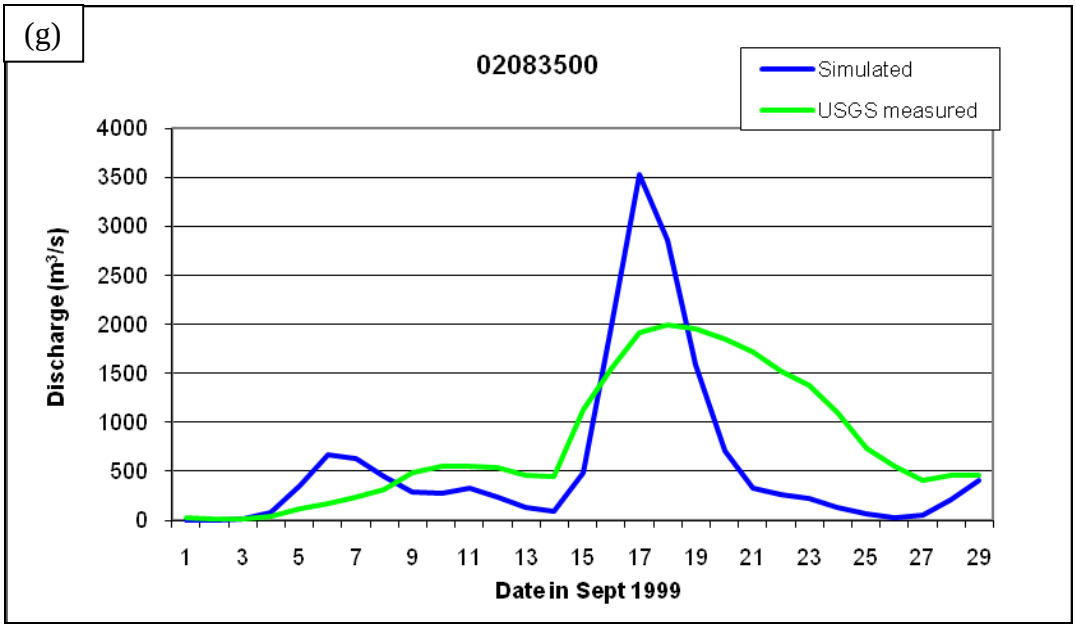
02083500
Simulated
USGS measured
Discharge (m³/s)
4000
3500
3000
2500
2000
1500
1000
500
0
1
3
5
7
9
11
13
15
17
19
21
23
25
27
29
Date in Sept 1999

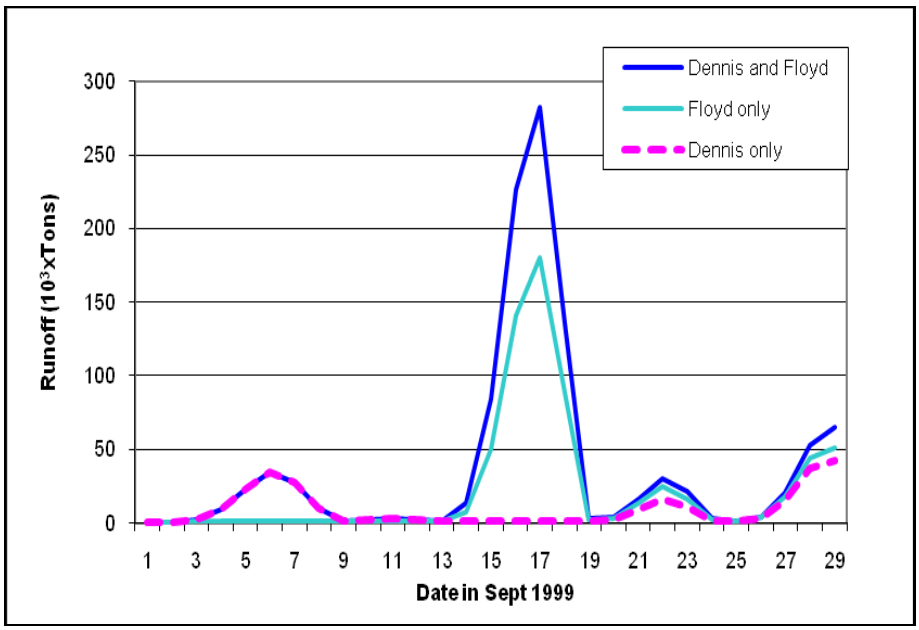

FIG 2.18 Simulated runoff (10^3 ton) at USGS Station 02083500 during Hurricanes Floyd and Dennis in September 1999.

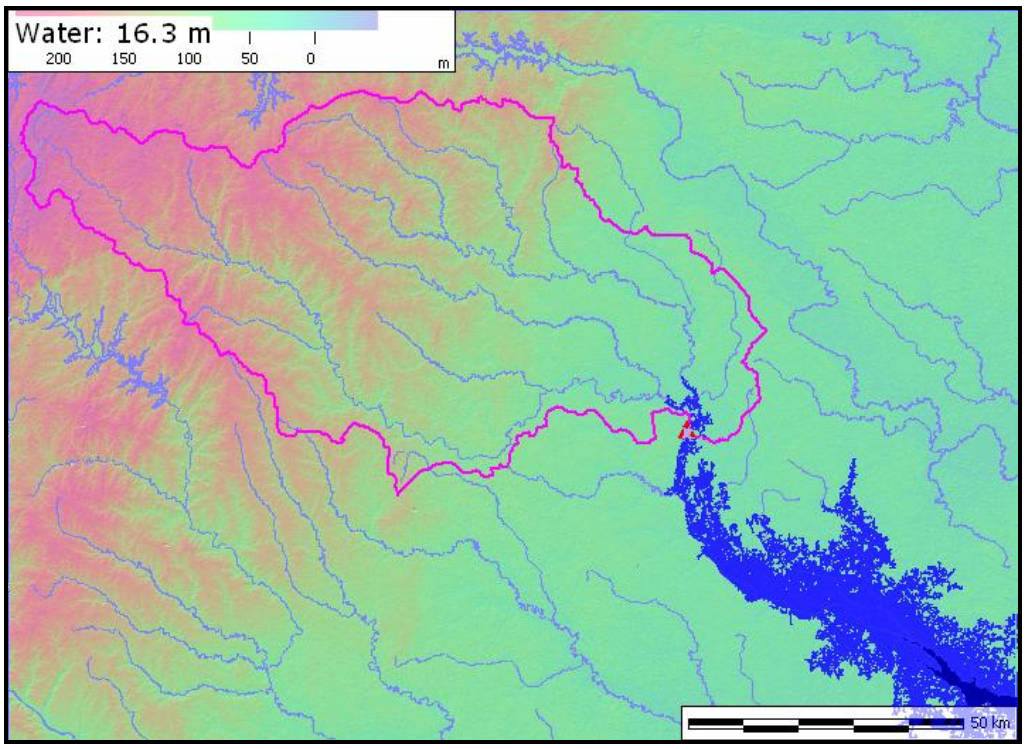

FIG 2.19 Calculated flood map at gage station 02083500 (Tarboro) when gage height is about 16.3 meters.

CHAPTER 3 Modeling the Impacts of Large-Scale Atmospheric Environment on Inland Flooding during Hurricane Floyd Landfall in 1999

3.1 Introduction

Hurricane Floyd in September 1999 caused disastrous flooding along the Atlantic coast from South Carolina to Massachusetts. Flooding was particularly severe and prolonged in eastern North Carolina, where the combined effects of Hurricanes Dennis and Floyd (see FIG 1.2 and FIG 1.3 for distribution of precipitation) resulted in greater flood-flow loadings of water and contaminants to Pamlico Sound, North Carolina, than any previously recorded events (Bales 2003). Over 50 cm of rain fell in isolated areas of North Carolina with widespread amounts exceeding 20 cm stretching from the Carolina Piedmont into southeastern New York (Lawrence et al. 2001). Previous studies (e.g. Atallah and Bosart 2003; Colle 2003; Atallah et al. 2007) indicated that this severe flooding is not only caused by the combination of Dennis and Floyd but also due to the enhancement of precipitation after interaction with a midlatitude trough during Floyd's landfall. The effect of the previous rainfall event - Hurricane Dennis has been studied and quantified in Chapter 2. However, the quantitative relations between atmospheric environment such as trough/ridge system and precipitation during hurricane landfall are still unclear.

The large-scale atmospheric environment hundreds to thousand kilometers away to the northwest of a Tropical Cyclone (TC) plays an important role in TC landfall in the southeastern United States. The intensity of troughs/ridges in that area will affect the track,

speed, intensity and duration of TCs (e.g. Rodgers and Pierce 1995; Hanley et al. 2001; Kimball et al. 2002; Atallah and Bosart 2003 and Peng et al. 2007). It will further affect the rainfall amount and distribution. Many efforts have been devoted to understanding how environmental features affect TC and resulting different precipitation distribution (e. g. Atallah and Bosart 2003; Colle 2003; Bales 2003 and Croke 2005). Those studies can be categorized into three aspects.

The first one is the influence of extratropical transition (ET). A significant number of tropical cyclones move into the midlatitude and transform into extratropical cyclones (usually occuring in 30 – 40 $^{\circ}$N). This process is generally referred to as extratropical transition (ET). During ET, a cyclone frequently acquires increased forward motion and sometimes intensifies substantially so that such systems pose a serious threat to land and maritime activities. Atallah and Bosart (2003) stated that the transport of tropical air masses into the midlatitudes resulted in a large increase in the available potential energy (APE) of the atmosphere. The approaching midlatitude trough provided a mechanism by which this APE was converted to kinetic energy through thermally direct circulations, resulting in a rather powerful extratropical cyclone. Hurricane David in 1979 regained power over land just prior to undergoing ET as it lifted the tropopause ahead of the midlatitude trough due to diabatic heating from deep convection associated with Hurricane David (Bosart and Lackmann 1995). Atallah and Bosart (2003) diagnosed the dynamics associated with the ET of Floyd and found that strong isentropic ascent can lead to copious amounts of precipitation. The juxtaposition of the relatively cool dry air of the midlatitude trough and the warm moist air associated with Floyd produced an intense, troposphere deep baroclinic zone. The

circulation center of Floyd then interacted with this baroclinic zone, producing deep isentropic ascent and precipitation north of Floyd. Harr and Elsberry (2000) and Harr et al. (2000) indicated that strong ET tends to produce significant precipitation to the northeast of the TC from their conceptual model. These features were favored when the main midlatitude trough was located northwest of the tropical cyclone.

The second aspect is hurricane and trough interaction. Hurricane and trough interactions have been discussed for many years (e.g. Molinari and Vollaro 1990; Molinari et al. 1995; Molinari et al. 1998; Bosart et al. 2000; Hanley et al. 2001; Kimball and Evans 2002). In a study of interactions between tropical cyclone and upper-tropospheric trough, Hanley et al. (2001) performed a composite of trough interactions with 121 Atlantic tropical cyclones in an attempt to differentiate between troughs which lead to intensification, and those which lead to decay. Trough interactions were classified into four categories, that is, favorable superposition (tropical cyclone intensifies with an upper-tropospheric PV maximum within 400 km of the tropical cyclone center), unfavorable superposition, favorable distant interaction (upper PV maximum between 400 and 1000 km from the tropical cyclone center), and unfavorable distant interaction. In the superposition case, there is an upper positive PV maximum within 400 km of the TC center. Within the 400 km, flow is still cyclonic around the storm center in the upper levels (Levine 2003). A distant interaction occurs when an upper positive PV maximum is between 400 km and 1000 km from the TC center. This is where flow is anticyclonic in the upper levels. No trough interaction is considered to occur when an upper PV maximum is at a distance greater than 1000 km. They found 78% of TCs with a superposition and 61% of TCs with a distant

interaction deepened. In superposition cases, the composite showed that a small scale upper PV anomaly approached the TC center and dissipated before crossing the TC center, similar to the results of Molinari et al. (1995, 1998).

Kimball and Evans (2002) simulated idealized cases of a hurricane interacting with four different types of upper-level troughs in the condition of low vertical shear environment. Their simulation results show that the hurricane interacting with the strongest trough (highest PV, HILOW) becomes the most intense while weaker low trough is advected away by the storm or dissipated sooner. All hurricanes interacting with troughs evolve to be larger and stronger but less intense than hurricanes intensifying in vertical wind shear alone (control case, no interaction). Their results are supported by Guard (1995), who observed that interaction with midlatitude troughs was associated with the largest and most intense western North Pacific typhoons, but often occurred without rapid deepening. Large storms may not necessarily have the strongest low level winds but do have the areal coverage of destructive winds and heavy rainfall.

The third aspect is distribution of precipitation before and after landfall. The distribution of precipitation induced by TCs varies in TC size and intensity (e.g. Klein et al. 2000; Peng et al. 2007; Atallah et al. 2007; Hill and Lackmann 2009; Matyas 2010). TC size is sensitive to environmental humidity. Hill and Lackmann (2009) performed four idealized high resolution numerical simulations to test the sensitivity of TC size to environmental humidity. Their results indicated that moist environments favor the development of larger TCs, with progressively larger storms evident with each incremental relative humidity (RH). Although more moist environment did not show heavier eyewall precipitation or a more

intense cyclonic PV tower, more precipitation in outer rainbands occurred in the more moist environment.

Matyas (2010) studied 31 US hurricane land falls. Her results showed that hurricanes, which did not become extratropical were the most symmetrically shaped at the time of landfall, while those within 2 days of becoming extratropical were the most asymmetrical. Although the edges of the rain fields did not precisely align with any of the measures of storm size, they were most closely co-located with the radius of gale-force winds in each quadrant. When Hurricane Floyd (1999) transitioned into an extratropical cyclone, it produced heavy rainfall farther away from circulation center but also on the left side of the track (Atallah et al. 2007; Atallah and Bosart 2003). During ET, the environment surrounding the hurricane becomes baroclinic and isentropic ascent occurs near the steep thermal gradient between tropical and continental air masses typically located north of the storm's center that enhances precipitation in this region (e.g. Klein et al. 2000; Peng et al. 2007). Besides interaction of Floyd with upper-level trough, the Appalachians and the coastal terrain played a secondary role in the devastating flooding for this particular event (e. g. Colle 2003 and Harville 2009). Colle (2003) studied high resolution numerical simulations of Floyd after interaction with the midlatitude trough and found that without evaporative effects from precipitation, a low-level front was 10%–20% weaker than the control, and Floyd's central pressure was about 4 hPa weaker. Another simulation without surface heat fluxes resulted in a 4–5 hPa weaker cyclone, and 20%–30% less precipitation shifted 100–150 km farther eastward than the control.

Despite the extensive study on the influences of different hurricane perspectives such as ET energy during trough-hurricane interaction, environmental moisture, distribution of precipitation in different situations, surface heat fluxes and coastal terrain, as described above, quantitative analysis has rarely been conducted to understand the role of the atmospheric environment in intensifying precipitation carried by hurricanes such as Hurricane Floyd. Specific questions to answer include how much of a role has the midlatitute trough played in the entire process of hurricane interaction and what is the percentage that midlatitude trough environment has contributed to precipitation.

FIG 3.1 depicts the interaction and relationship among: previous rainfall event, atmospheric environment and landfalling hurricane. The hurricane induced flooding in a coastal watershed is caused by 1) previous rainfall event through antecedent precipitation to saturate soil moisture and increase ground water level; 2) precipitation from the interaction of atmospheric environment (trough/ridge) and landfalling hurricane; 3) storm surge from ocean induced by strong hurricane winds. The role of previous rainfall event induced flooding has been studied in Chapter 2 and the results indicated that total runoff would be reduced by 37% without Hurricane Dennis. In this study, we now try to separate the rainfall contribution from the hurricane and synoptic environment.

3.2 Models, Research Domains and Data

In this study, two models are employed. One is the Weather Research and Forecasting (WRF) model. WRF version 3.1(see website http://www.wrf-model.org/index.php for details)

has been applied to simulate Hurricane Floyd's landfall in North Carolina from September 15 – 18, 1999. Hurricane Floyd was chosen because it represents a heavy precipitation event resultings from interaction with a midlatitude trough. The other model is a hydrological model - the Annualized Agricultural Nonpoint Source Pollution Model (AnnAGNPS). The AnnAGNPS (Bingner et al. 2007) is selected in the study because it accounts for detailed surface topology, soil, land use, ground water hydrology and river channel flow. In the same time, up to 99 distributed rainfall stations can be accepted in the model. All of such information is managed in the GIS system so that data processing is much faster. The detailed information to set up this model can be found in Chapter 2.

FIG 3.3 demonstrates the WRF model domain used in this study. An inner domain with 2-km grid spacing with horizontal grid dimension of 301 x 301 lies within an intermediate domain of 6-km grid length of the same dimension. The outer domain features 18-km grid spacing with similar grid dimension as well. The outer boundary covers most of the US continent and includes the area covered by the midlatitude trough/ridge. The intermediate domain covers the simulation time period that the hurricane passed by and the inner domain covers the watershed area of interest. The watershed of interest is Tar-Pamlico River Basin depicted in FIG 3.4 in blue color polygon and the details of the basin can be found in FIG 3.19 and FIG 3.18(see Chapter 2 for details).

The North American Regional Reanalysis (NARR) dataset has been employed in the research because it offers better resolution data (in 32 kilometer grid spacing with 29 pressure levels and reports at three-hour intervals) than FNL (Final) Operational Global Analysis data (1 x 1 degree resolution with 26 levels and six hour intervals) from National

Centers for Environmental Prediction (NCEP). NARR covers the period from 1979 to the present. The surface and ground observation data are provided by North Carolina State Climate Office and NOAA National Climate Data Center. The stream flow data at each station depicted in FIG 3.19 are obtained from USGS (U. S. Geological Survey). Digital data such as landuse, soil, digital elevation model (DEM) for the AnnAGNPS model is from North Carolina State University library website (see Chapter 2 for details).

3.3 Method

3.3.1 Model setup and experimental design

The WRF model was used to simulate Floyd for diagnosing the structural evolution and associated precipitation. For this simulation, the three stationary domain levels were nested using two-way feedback. The model top was set at 100mb. Thirty-one unevenly spaced full-sigma levels were used in the vertical, with the maximum resolution in the boundary layer. Five minute averaged terrain and landuse data were interpolated to the 18-km model grids. For the 6- and 2-km domains, 2 minute and 30 second topography and landuse datasets were interpolated to the grid in order to better resolve the inland hills and valleys. Initial atmospheric conditions at 0000 UTC 15 September 1999 were generated by interpolating the NARR model 301x301 grids (32-km grid spacing) to the WRF grid. Additional analyses were generated in the same manner using the 3 hourly forecasts and were linearly interpolated in time in order to provide the evolving lateral boundary conditions for the 18-km domain.

In order to rigorously investigate large scale midlatitude environmental impact on hurricane landfall, two sets of simulations were conducted: the control (CTRL) simulation and synoptic environment simulation (ENV). All configurations were same except one (CTRL) with hurricane Floyd and another (ENV) featured a weakened Floyd.

Both simulations used the explicit WSM 6-class graupel scheme (Hong and Lim 2006) which includes prognostic equations for cloud ice and water, snow, rain, and graupel processes suitable for high-resolution simulations. This microphysics parameterization scheme has been preliminarily tested for WRF-NMM. Mellor-Yamada Nakanishi Niino (MYNN) level 2.5 planetary boundary layer (PBL) scheme (Nakanishi and Niino, 2004) were used on all domains for all runs. The scheme is 1.5 order and local TKE based vertical mixing in boundary layer and free atmosphere. This is new in WRF version 3.1. The original Mellor-Yamada model underestimates the mixed-layer depth and the magnitude of the TKE (Nakanishi and Niino, 2004). MYNN Monin-Obukhov similarity theory is used for the surface scheme corresponding to MYNN-PBL scheme. RRTM and Dudhia shortwave physics are used for long and short wave radiation schemes respectively. The New Kain-Fritsch scheme was applied for cumulus parameter for outer domain only (18km).

The comparison simulation is done by removing hurricane Floyd vortex (method is detailed in section 3.3.2) at initial time of 0000 UTC 15 September 1999 in the outer domain (18km). After removal of the TC vortex, WRF simulation of three domains was run (results will be showed and discussed in section 3.4.3).

In order to match the period of daily rainfall observation data, all simulation time period is set starting at 1200 UTC on 15 September 1999. Hereafter, all 1200 UTC to 1200 UTC 24-hr periods will be referenced by the date upon which the 24-hr period ends. This is referenced from Palmer (2008). Thus, the accumulation from 1200 UTC on 15 September 1999 to 1200 UTC on 16 September 1999 will be simply known as the 24-hr accumulation for 16 September 1999.

In order to investigate the flooding effects from the large scale environment, the precipitation from WRF model outputs of the control (CTRL) simulation and synoptic environment simulation (ENV) then served as input data for AnnAGNPS to compare the discharge and the total volume of runoff water carried at the outlet of the watershed. The experimental design was set as two groups. One group compared surface runoffs at seven subwatersheds by using observed precipitation at Tar-Pamlico River Basin with surface runoffs by using precipitation in about 40 points from WRF control simulated results at seven simulated (FIG 3.4). Another group compared surface runoffs one simulated from precipitation of WRF control run and the other simulated from precipitation only containing with hurricane Floyd (substract ENV from CTRL under assumption of linear relationship during the interaction of atmospheric environment and TC).

3.3.2 Vortex removal

Bogussing and/or removing a tropical cyclone (TC) from the initial conditions are conducted through the utility program (tc_em.exe). The bogussing program has been ported

from MM5 for WRF in version 3.1 (Fredrick et al. 2009). In this version of the scheme, one can either introduce a new vortex or remove an existing vortex. The input to the scheme is a single file containing fields on isobaric surfaces that have been produced by running the WPS metgrid.exe program. In order to investigate the role of large scale environment, TC Floyd is mostly removed using this technique.

According to Fredrick et al. (2009), the TC bogus scheme starts by searching for the vortex corresponding to the storm in the first guess-field. This is done by looking for the maximum relative vorticity within a prescribed radial distance from the Best Track location of the Tropical Cyclone. 400 km searching radius has been currently used (FIG 3.5). The grid point where the maximum vorticity is located serves as the center of vortex to be removed. Once the vortex has been found, the first-guess vorticity and divergence within 600 km radius of the first guess storm is removed and then the velocity is re-calculated.

The schematic diagram of TC bogussing and vortex removal is depicted in FIG 3.6. The relationship of the vorticity is as follows:

$$\nabla^2 \psi = \zeta \qquad (1)$$

where ψ is the stream function for the non-divergent wind and ζ is the relative vorticity. To define the non-divergent wind associated with the first-guess storm, the vorticity is set to 0 outside a radius of 600 km. Then the Dirichlet boundary conditions stream function is defined to be 0 and the Successive Over-Relaxation (SOR) method is used to solve Equation 1 for the perturbation stream function on all pressure surfaces. The non-divergent wind is then calculated from the following relationship:

$$v_{\psi} = \hat{k} \times \nabla \psi \tag{2}$$

where v_{ψ} is the non-divergent wind. Once the non-divergent wind is calculated, it is subtracted from the first-guess U and V wind fields.

Removal of the divergent wind from the first-guess storm is similar. The following relationship is used:

$$\nabla^2 \chi = \delta \tag{3}$$

where χ is the velocity potential and δ is the divergence computed from the horizontal wind. In this case, the divergence is set to 0 outside a radius of 600 km. The velocity potential is calculated from the following equation:

$$v_x = \nabla \chi \tag{4}$$

where v_x is the divergent wind. Once the divergent wind is calculated with the equation above, it is subtracted from the first-guess U and V wind field. Then the geopotential height anomaly from the first-guess field is removed. The equation for the perturbation height and the geostrophic wind are calculated by the following equations:

$$\nabla^2 \phi = \zeta_g f_0 \tag{5}$$

$$v_g = \hat{k} \times \nabla \phi \tag{6}$$

where v_g is the geostrophic wind and is then subtracted from the first guess-field.

The temperature anomaly field due to the first guess-storm is calculated from the following equation:

$$\frac{\partial \phi'}{\partial \ln(p)} = RT' \tag{7}$$

where R is the gas constant and p is the pressure. After the temperature anomaly field is removed, the surface and sea-leval pressure perturbations associated with the height anomalies from the surface and sea-level pressure fields are removed. Finally only the background flow is left.

The configuration is set as follows: the center location of TC Floyd at 1500 UTC on 15 September 1999 was at 27.1^{o} N and 77.7^{o} W from the National Hurricane Center. The maximum observed sustained wind speed was 59.16m/s. The radius from the cyclone center to where the maximum wind speed occurs is set to 90 km. And the scale factor for model's Rankine vortex is 0.75.

3.4 Results

The history of Floyd can be described from the best track position (FIG 3.2) from the National Hurricane Center. Early stage of Hurricane Floyd started as a tropical wave off the coast of Africa in early September 1999. It traveled across the Atlantic until becoming a tropical depression on 7 September 1999 located at 14.6 ºN and 45.6 ºW with central pressure of 1008 hPa and 13 m/s wind speed (Pasch et al. 1999). At 0600 UTC on 8 September

(hereafter using 0600/8th for UTC time and date in September 1999), it was upgraded to a tropical storm (TS) with low pressure of 1005 hPa and the wind speed up to 18 m/s. By the time of 1200/10th, approximately 370 km northeast (NE) of the Leeward Islands, Floyd was upgraded into hurricane status with the pressure of 989 hPa and wind speed reached up to 36 m/s.

As moving westward, Floyd reached its maximum strength on 13 September 1999, with a central minimum pressure of 921 hPa and maximum sustained winds up to 69 m/s, making the storm a Category 4 on the Saffir-Simpson Scale. When passing the Bahamas on September 14, Floyd began to move northwest due to the influence of a large upper mid-trough located in Ontario, Canada (Pasch et al. 1999).

The simulations in this research cover the period from 0000/15th to 1200/17th and the results are described as below. After 1200/17th, Floyd moved from Maine toward the northeast and then east-northeast and soon dissipated after 18th which is out of this study interested area and time frame.

3.4.1 Control simulation and synoptic features of Hurricane Floyd

FIG 3.7 displays the sea level pressure and 10 meter wind 18 km domain 1 from control simulation every 12 hours from 0000/15th – 1200/17th. The figures clearly describe the Hurricane Floyd's step by step movements from near coastal Florida to Maine. Floyd continued to turn gradually to the north during the time of 0000/15th to 1200/15th (

FIG 3.7a, b). The center of the hurricane was moving parallel to the eastern Florida coast till 1200/15th. FIG 3.9 depicts the 500 hPa Potential Vorticity (shaded in every 0.5 PVU, 1 PVU = 10^{-6} K kg^{-1} m^2 s^{-1}) and Geopotential Height from WRF control simulation in every 12 hours from 0000/15th to 1200/17th. The large upper mid-latitude trough can be seen at 500 hPa from FIG 3.9a (0000 UTC 15th is 8 pm of 14th eastern daylight time).

FIG 3.7c is similar to the manual surface analysis map from Colle (FIG 1a, Colle 2003) in the terms of the central location of Floyd (about 200 km south of North Carolina) and pressure field at time 0000/16th. The only differences are the former has a greater minimum pressure (980 hPa vs. 951 hPa) and slower maximum wind (25m/s vs. 59 m/s). This is probably due to the initial minimum pressure from NARR at time 0000/15th which was higher and maximum wind is lower than observed. At 500 hPa (FIG 3.9c), Floyd began to interact with a broad baroclinic zone that extended along the coast of the south-eastern and mid-Atlantic states. The comparison of 500 hPa geopotential height demonstrated much better agreement with NCEP analysis (FIG 3.11, Colle 2003) both Floyd and mid-latitude trough geopotential height contours are laid in very similar places.

The WRF model result on the 6 km grid in domain 2 at 0300/15th in FIG 3.13a demonstrates much better agreements with observed data (FIG 3.11, Colle 2003). Comparing to FIG 3.12a of 18 km grid spacing (same map but different grid spacing), FIG 3.13a showed much better wind and pressure field structure of Floyd. The wind is stronger than 18 km field. Although the difference of minimum pressure doesn't have big differences, the maximum wind speed is stronger than 18 km grid spacing field (24.75 m/s vs. 23.76 m/s).

Floyd made landfall at Bald Head Island, NC at 0630 UTC 16 September. Although the central pressure of Floyd gradually weakened after 13th, the potential vorticity of Floyd center at 500 hPa increased from 3.5 PVU at 0000/15th (FIG 3.9a) to 4 PVU at 1200/15th (FIG 3.9b) and up to 4.5 PVU at time 0000/16th (FIG 3.9c) and 1200/16th (FIG 3.9d) (1 PVU = 10^{-6} K kg^{-1} m^2 s^{-1}). The northwest trough gradually deepened and moved southeastward while Floyd continued moving northward until the two systems merged at 1200/16th (FIG 3.9d).

By 0000/17th, the two systems completely merged with each other and Floyd had made extratropical transition (FIG 3.9e). At 1200/17th, Floyd had weakened to 984 hPa from observation along the northern New England. The area of PV greater than 1.5 PVU became larger and the merged extratropical cyclone moved toward the northeast although the maximum PV at the center of the extratropical cyclone weakened to 3.5 - 4 PVU. The heaviest rainfall occurred during this period between 1200/16th – 1200/17th. Although the pressure field was weaken, however, the PV field did increase after landfall during ET and the interaction of the trough and Floyd. Colle (2003) proved that the surface temperature gradient to the north of the cyclone center had doubled in magnitude from 1200/16th – 0000/17th although surface pressure slightly weakened. The combined effects of an intensified baroclinic zone in this period are consistant with the view point of Atallah and Bosart (2003). But this intensification was not as strong as some other documented ET events (e.g. Bosart and Lackmann 1995; Klein et al. 2000) which both featured pressure decrease and a temperature increase.

Floyd further weakened to 992 hPa by 1200/18th and maintained this intensity for the next 24 h (Pasch et al. 1999).

3.4.2 Precipitation distribution of Floyd from control simulation

The precipitation of control run in the inner domain (2x2km) is shown in FIG 3.14a. It is comparable to the NOAA observed result in FIG 3.14b and FIG 3.14c from Climate Prediction Center. The color scheme of NOAA map has been modified for comparison purposes. The original map can be found in Pasch et al. (1999). The time period of NOAA map was accumulated from 14 – 19 September 1999 while the WRF model result is from 16 – 17 September 1999. This is because precipitation before the 16th and after the 17th was very little in North Carolina. Rainfall after the 17th moved from Virginia northward. It is obvious that the pattern of accumulated rainfall is very similar although the highest rainfall area of the simulated precipitation is located in South Carolina rather than North Carolina as observed and the area over 380 mm rainfall is smaller than the observed one.

After making landfall in South Carolina and moving north to North Carolina, the heavy precipitation fell from the coast to central piedmont region up to the Appalachian Mountains in the west as demonstrated. The precipitation pattern of Floyd is highlighted by a linear Northeast and Southwest axis and maximum accumulations as stated by Atallah et al. (2007) that hurricane lost its symmetry after landfall as shown in FIG 3.15 where rainfall distributed most in northeast part of Floyd.

To examine the cumulative precipitation from 1200/15th – 1200/17th at watershed area, FIG 3.16 compares the WRF simulated precipitations in domains 1, 2, 3 with observations at selected weather stations. Distribution of these stations can be found in FIG 3.4. Stations in the chart listed from left to right axis are in the order from upper to lower watershed which also means from west to east. There are no significant differences among the simulated results for domains 1, 2 and 3. In the upper watershed, the simulated precipitation is lower than observed for such stations as Roxboro 7 ESE, Roughment and Oxford AG. However, the simulated precipitation is higher than observed in some lower parts of the watershed. TABLE 3.1 compares the WRF simulated precipitations with observed cumulative precipitation during Floyd in North Carolina in Domains 1, 2 and 3. There are no significant differences among the results for the three domains, except for the Scotland Neck No 2 station where the differences between the simulated and the observed precipitation is more than 30%. Five out of 13 simulated station precipitation totals differ by less than 10% of the observed values in Domain 1.

3.4.3 Comparison of precipitation from TC vortex removal with CTRL

FIG 3.8 shows sea level pressure and 10 meter wind from WRF TC vortex removal simulation in every 12 hours from 0000/15th – 1200/17th. Compared with

FIG 3.7, Floyd has been removed from pressure field although there is still a cyclonic circulation existing to the south of the Carolinas. This might be due to the large size of Hurricane Floyd. Vortex removal may not cleanly eliminate the effects from surrounding environment. However, this circulation did not move through the entire processes as is the

case shown in FIG 3.8 where the vortex moves to the northeast gradually. FIG 3.12b and FIG 3.13b shows the simulation of vortex removal from 18 km and 6 km grid spacing WRF output at 0300/15th, the 6 km result is still shown better result and cyclonic circulation is not as strong as at 18 km grid spacing although part of Floyd is out of the Domain 2 area.

FIG 3.10 presents potential vorticity and geopotential height every 12 hours at 500 hPa after removing Floyd at the initial time of 0000/15th. Without the Floyd vortex, the northwest trough is still located in the same place and geopotential height did not change. At 1200/15th in FIG 3.10b, the highest PV of 1.5 PVU moved southeastward and is located in eastern Dakotas which are the same as FIG 3.9b without removing Floyd vortex. This trough continued moving southeastward at 0000/16th and PV fields are similar to where the 1.5 PVU field was located at the boundary between Iowa and Missouri. Until 1200/16th, the differences of PV field can be seen clearly with/without Floyd. The area of PV larger than 1.5 PVU expanded and deepened as described in FIG 3.9a and FIG 3.9d. However, the 1.5 PVU field without Floyd is just shifted to the southeast to Indiana and Ohio with a little expansion but not strengthening. This 1.5 PVU area moves northeastward at 0000/17th and further moves to the north at time 1200/17th without strengthening.

The accumulated atmospheric environmental precipitation is shown in FIG 3.18b. The environmentally induced precipitation is mostly distributed in eastern area along the coastal region. In the study area, there is only a small amount of environmental precipitation while more precipitation is distributed downstream of Tar Pamlico Sound. There is more precipitation in the northeast than the west and southwest. FIG 3.17 demonstrates the environmental precipitation as a percentage of the total precipitation (control run) in

Domains 1, 2 and 3. The environmental precipitation is relatively less. Only coastal stations of Greenville and Williamston 1 E are over 15% of the total precipitation. TABLE 3.2 demonstrates the results of environmental precipitation at observation stations. The results indicate that on average, only 7.3% of the total event precipitation is created by atmospheric environment in the study area since all stations surround the study area. In Domain 3, however, 21.5% of the total precipitation is induced by the large-scale atmospheric environment. Again, this result is under the assumption of linear interaction. The real environment contributed more than this with the interaction.

This analysis comfirms that the interaction of Floyd with the synoptic environment is what led to the heavy observed rainfall, consistent with Colle (2003) and Atallah and Bosart (2003).

3.4.4 Comparison of surface runoffs

The distributed precipitation at about 40 points from the WRF model (see FIG 3.4 and FIG 3.18) serve as input data into AnnGNPS model to simulate the total runoff. FIG 3.20 presents comparisons of three surface runoffs from 1) AnnAGNPS simulated runoff from input precipitation by WRF model output; 2) AnnAGNPS simulated runoff from input precipitation of Climate Set 2 observations; and 3) USGS measured runoff (unit is mm per day per unit area). To see the distribution of climate station set 2 please refers in FIG 3.4 as red triangle points. The simulation was conducted for seven USGS stations (see FIG 3.19 for their locations). Station Tarboro (02083500, hereafter referred to as 3500) is the outlet of the watershed. Each station represents part of the sub-watershed from the upper portion of the

stream to downstream. It can be seen that the values of the runoffs simulated from WRF output are closer to USGS measured values for most of the gage stations than runoff simulated by observed precipitation from Climate Station Set 2. For station 3500, the simulated surface runoff from WRF output matches to the USGS measured results better. For the upper stream stations 1500, 1747 and 2505 simulated results from WRF output also agree with USGS measured values better than simulated results from Climate Station Set 2 as input precipitation. This might be due to the WRF outputs provide better resolution precipitation data for the hydrological model. However, for some middle stations (2770 and 2950), the simulated results tends to underestimate surface runoff. It needs to be pointed out that USGS stream flow data at station 2950 during Floyd were estimated values and might not be very accurate.

FIG 3.21 demonstrates the simulated daily discharge hydrographs using precipitation from WRF output in domain 3 on September 16 and 17 (rest of days using observed precipitation) at the above-mentioned seven USGS gages after applying Muskingum stream routing (see Chapter 2 section 2.3.8 for details of the method). The unit is m^3s^{-1}. It compares with USGS measured river discharge in September 1999 (Note: Hurricane Dennis on Sept 5 and Floyd on Sept 16, 1999). The results show good agreement with USGS measured discharges. The simulated results for upper stations 1500 and 1747 are very close to USGS measured ones as it is easier to parameterize smaller sub-watersheds at upper stream than larger sub-watershed at downstream. The stream flow over Dennis can be clearly simulated at upper stream stations. However, downstream hydrographs demonstrate delay effects after rainfall so that discharge from Dennis cannot be reflected at station 3500 and is only slightly

reflected at stations 2585 and 2950, where AnnAGNPS model may not work exactly as measured at these gauges. These are still much better results than data from Climate Station Set 2 (see Chapter 2).

Environmentally induced precipitation only accounts for 7% of the total precipitation in the watershed area. Therefore without interaction with mid-latitude trough, total runoff is reduced by about 10% in the Tar Pamlico River Basin although Floyd would change its track if without the Midlatitude trough.

3.5 Summary and discussion

In this study, large-scale atmospheric environmental impacts on inland flooding during Floyd in 1999 have been investigated. The percentage of environment- induced precipitation has been quantified via the WRF vortex removal technique. Tropical cyclone Floyd in 1999 was simulated using a nested grid system with the highest resolution grid nested down to 2 km horizontal grid spacing using WRF version 3.1 with NARR data. The WRF model reproduced the narrow axis and intense band of heavy precipitation that developed inland of the coast over North Carolina. The distribution pattern of accumulated precipitation is much closer to NOAA observations. The simulated precipitation is within 30% of the observed values at all selected stations in the study area except for one station which is located in the northeastern corner and just outside of the study area (Scotland Neck No. 2). The simulated results are within 10% of the observed values for 5 out of the 13 stations in Domain 1. There are no major differences among Domain 1, 2 and 3 and no big signal to state that the precipitation is over or underestimated as compared to observations.

PV analysis in this study confirmed that Floyd did intensify shortly after landfall during the interaction with mid-latitude trough. This point has been stated by Atallah and Bosart (2003) but contested by Colle (2003). During Hurricane Floyd is landfall, the environmentally created precipitation was as high as 21.5% in Domain 3, which covers most of North Carolina and 7.3% of the focused hydrological study area. Surface runoff would be reduced by about 10% without large scale mid-latitude trough impacts on hurricane at gage station Tarboro where severe flooding happened in September 1999. Thus a complete study of the "perfect flooding" of hurricane Floyd in September 1999 has been conducted and investigated (see FIG 3.1). The storm surge induced flooding in this event can be separated for further study in the future.

Although the WRF vortex removal is conducted in this study, more sensitivity analyses are needed to further test this method. More hurricane cases can be applied in the future study in order to compare the role of the environment in different cases. The limitation of the vortex removal method in this study is that it is impossible to completely remove all of the vortex. Sea level pressure and wind outside of Floyd would create another circulation after removal of Floyd vortex in 600 km radius. This might be due to the large Floyd system impacting the surrounding environment. QGPV or EPV inversion techniques can be applied to compare with vortex removal method. In general, the main point of using WRF model here is to forecast precipitation when hurricane landfalling so that total runoff can be predicted. This provides a couple of days in advance for flooding warning.

REFERENCES

Atallah, E. H. and L. F. Bosart, 2003: The extratropical transition and precipitation distribution of Hurricane Floyd (1999). *Mon. Wea. Rev.,* **131**, 1063–1081.

Atallah, E. H., L. F. Bosart and A. R. Aiyyer, 2007: Precipitation distribution associated with landfalling tropical cyclones over the eastern United States. *Mon. Wea. Rev.,* **135**, 2185–2206.

Bales J. D., 2003: Effects of Hurricane Floyd inland flooding, September–October 1999, on tributaries to Pamlico Sound, North Carolina. *Estuaries,* **26**, 1319–1328.

Bingner, R. L., F. D. Theurer and Y. Yuan, 2007: AnnAGNPS technical processes. Version 4.0. USDA-ARS documentation.

Bosart, L. F., and G. M. Lackmann, 1995: Postlandfall tropical cyclone reintensification in a weakly baroclinic environment: A case study of Hurricane David (September 1979). *Mon. Wea. Rev.,* **123,** 3268–3291.

Colle, B. A., 2003: Numerical simulations of the extratropical transition of Floyd (1999): Structural evolution and responsible mechanisms for the heavy rainfall over the Northeast U.S. Mon. Wea. Rev., **131**, 2905-2926.

Croke, M. S. 2005: Examining Planetary, Synoptic and Mesoscale Features That Enhance Precipitation Associated With Landfalling Tropical Cyclone in North Carolina. M. S. thesis, North Carolina State University.

Fredrick, S., C. Davis D. Gill and S. Low-Nam, 2009: Bogussing of tropical cyclones in WRF version 3.1. Abstract of Workshop, National Center for Atmospheric Research, Boulder. June, 2009.

Hanley, D., J. Molinari and D. Keyser, 2001: A composite study of the interactions between tropical cyclones and upper-tropospheric troughs. *Mon. Wea. Rev.,* **129**, 2570 -2584.

Harville, S. 2009: Effects of Appalachian Topography on Precipitation from Landfalling Hurricanes. MS thesis, North Carolina State University.

Kimball, S. K., and J. L. Evans, 2002: Idealized numerical simulations of hurricane–trough interaction. *Mon. Wea. Rev.,* **130,** 2210–2227.

Matyas, C. J., 2010: Associations between the size of hurricane rain fields at landfall and their surrounding environments. *Meteor. Atmos. Physi.*, **106**, 135-148.

Nakanishi, M. and H. Niino, 2004: An improved Mellor-Yamada level 3 model with condensation physics: Its design and verification. *Bound.-Layer Meteor*., **112**, 1-31.

Palmer, J. M., 2008. Geostatistical Modeling of Subclimatic Tropical Precipitation in the Carolinas. MS thesis. North Carolina State University.

Pasch, R. J., T. B. Kimberlain and S. R. Stewart, 1999: Preliminary Report Hurricane Floyd 7 - 17 September, 1999. National Hurricane Center, NOAA. http://www.nhc.noaa.gov/1999floyd_text.html

Peng, M. S., R. N. Maue, C. A. Reynolds and R. H. Langland, 2007: Hurricanes Ivan, Jeanne, Karl (2004) and mid-latitude trough interactions. *Meteor. Atmos. Physi.*, **97**, 221-237.

Rodgers, E. B. and H. F. Pierce 1995: Environmental influence on Typhoon Bobbie's precipitation distribution. *Amer. Meteor. Socie.*, **34,** 2513-2532.

TABLE 3.1 Comparison of WRF simulated with observed total precipitation during Floyd landfall in NC

Station Name	Station ID	Latitude	Longitude	Observed Total Precipitation (mm) on Sept 16 and 17, 1999	Simulated Total Precipitation (mm) Sept 16 and 17, 1999			Differences in Percentage (Simulated – observed)		
					Domain1	Domain2	Domain3	Domain1	Domain2	Domain 3
Arcola	310241	36.29	-77.98	224	225	244	251	1	9	12
Enfield	312827	36.17	-77.68	259	310	321	323	20	24	25
Greenville	313638	35.64	-77.40	314	318	307	312	1	-2	-1
Henderson 2 NNW	313969	36.35	-78.41	134	143	152	154	7	14	15
Louisburg	315123	36.10	-78.30	204	161	162	161	-22	-21	-21
Oxford AG	316510	36.31	-78.61	138	125	116	117	-10	-16	-15
Roxboro 7 ESE	317516	36.35	-78.89	123	92	90	91	-25	-27	-26
Rougemont	317499	36.22	-78.85	115	92	98	96	-20	-15	-16
Snow Hill 2 SW	318060	35.53	-77.68	387	385	404	386	-1	5	0
Scotland Neck No 2	317725	36.14	-77.42	277	377	407	409	36	47	48
Williamston 1 E	319440	35.85	-77.03	326	292	308	308	-11	-6	-6
Wilson 3 SW	319476	35.70	-77.95	259	253	284	300	-2	10	16
Zebulon 3 SW Average	319923	35.78	-78.35	237	175	178	189	-26	-25	-20

TABLE 3.2 Atmospheric environmental induced precipitation during Floyd landfall in NC

Station Name	Station ID	Observed Total Precipitation (mm) on Sept 16 and 17, 1999	Simulated Total Precipitation (mm) Sept 16 and 17, 1999			Simulated environmental precipitation (mm)			Environmental Precipitation Percentage		
			Domain1	Domain2	Domain3	Domain1	Domain2	Domain3	Domain1	Domain2	Domain3
Arcola	310241	224	225	244	251	11	8	8	5.00	3.24	3.38
Enfield	312827	259	310	321	323	21	16	14	6.63	5.05	4.19
Greenville	313638	314	318	307	312	29	54	34	9.04	17.63	10.79
Henderson 2 NNW	313969	134	143	152	154	15	5	3	10.55	3.32	1.76
Louisburg	315123	204	161	162	161	11	4	5	6.74	2.61	2.92
Oxford AG	316510	138	125	116	117	13	16	10	10.74	13.72	8.47
Roxboro 7 ESE	317516	123	92	90	91	3	2	4	2.72	2.55	3.91
Rougemont	317499	115	92	98	96	3	5	5	2.72	5.24	5.64
Snow Hill 2 SW	318060	387	385	404	386	21	16	22	5.41	4.03	5.57
Scotland Neck No 2	317725	277	377	407	409	14	23	24	3.63	5.68	5.92
Williamston 1 E	319440	326	292	308	308	57	55	55	19.72	17.95	17.88
Wilson 3 SW	319476	259	253	284	300	17	8	4	6.84	2.66	1.17
Zebulon 3 SW	319923	237	175	178	189	14	20	25	7.88	11.25	13.29
Average		**231**	**227**	**236**	**238**	**18**	**18**	**16**	**7.51**	**7.30**	**6.53**

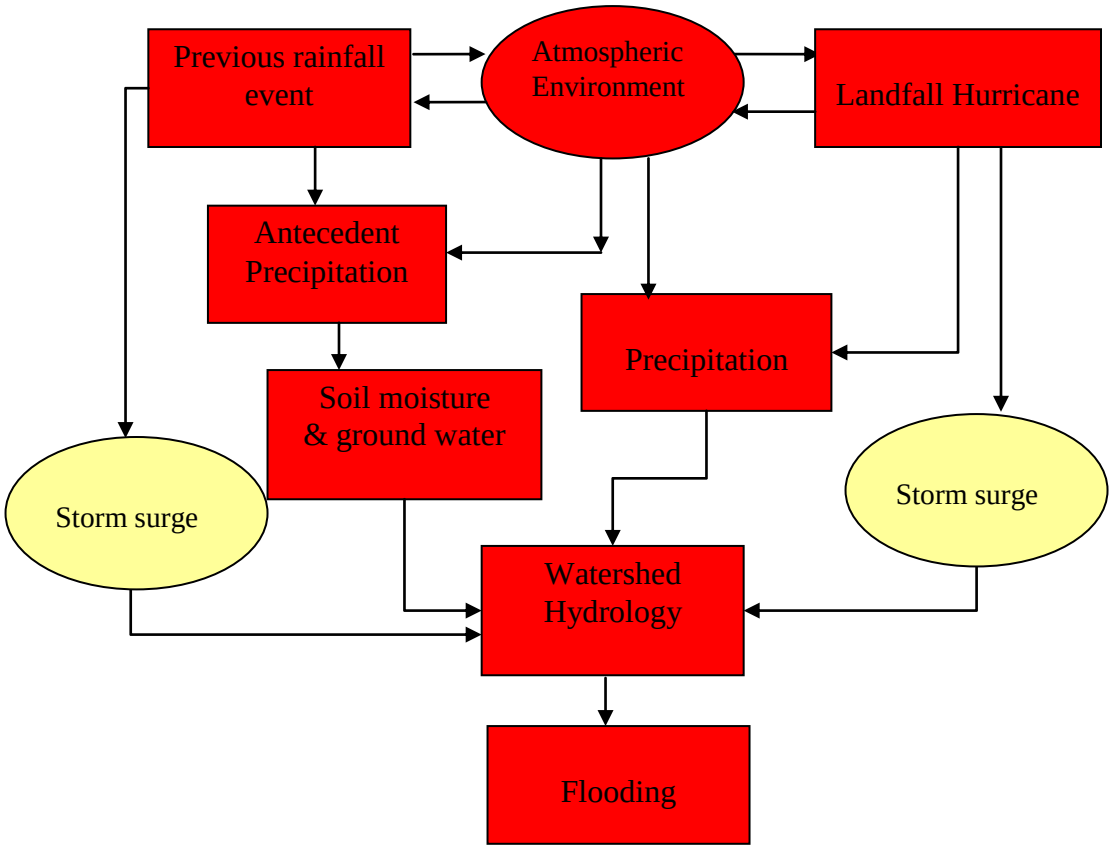

FIG 3.1 The schematic interaction map of antecedent precipitation, atmospheric environment and landfall tropical cyclone induced precipitations, watershed hydrological response and storm surges. The yellow color boxes are not studied in the research.

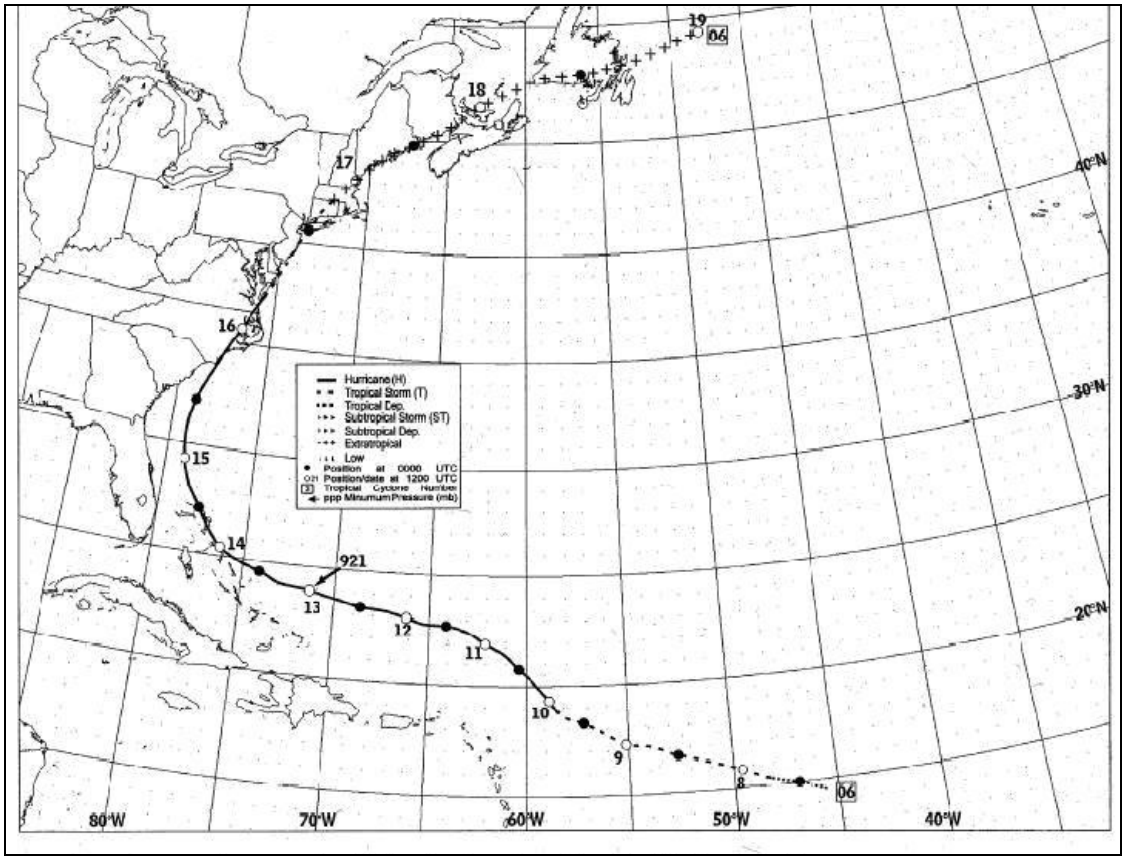

FIG 3.2 The Best Track for Hurricane Floyd from National Hurricane Center during the period of September 7 – 19, 1999. Each point represents an adjusted storm location as part of a post-storm data analysis. Best Track locations occur in 6 hour intervals at 0000 UTC (black point) and 1200 UTC (white circle point), respectively. The various line type indicate the storm classification.

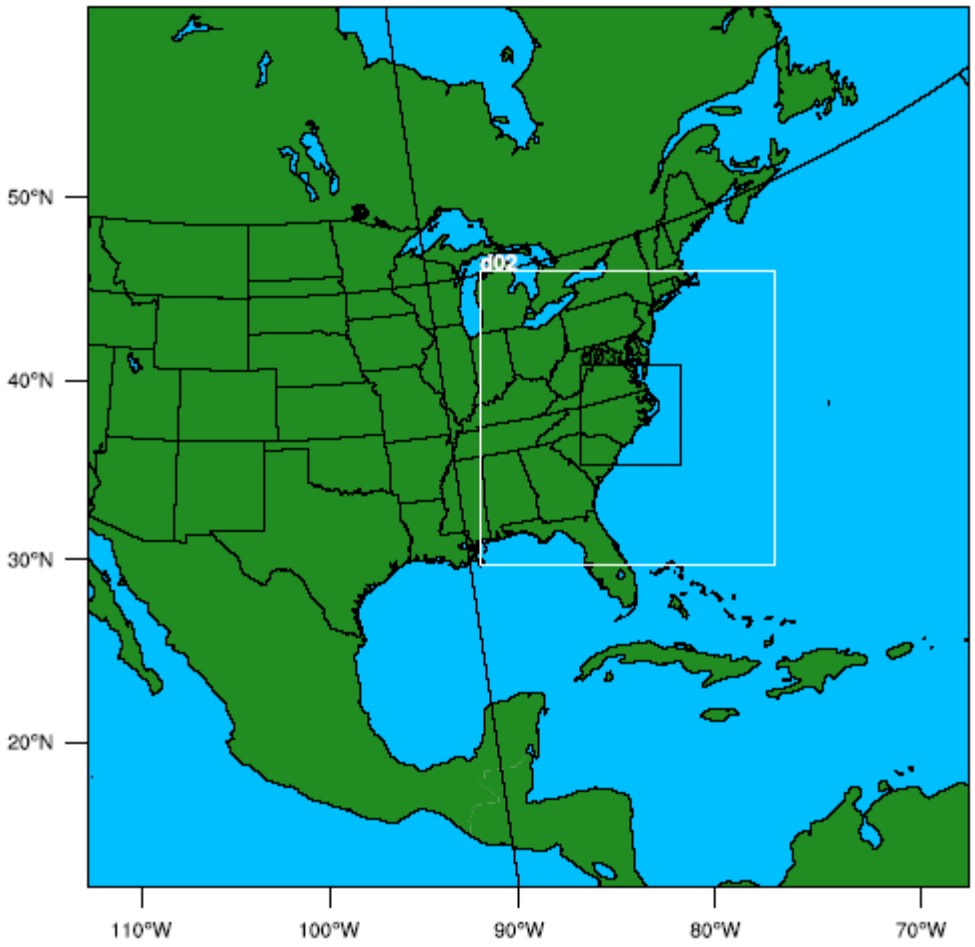

FIG 3.3 WRF model domains. Domain 1 is outside of boundary, domain 2 is white color square boundary and domain 3 is inside black color square boundary covered study area.

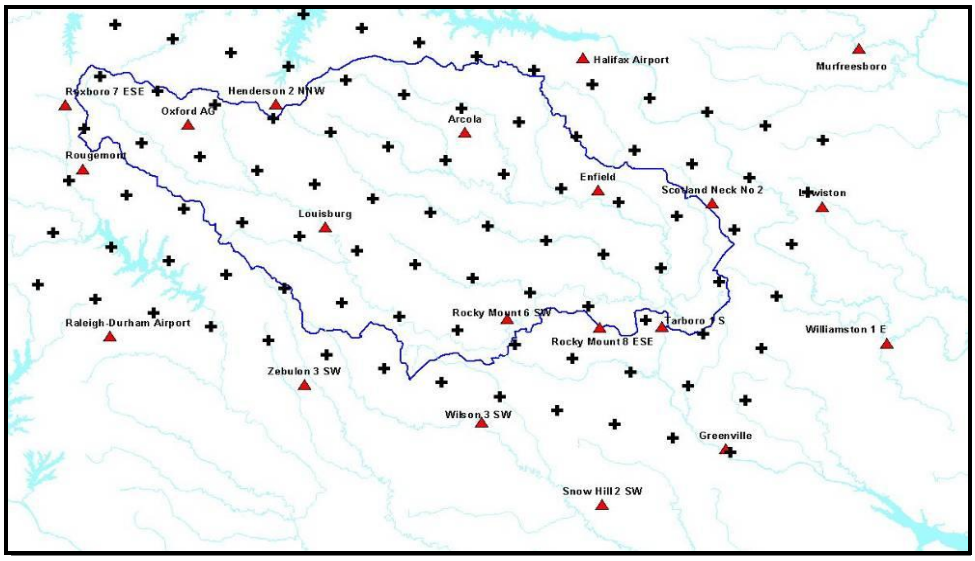

FIG 3.4 Locations of weather stations (red triangle points) in Tar-Pamlico River Basin and AnnAGNPS model input precipitation points from WRF model output (Black crosses).

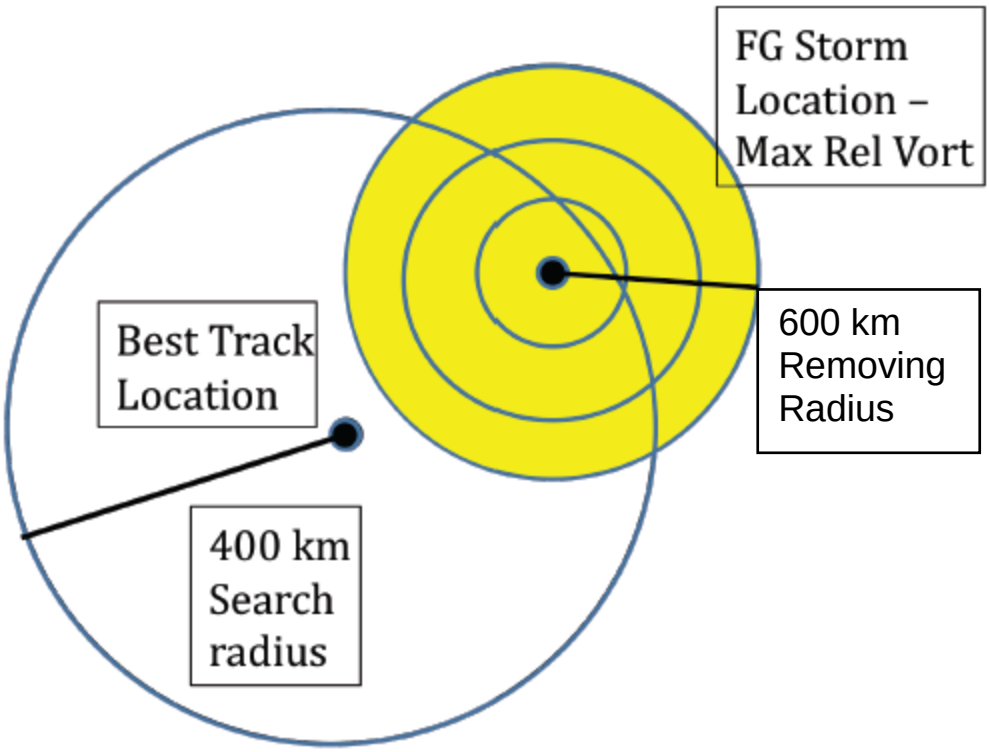

FIG 3.5 Bogussing of Tropical Cyclone (modified from Fredrick et al. 2009). TC bogus scheme searches for vortex within 400km radius from the Best Track location. The point where the maximum vorticity is located serves as the center of the vortex to be removed (the center of yellow circles) and the removing radius is 600 km.

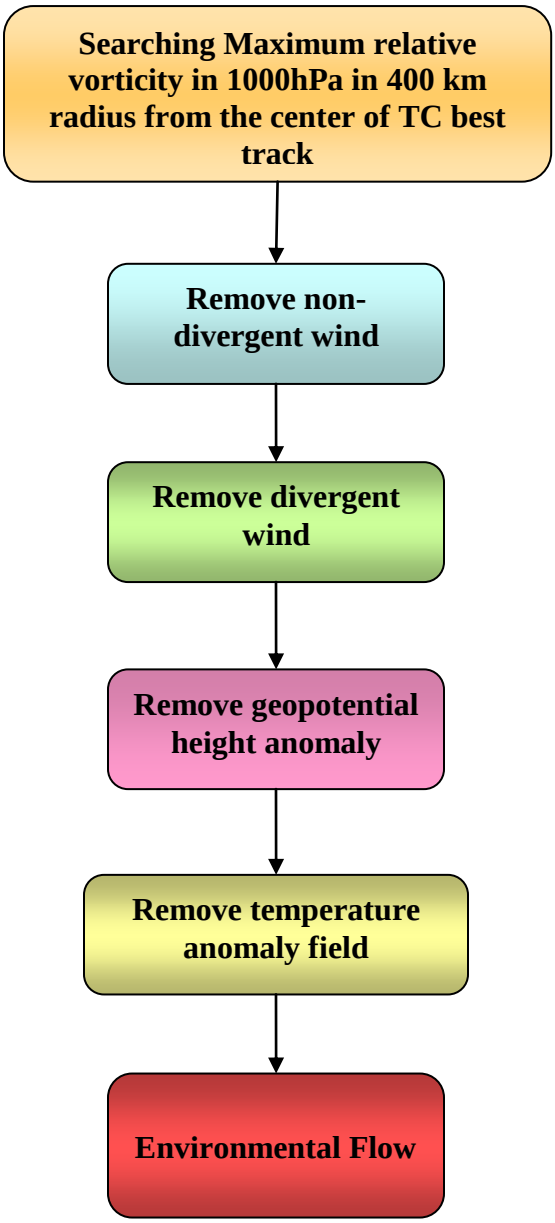

FIG 3.6 Schematic diagram of bogussing TC and removing vortex from background flow.

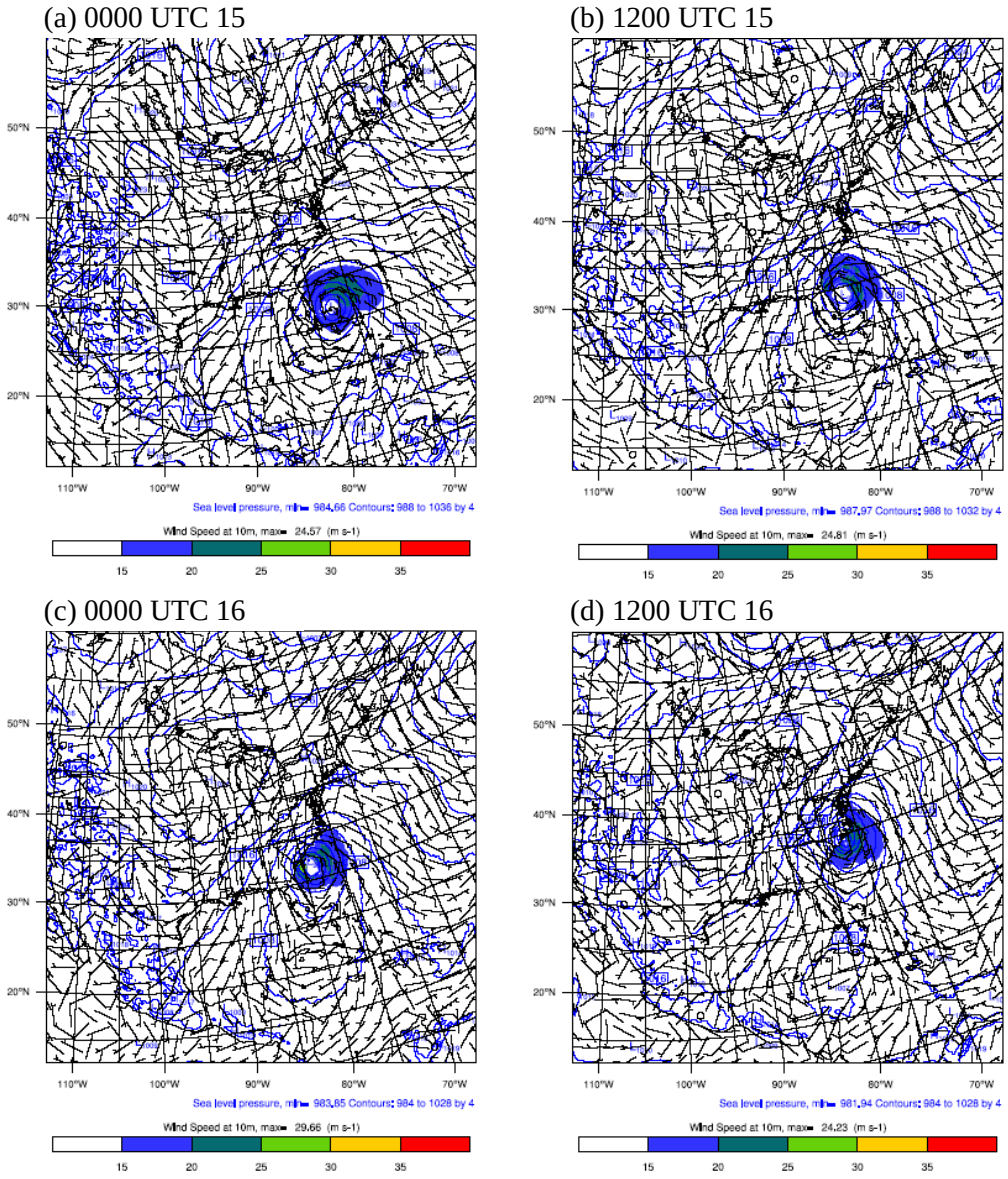

FIG 3.7 Sea level pressure and 10 meter wind from control simulation in every 12 hours starting from 0000 UTC 15 Sep 15 to 1200 UTC 17 Sep 1999 (a) 0000/15th, (b) 1200/15th, UTC Sept. 15, (c) 0000/16th, (d) 1200/16th.

(e) 0000 UTC 17 (f) 1200 UTC 17

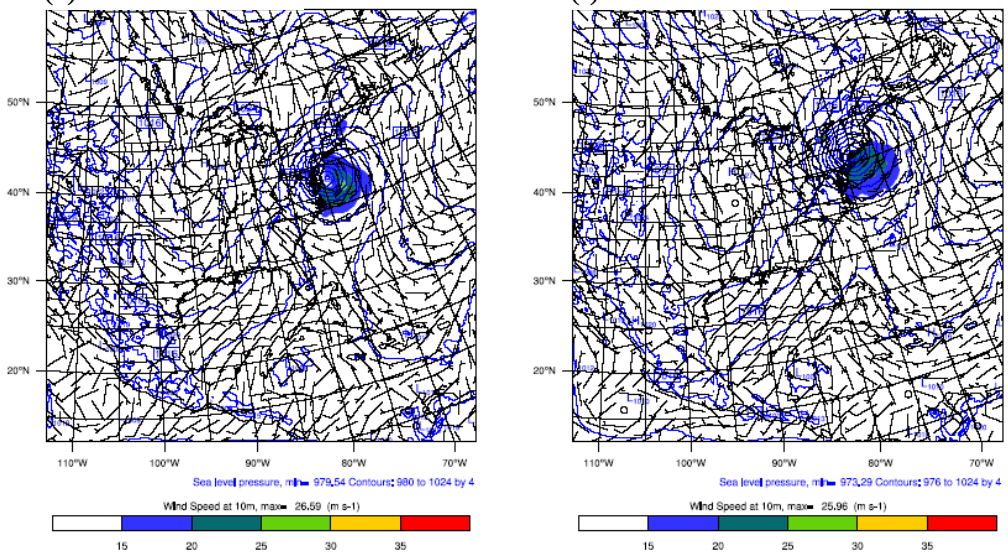

FIG 3.7 Sea level pressure and 10 meter wind from control simulation in every 12 hours starting from 0000 UTC 15 Sep 15 to 1200 UTC 17 Sep 1999 (e) 0000/17th and (f) 1200/17th.

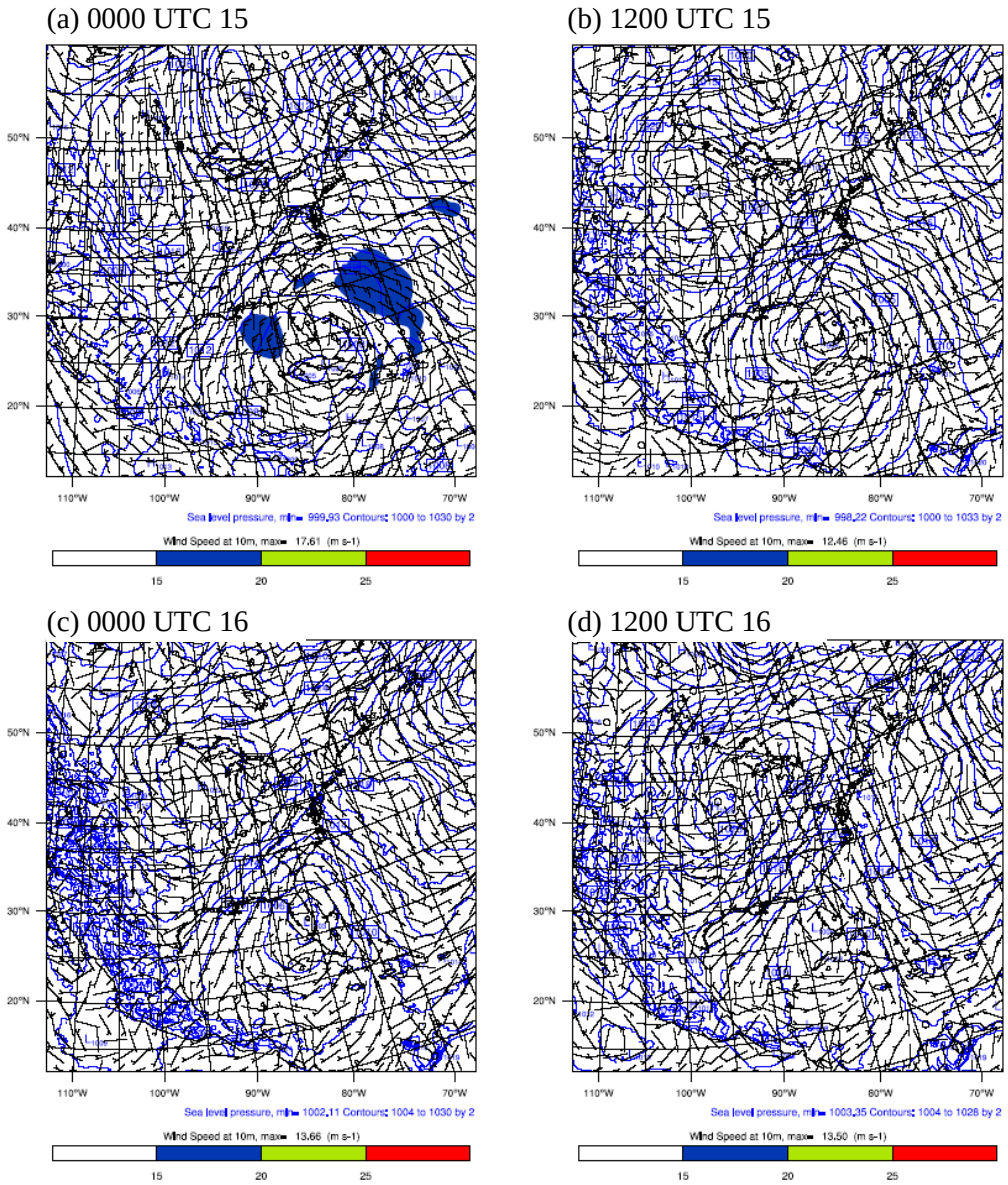

FIG 3.8 Sea level pressure and 10 meter wind from WRF TC vortex removal simulation in every 12 hours starting from 0000 UTC 15 Sep 15 to 1200 UTC 17 Sep 1999 (a) 0000/15th, (b) 1200/15th, UTC Sept. 15, (c) 0000/16th, (d) 1200/16th.

(e) 0000 UTC 17 (f) 1200 UTC 17

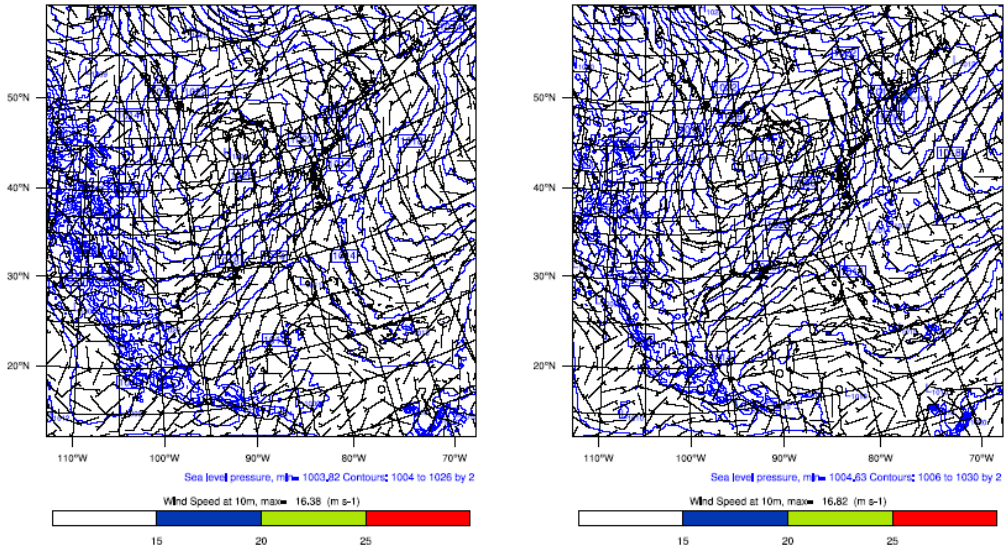

FIG 3.8 Sea level pressure and 10 meter wind from WRF TC vortex removal simulation in every 12 hours starting from 0000 UTC 15 Sep 15 to 1200 UTC 17 Sep 1999 (e) 0000/17th and (f) 1200/17th.

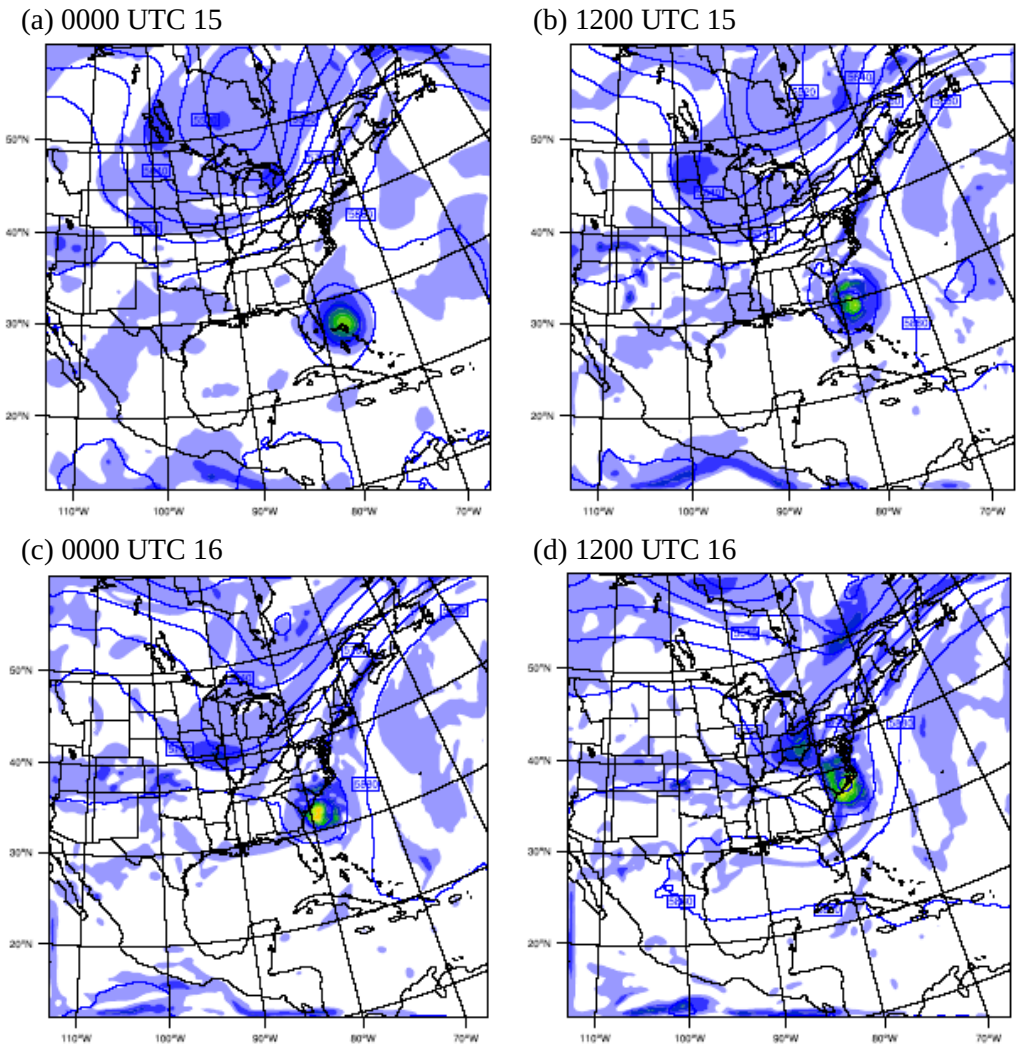

FIG 3.9 The 500 hpa Potential Vorticity (shaded in every 0.5 PVU, 1 PVU = 10^{-6} K kg^{-1} m^2 s^{-1}) and Geostrophic Height (blue line) from WRF output in every 12 hours starting from 0000 UTC 15 Sept. 15 to 1200 UTC Sept. 17, 1999 (a) 0000/15th, (b) 1200/15th, (c) 0000/16th, (d) 1200/16th.

(e) 0000 UTC 17 (f) 1200 UTC 17

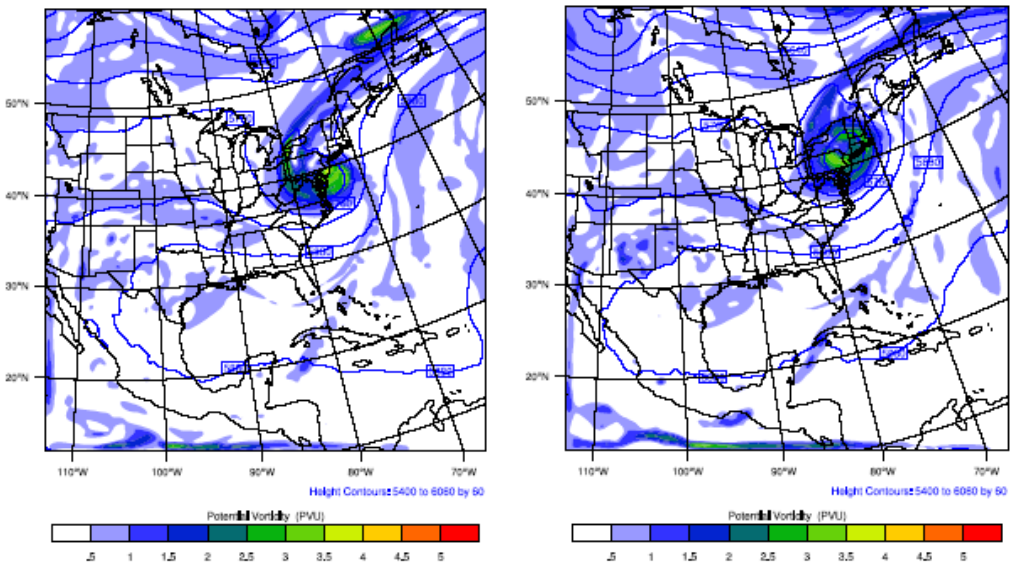

FIG 3.9 The 500 hpa Potential Vorticity (shaded in every 0.5 PVU, 1 PVU = 10^{-6} K kg^{-1} m^2 s^{-1}) and Geostrophic Height (blue line) from WRF output in every 12 hours starting from 0000 UTC 15 Sept. 15 to 1200 UTC Sept. 17, 1999 (e) 0000/17th and (f) 1200/17th.

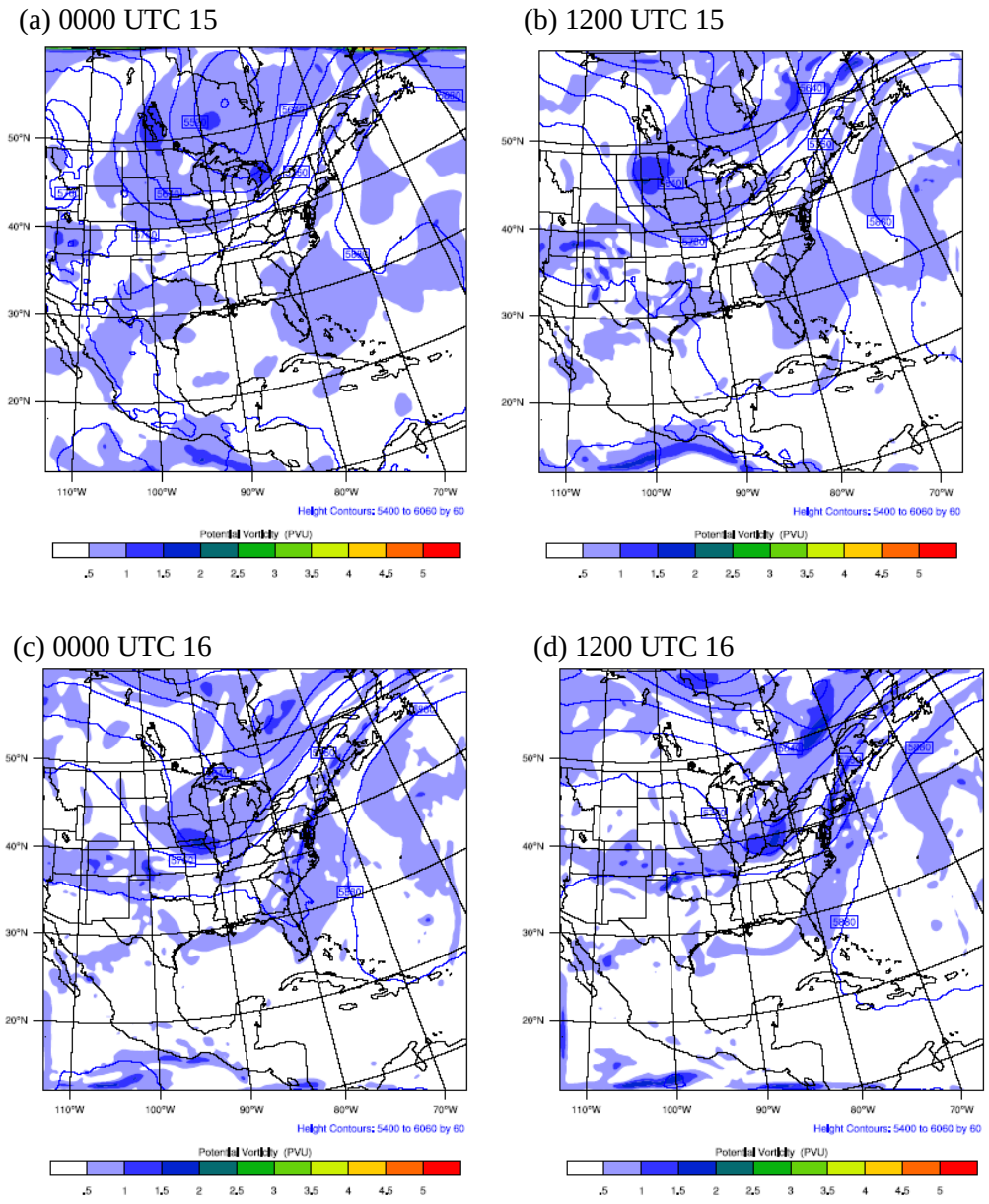

FIG 3.10 The 500 hPa Potential Vorticity (shaded in every 0.5 PVU) and Geostrophic Height (blue line) from WRF output in every 12 hrs starting from 0000 UTC Sept. 15 to 1200 UTC Sept. 17, 1999 (a) 0000/15th, (b) 1200/15th, UTC Sept. 15, (c) 0000/16th, (d) 1200/16th.

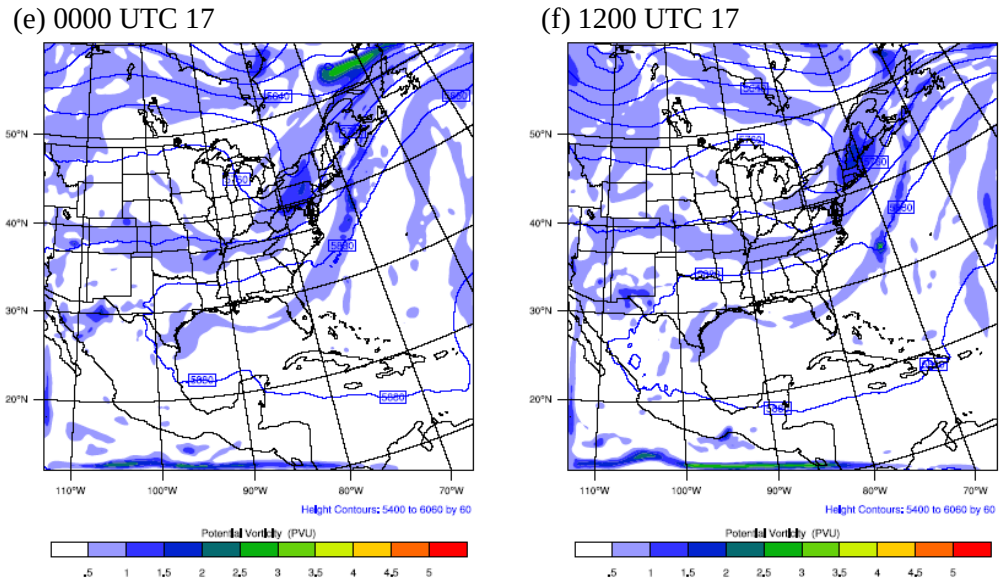

FIG 3.10 The 500 hPa Potential Vorticity (shaded in every 0.5 PVU) and Geostrophic Height (blue line) from WRF output in every 12 hrs starting from 0000 UTC Sept. 15 to 1200 UTC Sept. 17, 1999 (e) 0000/17th and (f) 1200/17th.

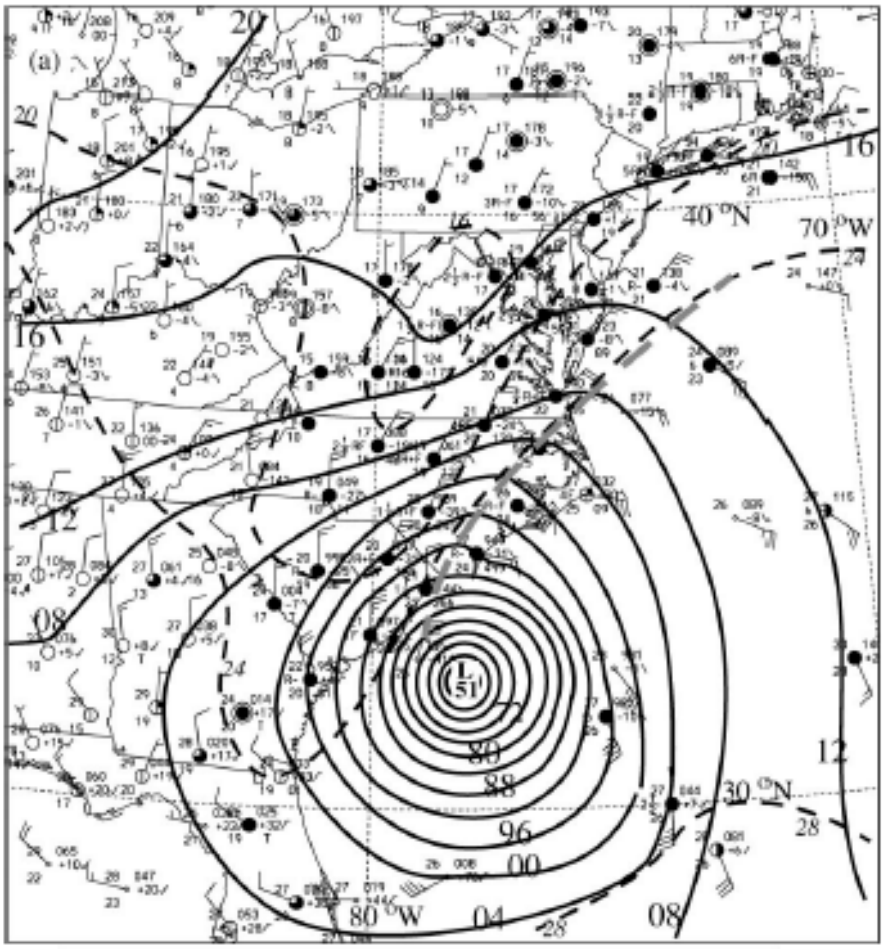

FIG 3.11 Manual surface analysis at 0000 UTC 16 September 1999 (Colle 2003)

(a)

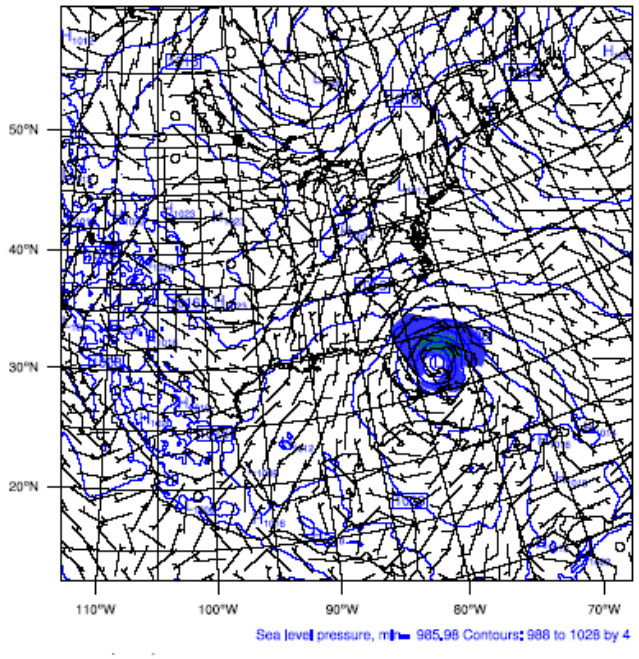

(b)

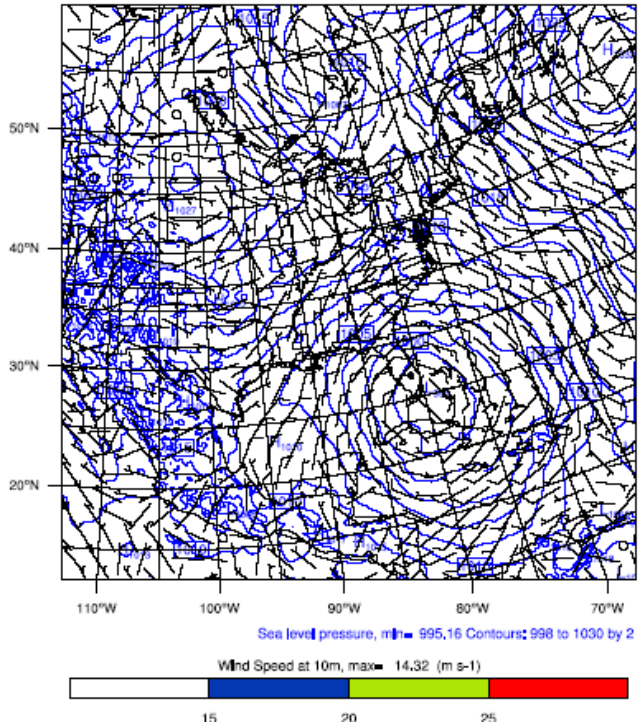

FIG 3.12 Sea level pressure and 10 meter wind at 0300 UTC 15 Sep 1999 from WRF simulation result in 18 km grid space in a) control simulation (CTRL) b) hurricane vortex removal (ENV).

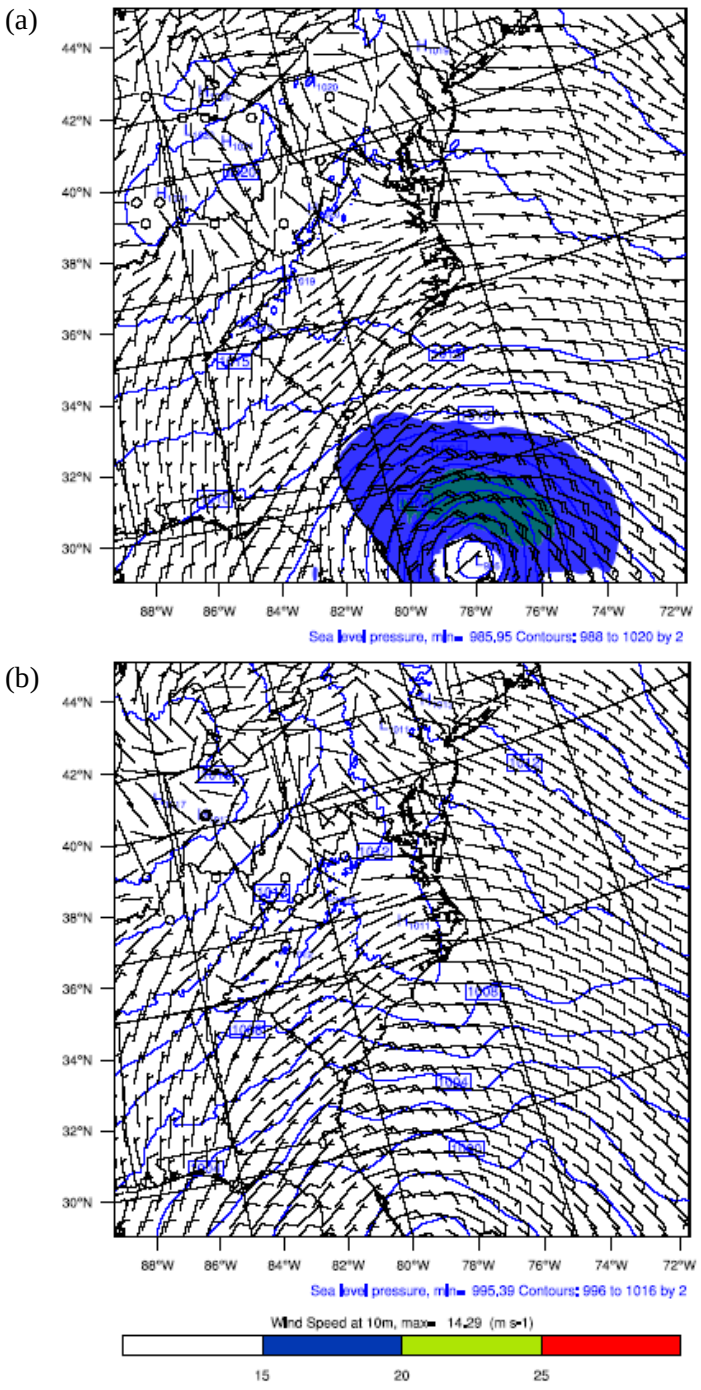

FIG 3.13 The same with FIG 3.12 but in 6 km grid space in a) control simulation (CTRL) b) hurricane vortex removal (ENV).

(a)

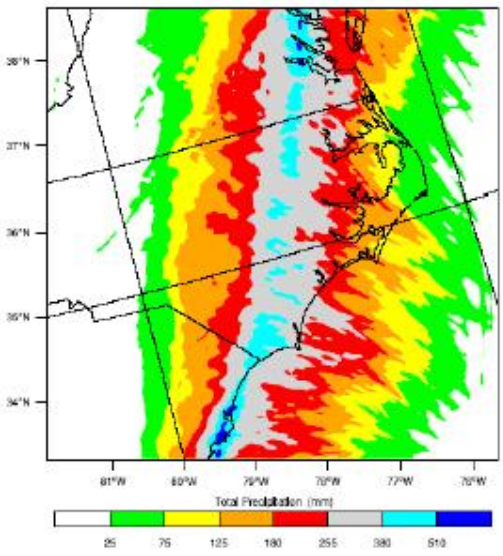

(b)

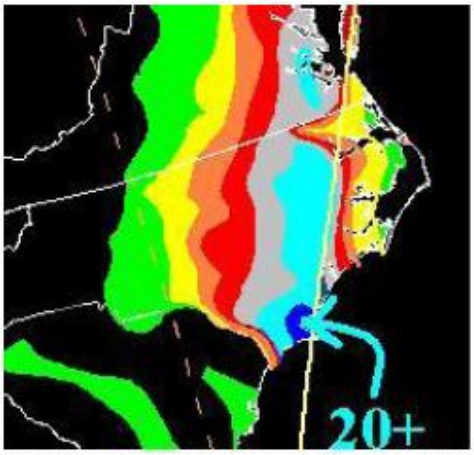

Note: Blue is 510mm; Cyan is 380mm; Gray is 255mm; Red is 180 mm; Orange is 125mm; Yellow is 75mm and green is 25mm (Modified color scheme from NOAA).

(c)

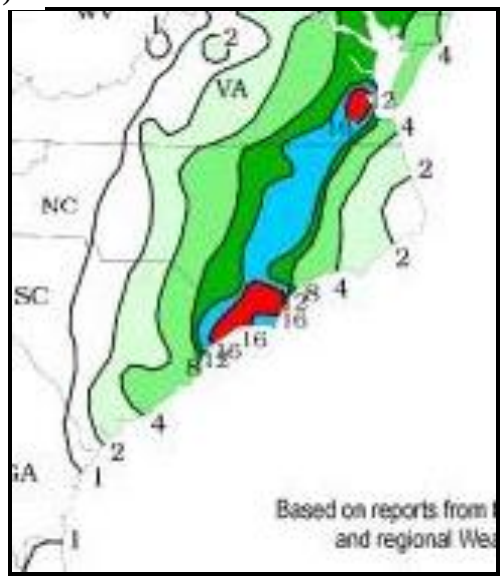

FIG 3.14 Cumulated precipitation during TC Floyd landfall from Sep 14 – Sep 19, 1999 from a) WRF model control simulation, b) NOAA observed precipitation map (modified color scheme from NOAA, Pasch et al. 1999) and the yellow line indicated the Floyd track, and c) Climate Prediction Center based on reports from the River Forecast Centers and regional Weather Service Offices (precipitation in inches)

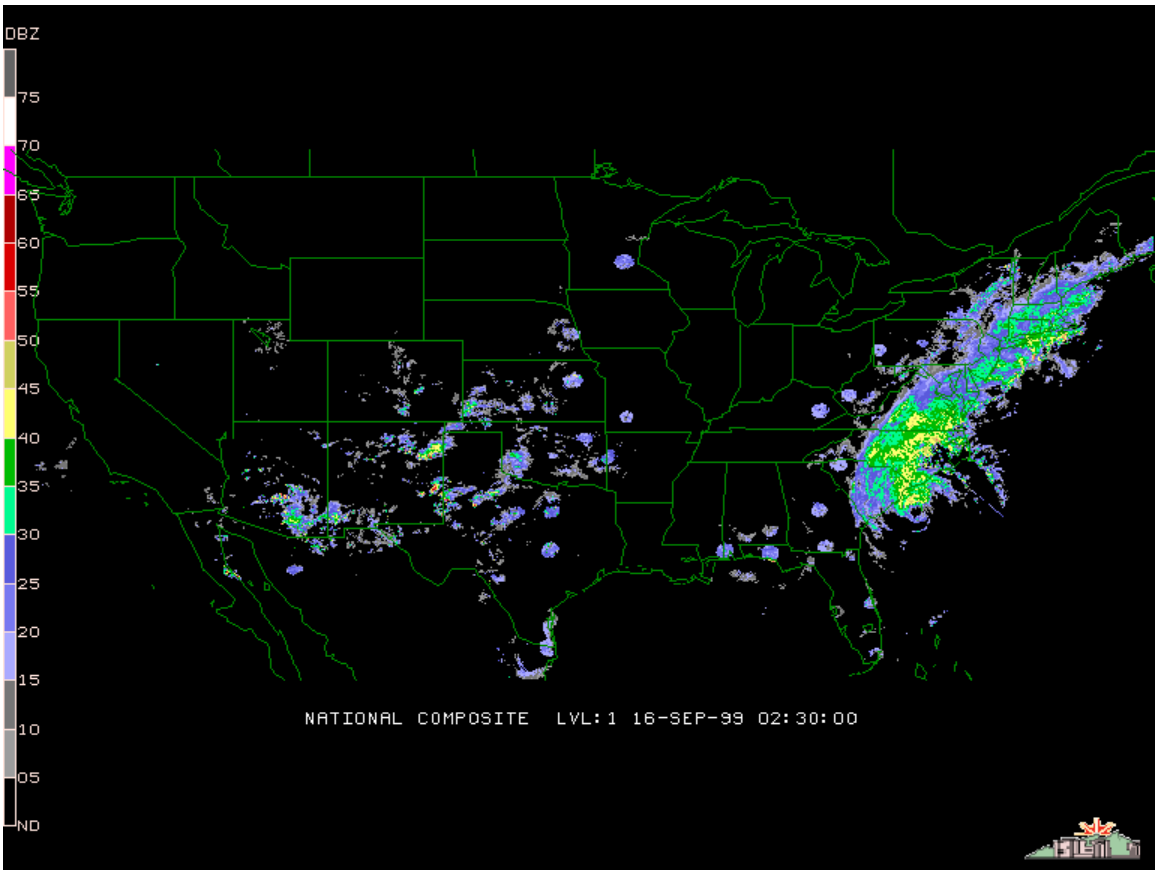

FIG 3.15 Radar reflectivity on 16 September 1999 from National Center for Atmospheric Research (http://locust.mmm.ucar.edu/)

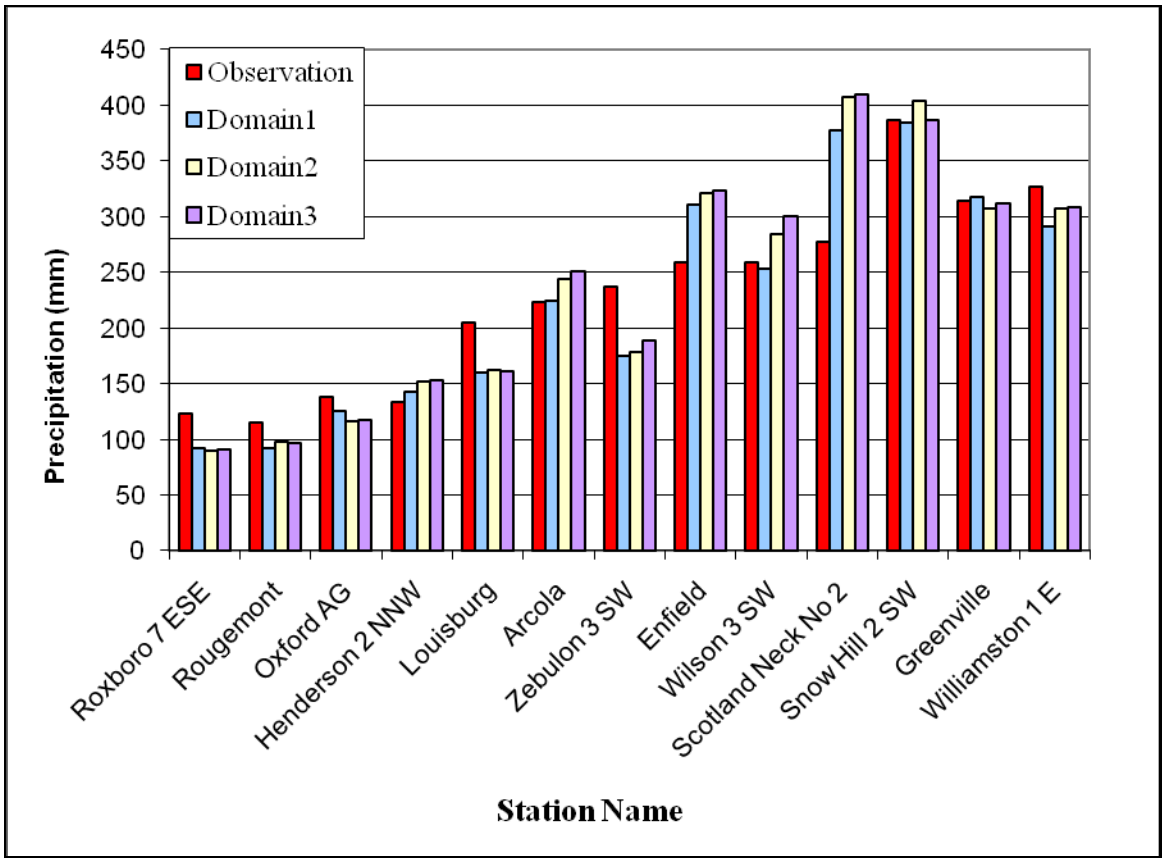

FIG 3.16 Comparison of WRF simulated precipitation in domain 1, 2, 3 and observation at selected weather stations. Please see Fig. 4.9 for the distribution of weather stations, the stations from left to right present stations from upper in the west to lower watershed in the east.

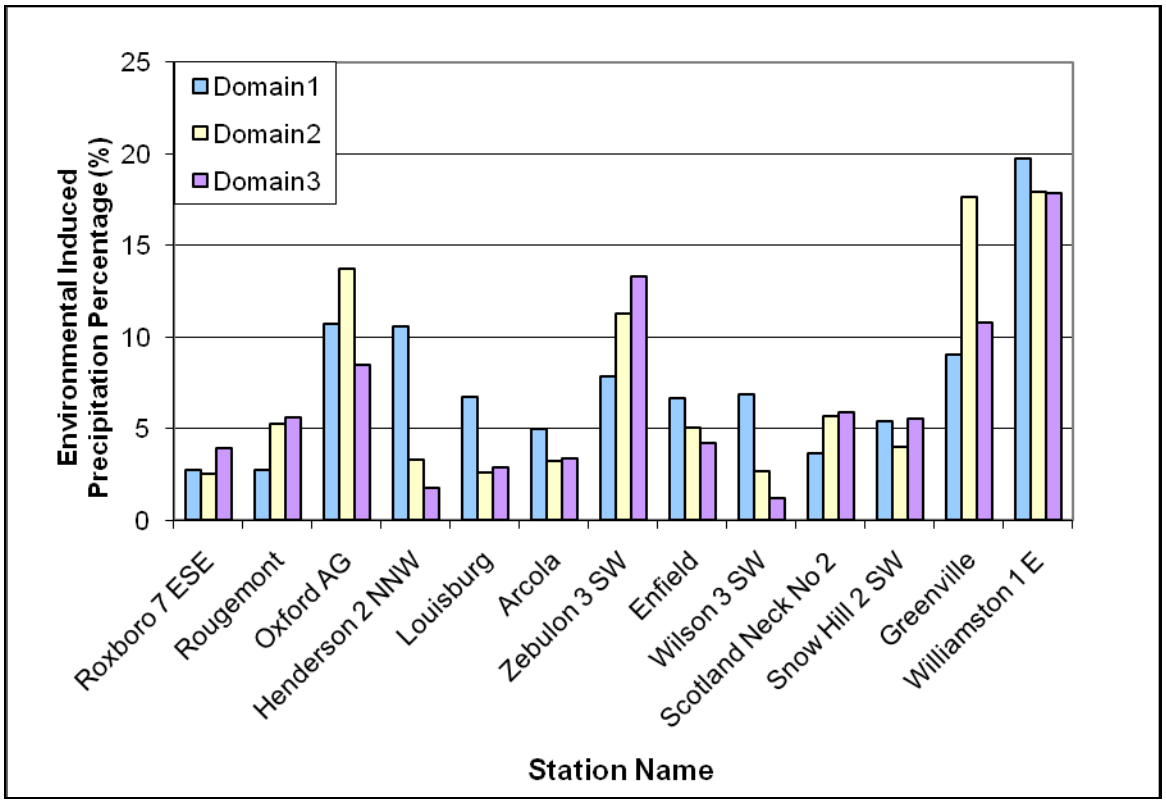

FIG 3.17 WRF simulated environmental precipitation in domain 1, 2 and 3 at selected weather stations. Please see Fig.4.9 for the distribution of weather stations, the stations from left to right present stations from upper in the west to lower watershed in the east.

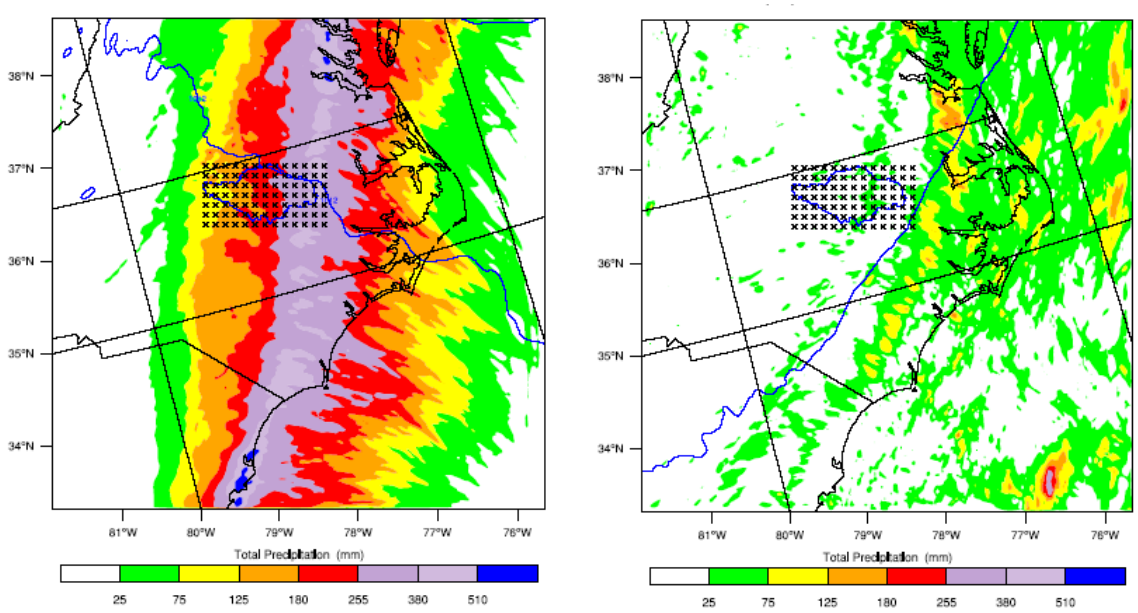

FIG 3.18 Simulated precipitation cumulated from 1200 UTC 15 Sep 1999 to 1200 UTC 17 Sep 1999. Marked area is the study area for hydrological model in Tar Pamlico River Basin. The cross points represent the precipitation data from WRF output into AnnAGNPS model. (a) Control run from WRF model (b) Environmental precipitation.

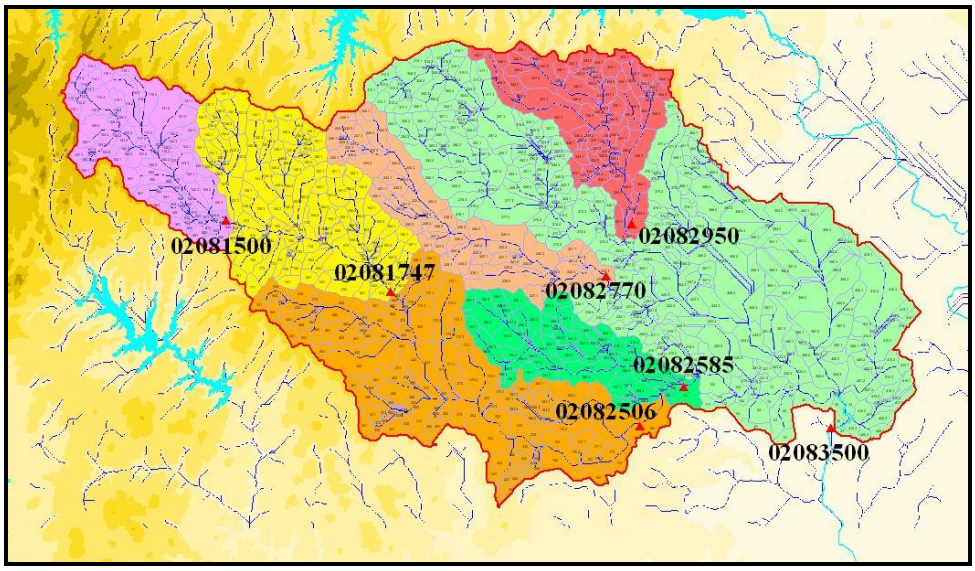

FIG 3.19 USGS streamflow gages (triangle points) and corresponding areas in AnnAGNPS in Tar-Pamlico River Basin (Each downstream gage area covers all upper gage areas).

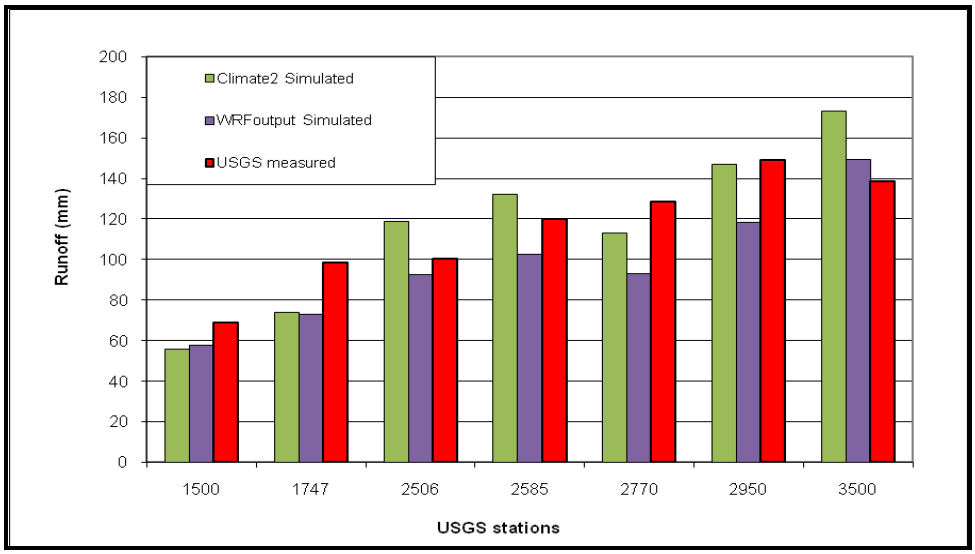

FIG 3.20 Comparison of climate station set 2 and WRF output simulated runoff with USGS observed runoff at seven gage stations in Tar Pamlico River Basin (unit is in mm/day/unit area).

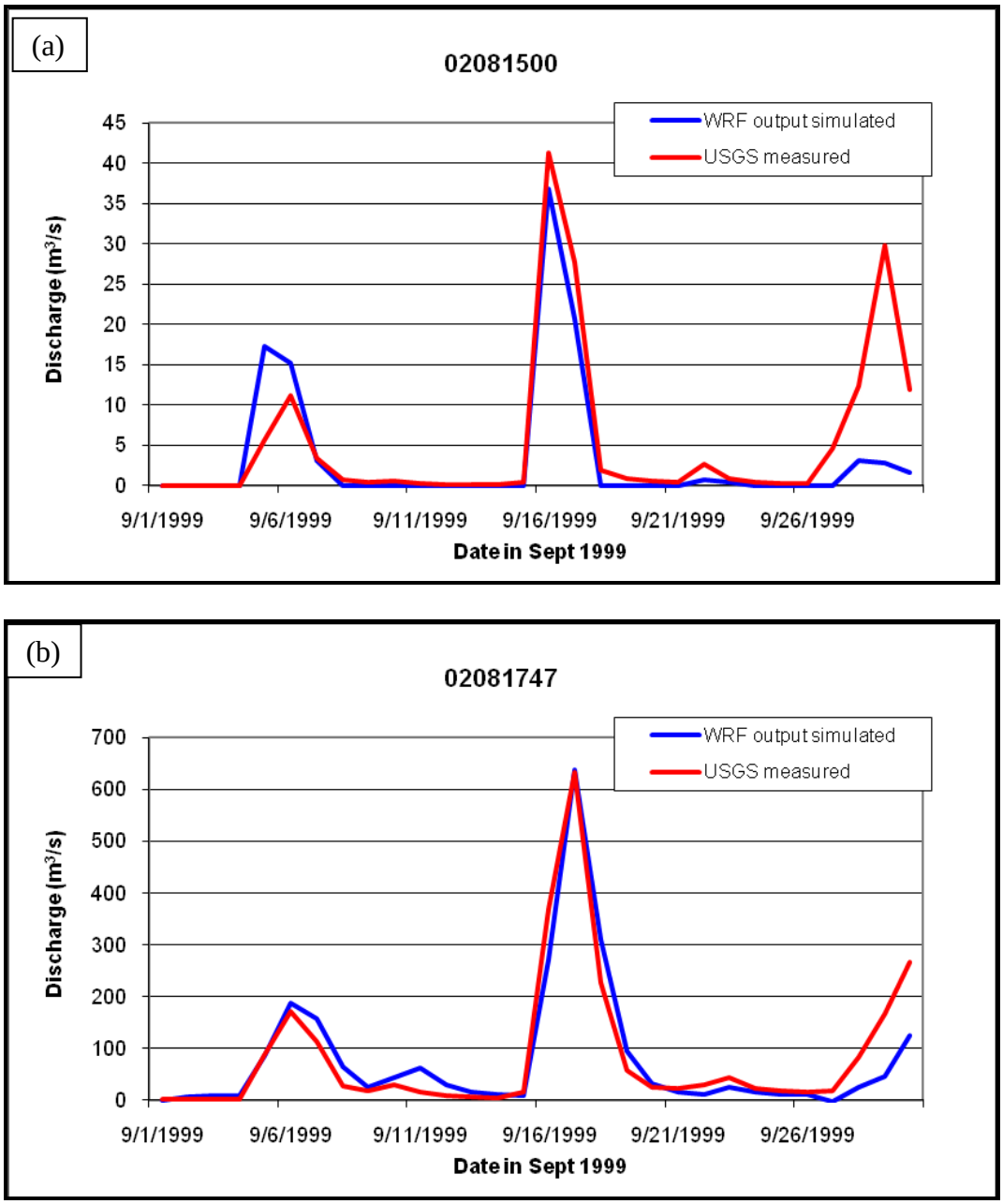

FIG 3.21 Hydrographs comparison of AnnGNPS simulated river discharge using WRF output with USGS measured ones in September 1999 at gages (a) 02081500 and (b) 02081747 (Note: Dennis on Sept 5 and Floyd on Sept 16, 1999).

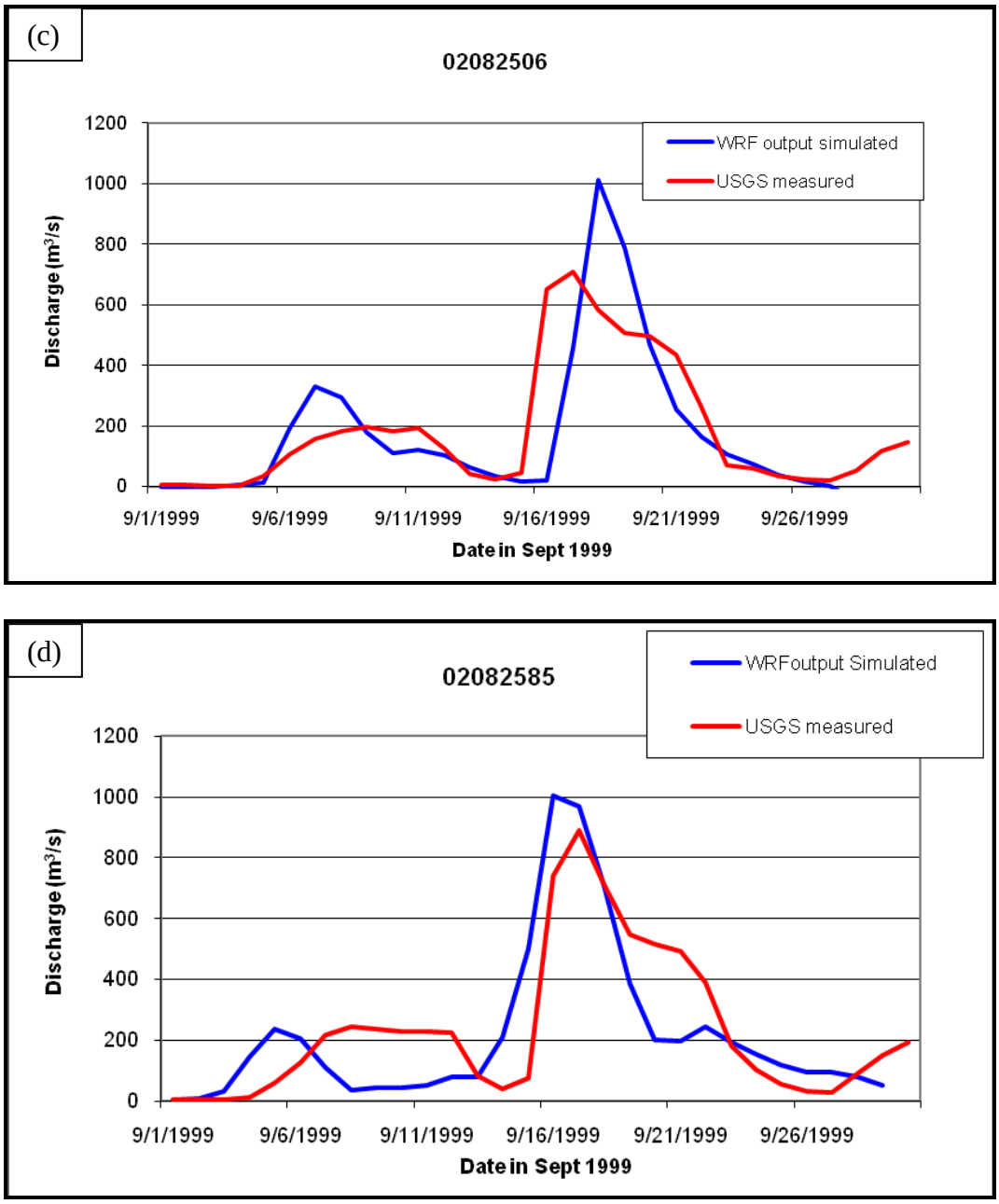

FIG 3.21 Hydrographs comparison of AnnGNPS simulated river discharge using WRF output with USGS measured ones in September 1999 at gages (c) 02082506 and (d) 02082585 (Note: Dennis on Sept 5 and Floyd on Sept 16, 1999).

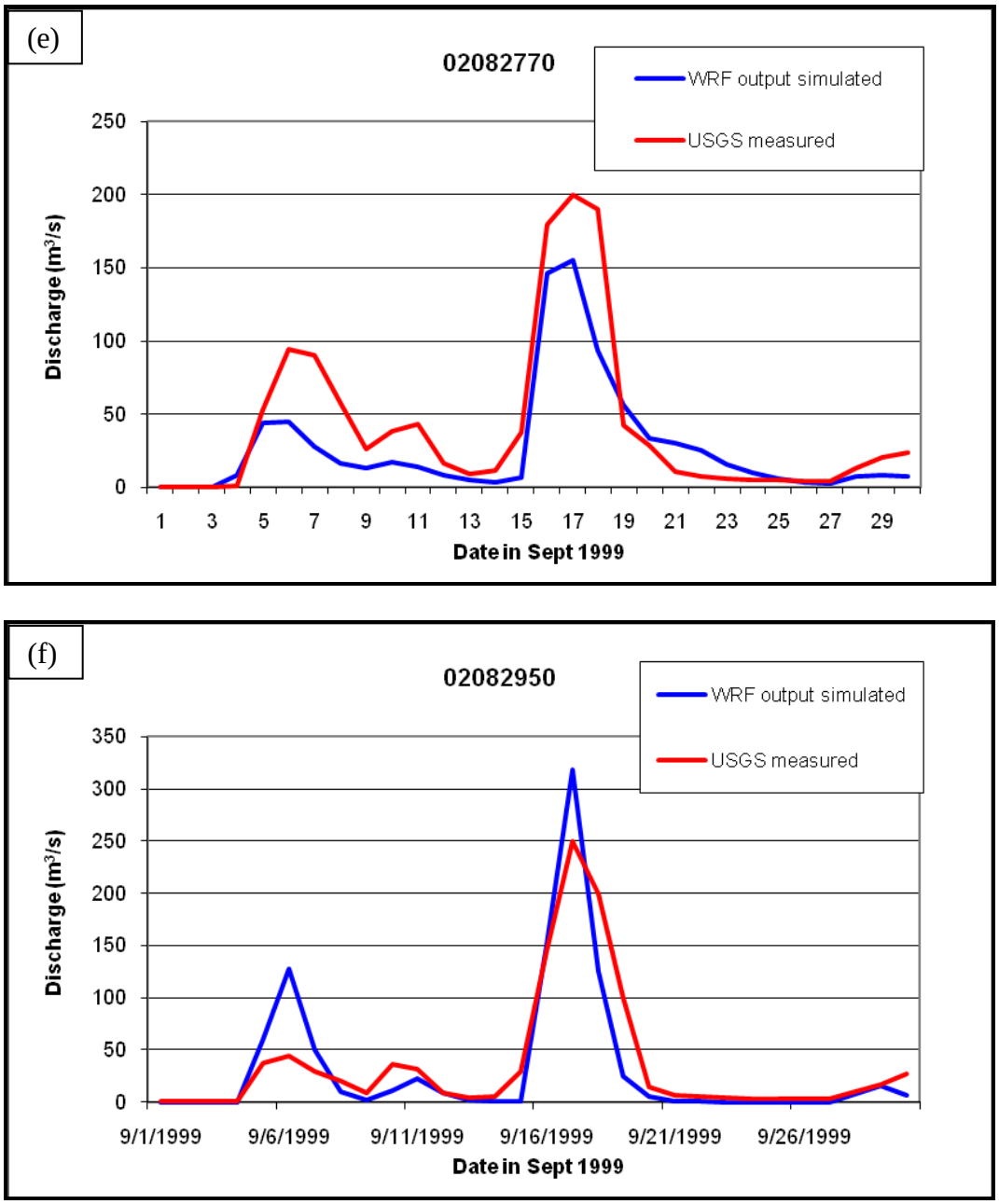

FIG 3.21 Hydrographs comparison of AnnGNPS simulated river discharge using WRF output with USGS measured ones in September 1999 at gages (e) 02082770 and (f) 02082950 (Note: Dennis on Sept 5 and Floyd on Sept 16, 1999).

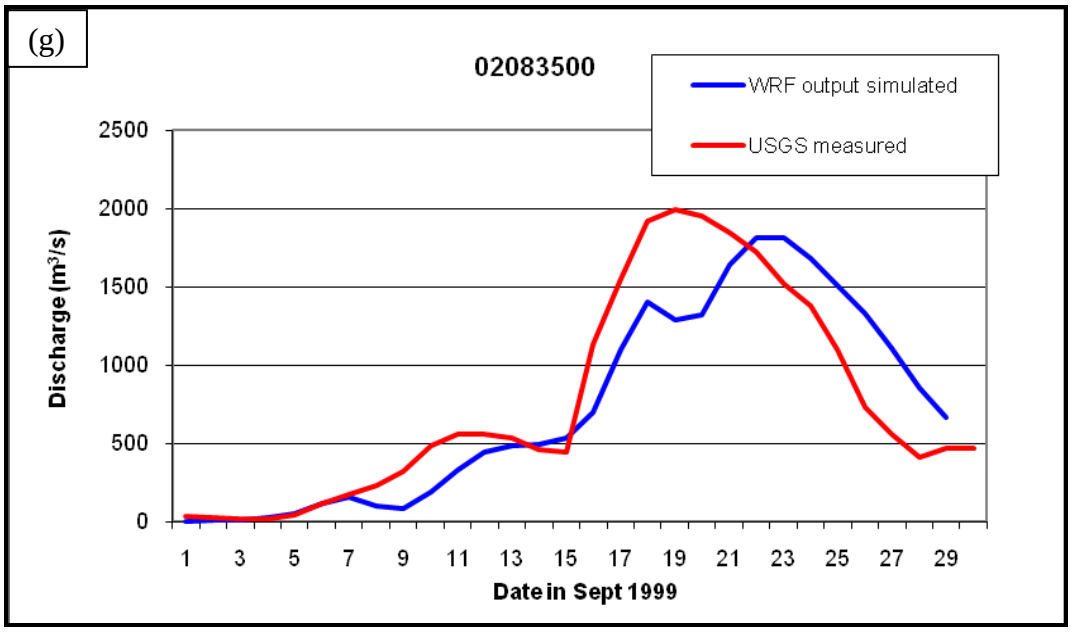

FIG 3.21 Hydrographs comparison of AnnGNPS simulated river discharge using WRF output with USGS measured ones in September 1999 at gages (g) 02083500 (Note: Dennis on Sept 5 and Floyd on Sept 16, 1999).

CHAPTER 4 Concluding Remarks and Future Works

Concluding remarks

Tropical Cyclone induced inland flooding at Tar Pamlico River Basin of North Carolina by Floyd 1999 has been simulated by using the watershed hydrological model of AnnAGNPS and the Weather Research Forecast model (WRF). AnnAGNPS reproduced surface total runoff at each subwatershed and the outlet of an entire watershed to create total volume of water so that flooding can be further generated by the MicroDem program. The study indicates that for large watersheds, Muskingum channel routing must be incorporated into the model in order to create accurate hydrographs. The WRF model could reproduce the northeast and southwest stretched narrow and intense band of precipitation. The study investigated four hydro-meteorological identities of previous rainfall events, synoptic atmospheric environment, hurricane Floyd and watershed surface runoff since the severe flooding in the coastal watershed during hurricane Floyd landfall is caused by the combination effects of antecedent precipitation, synoptic atmospheric environment and hurricane induced precipitations. It is found that previous TC or precipitation saturated the soil of the watershed so that additional rainfall would more easily produce flooding. In the case of Hurricane Dennis which immediately preceded Hurricane Floyd, total runoff caused by Hurricane Floyd at the outlet without Hurricane Dennis would have been as much as 37% lower than the actual observations. Meanwhile, hydrological simulation results demonstrate that the surface runoff in the Tar Pamlico river basin is reduced by about 10% without

interaction of Floyd and the large scale mid-latitude trough. This is under assumption of linear relationship of the interaction. Using WRF model output of precipitation at 40 points as input for the AnnAGNPS model, the simulated discharge and volume of water are better than using observed data from 10 climate stations. Thus a more thorough study on the "perfect flooding" of hurricane Floyd in September 1999 has been conducted (see FIG 3.1). The other findings from this research include:

a. For the large watershed of Tar-Pamlico River Basin with a total area of 5605 km^2, subwatershed simulations are necessary. The study indicated that simulated hydrographs in the upper small sub-watersheds at stations 02081500 and 02081747 are better than larger sub-watershed such as stations 02082770 and 02082950. But overall, it still provides good hydrographs.
b. Scale analysis indicates that the important parameters affecting watershed flooding are precipitation, surface runoff and subsurface flow.
c. The sensitivity analysis and calibration through TCs of Bertha (1996), Fran (1996), Floyd (1999), Isabel (2003) and Hanna (2008) indicate that the AnnAGNPS model can reliably be used to simulate event total runoff.
d. Sensitivity analysis of soil saturated hydrological conductivity K_s indicates that peak runoff at gages exponentially decreases as K_s increases and base flow increases as K_s increases at lower level of K_s value (0 – 15 m/day) while base flow slightly decreases when K_s value increases at higher level of K_s value (> 15 m/day).
e. The WRF model output of distribution pattern of accumulated precipitation is very close to observed ones. The magnitudes of simulated precipitation is within 30% of

the data from stations in the study area except one station located in northeastern outside of study area named Scotland Neck No. 2. Seven out of thirteen stations are less than 15% of differences in domain 1. There are not much differences in simulated results among Domain 1, 2 and 3 and there is no indication that the precipitation is over or underestimated.

Future works

This study is limited to the flooding caused by Hurricanes Dennis and Floyd in Tar-Pamlico River Basin of North Carolina. More hurricane cases should be applied in the future study in order to compare the role of previous rainfall event and synoptic atmospheric environment in different cases. More sensitivity analyses are needed to test the accuracy of the hydrological model used in this study and the validity of using WRF rainfall forecasts in hydrological prediction. The limitation of vortex removal method used in this study is that it is impossible to completely remove all vortex of the environment surrounding Floyd. Sea level pressure and wind outside of Floyd may create another cyclonic circulation after removal of Floyd vortex in 600 km radius. This might be due to large Floyd system impacting on the surrounding environment. QGPV or EPV inversion techniques can be applied to compare with vortex removal technique in future study. Additionally, flooding from storm surge and the interaction between storm surge and inland flooding should be examined.